NAVAL POSTGRADUATE SCHOOL
Monterey, California

THESIS

DESIGN AND EVALUATION OF ION SOURCE FOR SATELLITE CHARGE CONTROL

by

Michael Edward Melvin

June 1992

Thesis Advisor: R.C. Olsen

REPORT DOCUMENTATION PAGE

Form Approved
OMB No 0704-0188

1a REPORT SECURITY CLASSIFICATION Unclassified	1b RESTRICTIVE MARKINGS
2a SECURITY CLASSIFICATION AUTHORITY	3 DISTRIBUTION / AVAILABILITY OF REPORT Approved for public release; distribution is unlimited.
2b DECLASSIFICATION / DOWNGRADING SCHEDULE	
4 PERFORMING ORGANIZATION REPORT NUMBER(S)	5 MONITORING ORGANIZATION REPORT NUMBER(S)
6a NAME OF PERFORMING ORGANIZATION Naval Postgraduate School 6b OFFICE SYMBOL (If applicable) 33	7a NAME OF MONITORING ORGANIZATION Naval Postgraduate School
6c. ADDRESS (City, State, and ZIP Code) Monterey, CA 93943-5000	7b ADDRESS (City, State, and ZIP Code) Monterey, CA 93943-5000
8a NAME OF FUNDING / SPONSORING ORGANIZATION 8b OFFICE SYMBOL (If applicable)	9 PROCUREMENT INSTRUMENT IDENTIFICATION NUMBER
8c ADDRESS (City, State, and ZIP Code)	10 SOURCE OF FUNDING NUMBERS PROGRAM ELEMENT NO / PROJECT NO / TASK NO / WORK UNIT ACCESSION NO

11 TITLE (Include Security Classification)

DESIGN AND EVALUATION OF ION SOURCE FOR SATELLITE CHARGE CONTROL

12 PERSONAL AUTHOR(S)

Melvin, Michael E.

13a TYPE OF REPORT	13b TIME COVERED	14 DATE OF REPORT (Year, Month, Day)	15 PAGE COUNT
Master's Thesis	FROM _____ TO _____	June 1992	118

16 SUPPLEMENTARY NOTATION

The views expressed in this thesis are those of the author and do not reflect the policy or position of the Department of Defense or the U. S. Government.

17 COSATI CODES			18 SUBJECT TERMS (Continue on reverse if necessary and identify by block number)
FIELD	GROUP	SUB-GROUP	Satellite Charging, Satellite Charge Control, Differential Charging, Lithium Ion Source, Potassium Ion Source

19 ABSTRACT (Continue on reverse if necessary and identify by block number)

This thesis describes the design of a new spacecraft charge control device that incorporates a solid ion source made of Lithium or Potassium salt impregnated into a porous tungsten plug. The ion source was configured with a reentrant thin-wall heat shield to reduce heat loss and an experimental thermocouple imbedded in the plug to accurately measure emission temperature. The initial design of the charge control device included an extraction grid, deceleration grid, and an electron filament source. Experiments were conducted on the charge control device and results were used to modify the design for optimization of current out of the device versus power used. Incremental testing and modifications resulted in the deceleration grid being removed and the extraction plate's wire mesh being removed to allow a clear path for the ions. With these changes the requirement of 10 microamps was achieved at 13 watts with the Potassium ion source.

20 DISTRIBUTION / AVAILABILITY OF ABSTRACT ☒ UNCLASSIFIED/UNLIMITED ☐ SAME AS RPT ☐ DTIC USERS	21 ABSTRACT SECURITY CLASSIFICATION Unclassified
22a NAME OF RESPONSIBLE INDIVIDUAL Richard C. Olsen	22b TELEPHONE (Include Area Code) (408)646-2019 22c OFFICE SYMBOL PH/Os

DD Form 1473, JUN 86 *Previous editions are obsolete.* SECURITY CLASSIFICATION OF THIS PAGE

S/N 0102-LF-014-6603

Approved for public release; distribution is unlimited.

Design and Evaluation of Ion Source for Satellite Charge Control

by

Michael Edward Melvin
Lieutenant Commander, United States Navy
B.S., University of Colorado, 1979

Submitted in partial fulfillment of the
requirements for the degree of

MASTER OF SCIENCE IN PHYSICS

from the

NAVAL POSTGRADUATE SCHOOL
June 1992

K. E. Woehler, Chairman,
Department of Physics

ABSTRACT

This thesis describes the design of a new spacecraft charge control device that incorporates a solid ion source made of Lithium or Potassium salt impregnated into a porous tungsten plug. The ion source was configured with a reentrant thin-wall heat shield to reduce heat loss and an experimental thermocouple imbedded in the plug to accurately measure emission temperature. The initial design of the charge control device included an extraction grid, deceleration grid, and an electron filament source. Experiments were conducted on the charge control device and results were used to modify the design for optimization of current out of the device versus power used. Incremental testing and subsequent modifications resulted in the deceleration grid being removed and the extraction plate's wire mesh being removed to allow a clear path for the ions. With these changes the requirement of 10 microamps was achieved at 13 watts with the Potassium ion source.

TABLE OF CONTENTS

LIST OF FIGURES

I. INTRODUCTION

Spacecraft charging is a natural result of the interaction of a satellite with charged particles and high energy photons in the space environment. Numerous natural and man-made sources contribute to the charging phenomena but it is primarily determined by the collection of ambient ions and electrons and the emission of photoelectrons and secondary electrons from the satellite surface. Typical values for spacecraft potential relative to the ambient plasma can exceed -1 kV in sunlight and potentials as high as -19 kV have been recorded on the ATS-6 spacecraft in eclipse (Olsen, 1987). In the absence of measures to control the charge accumulation, the subsequent discharges have caused anomalous satellite behavior including problems with telemetry, spurious electronic commands, damage to satellite surfaces, and even satellite failure (Nanevicz and Adams, 1980). Additionally on spacecraft designed for experimental work the buildup of charge can impact dramatically on results and even limit the types and degree of experiments.

Control of large negative potentials has been partially achieved onboard satellites by emitting electrons which drives the spacecraft potential to zero. The same result is accomplished for positively charged satellites with the use of an ion source. However, since most satellites are not made of uniform material, a differential charge forms across these materials of different conductive properties. If an electron source is used to discharge a negatively charged satellite the charge on insulated sections of the satellite will not be modified by the electron source and the difference in charge between the sections of the

satellite will grow. At some point this differential charge will cause an arc or discharge which has been found to correlate with observed anomalies. (Olsen, 1985)

It has been found that discharging both electrons and ions together will control the spacecraft potential and at the same time reduce differential charging between the sections of the satellite. Present methods to create a neutral plasma emission incorporate a heavy and bulky gas discharge system. A simpler and smaller ion and electron charge control device is desired that uses a solid ion emitter rather than gas or liquid.

The purpose of the research described in this thesis was to design a charge control device that incorporates improvements over the gas discharge system presently used. Once designed the charge control device was tested in a vacuum chamber for the optimum modifications that would maximize the current out of the charge control device at the lowest power. The results found at each step of the experiment were then used to steer the design process towards better designs and further testing. The results of the experiments are presented and discussed and recommendations for further improvements are given.

II. SPACECRAFT CHARGING

Early rockets and satellites launched into low earth orbit experienced a low energy plasma environment. Basic (Langmuir) probe theory indicated the ambient plasma currents would be dominated by electron current which would build the spacecraft potential up to ~ -1.0 V. As later satellites probed into higher energy plasma at higher altitudes it was predicted that spacecraft potentials would reach higher values. (Grard, 1983)

Subsequent test flights confirmed this hypothesis and additionally demonstrated that large potentials were most frequently observed on the night-side in geosynchronous orbit. Low earth orbit satellites were charged to a negative potential on the order of -1 V with respect to the environment, while large electrostatic potentials of the order of tens of kV have been measured on geosynchronous spacecraft in the earth's magnetosphere. (Whipple, 1981)

A. ANOMALIES

As satellite flights have become commonplace a pattern of anomalous behavior onboard the spacecraft has been observed. Satellite anomalies are defined as any behavior that is unordered or unexplained that directly affects the satellite, its control, or experimental measurements. Anomalies can include unordered commands to satellite components, disruption of electronic equipment, loss of data, and numerous other unwanted behavior.

This anomalous behavior is distracting at best but can be very serious to the operation and success of a satellite. Table 1 lists a summary of some known anomalies for a few satellites. Because of the potential for failure of a satellite or

loss of control, the cause of anomalies and their elimination or control has been of interest to the space community for years.

Numerous studies of anomalous behavior of satellites have correlated the unwanted action with a buildup of charge on the satellite (Whipple, 1981). Almost all satellites have been affected by this behavior at some time with a correlation observed between the anomaly and where the satellite is in local time. A compilation of data from several geosynchronous satellites collected in Figure 1 shows a concentration of anomalous behavior in the 2000 to 1000 local time frame. This is also the time frame of significant charging for geosynchronous satellites. Figure 1 indicates that anomalies are more prominent during the night side orbit or soon after entering sunlight. Data suggests that sudden changes in the electrical environment of the spacecraft may trigger a discharge. In fact, the movement of the satellite from night to day during its orbit provides a change in environment that makes charging and subsequent discharge possible.

B. Charge Development

Typical values of geosynchronous satellite potentials range from -1 to -20 kV in eclipse, and ~0 to -1 kV in sunlight. This potential that develops between a satellite and its space environment is a result of the charging currents which must balance. Important contributors of the charging equation are photoemission, plasma bombardment, secondary electron emission, backscattering electrons, and other charging mechanisms.

1. Charging equation

Many charge and current sources contribute to the satellite overall buildup of charge and eventual balance of currents. The satellite's potential is governed by the charging equation

$$I_{tot} = I_e + I_i + I_{se} + I_{si} + I_{bsce} + I_{hv} + I_{exp} + I_{oth} \qquad (1)$$

where

I_e = ambient electron current

I_i = ambient ion current

I_{se} = secondary electron current

I_{si} = secondary ion current

I_{bsce} = backscattered electron current

I_{hv} = photoemission current

I_{exp} = active current sources such as electron or ion beam experiments

I_{oth} = other current source.

At equilibrium ($\frac{dV}{dt} = 0$), the total current (I_{tot}) is zero.

The most important factors are the net flux of ambient plasma current, the secondary emission of electrons, and photoelectric emission due to sunlight. Additional currents include backscattered electron fluxes associated with impacting electrons and ions. More subtle sources consist of current generated by the movement of the satellite across an ambient magnetic field and by high energy (> 10 keV) electrons which deposit charge inside insulating surfaces. Finally any onboard components such as ion thrusters or induced current flows to exposed satellite surfaces with high potentials also contribute (Garrett, 1980).

The rate of charge transfer, positive or negative, is dependent on the characteristics of the satellite and the operating environment (Whipple, 1981). Specifically, it depends on charge already residing on the vehicle, the motion of the satellite, the design of the satellite, and by local magnetic and electric fields.

2. Charging Currents

In general the equilibrium charge will not be zero. Where photoemission plays no role, such as in eclipse, the equilibrium charge will be negative because of the higher flux of electrons to an uncharged surface compared to ions. In regions where photoemission is the dominant process, the equilibrium charge will be positive. (Whipple, 1981)

The major natural sources of high voltage potentials are discussed next: ambient space plasma interaction with the satellite, secondary electron emission, and photoelectric emission.

a) Ambient Plasma Currents

One of the underlying principles of a plasma is the assumption of "quasi-neutrality". This charge neutrality requires that, on average, electron and ion densities are generally equal. However, assuming the simplest case of equal temperature, the ion and electron velocities are then quite different. Given equal temperature, the ion and electron thermal energies are equal and given by equations (2) and (3)

$$E_{th} = \tfrac{1}{2}KT \qquad (2)$$

$$= \tfrac{1}{2}m_p v_p^2 = \tfrac{1}{2}m_e v_e^2 \qquad (3)$$

therefore

$$\frac{v_e}{v_p} = \sqrt{\frac{m_e}{m_p}} = 43 \qquad (4)$$

assuming an H^+ plasma. Then with equal charge and density for both ions and electrons the higher electron velocity term changes the current density equation

$$J = qnv \qquad (5)$$

for electrons. Therefore the current density for electrons is about 43 times higher than for ions which causes a net negative charge buildup on the satellite. This negative potential increases on the satellite surface until the repulsive force on the incoming electrons produced by the electrons residing on the satellite's surface reduces the electron flux to a balance with the ion flux as shown in Figure 2(a).

In the plasma sheet, the hotter plasma distributions are found in the midnight to dawn region (DeForest and McIlwain, 1971). As the plasma temperature increases the velocity and current density also increase. Additionally, the degree to which ambient plasma bombardment affects the satellite potential is also determined by the design and structure of the individual satellite.

b) Photoelectric Effect

Photoemission is an important source of current for satellites. At geosynchronous orbit photoemission is the major current from the spacecraft (Grard, *et al*, 1983). Indeed, at plasma densities below ~1000 e^-/cm^3, photoemission current will dominate (outside L~2) (Olsen, 1989). In the absence of differential charging the spacecraft surface develops a positive charge as photons (mostly due to H Lyman-alpha) of sufficient energy strike the satellite's surface material and knock electrons free as shown in Figure 2(b). The actual buildup of positive charge is influenced by the ability of the photoemission induced current of 10-100 microamps/m^2 to leave the satellite. This can be

affected by the design of the satellite and the formation of potential barriers near the satellite surface.

c) Secondary Electron Emission

Secondary emission of electrons is an important charging concern in the magnetosphere. The impact of ambient plasma on a negatively charged spacecraft produces secondary electron emission. When a particle hits the spacecraft it loses energy and a portion of this energy can be used to "excite" other electrons which may then escape the spacecraft at an energy of about 1 - 2 eV. This process can cause a spacecraft to charge positively in eclipse in spite of the supposed dominance of the ambient electron currents.

The actual number of electrons that are emitted by the impact is a function of the incident electron's energy, the angle of incidence, and the spacecraft material's emission characteristics (Garrett, 1980). The yield is typically greater than one for incident electron energies of 10 - 1000 eV, and less than one at higher energies. The ratio of secondary emission current to ambient plasma current can be related to the plasma temperature. For distributions with average energies of less than a few keV, secondary electrons will exceed the ambient electrons resulting in net positive current. For temperatures above ~5 keV, the ambient electrons dominate though ~90% of the incident current is compensated for by the secondary emission. In the magnetosphere the incident ion flux is considerably less than the electron flux and therefore less important.

In the absence of photoemission, equation (5) then becomes

$$J = qn\sqrt{\frac{KT_e}{m_e}} \qquad (6)$$

and for an electron energy of $KT_e = 10^4$ eV and a density of $n=10^6/m^3$, equation (6) yields a current density of ~7 microamps/m^2.

The nature of the various current flows to and from the satellite is shown in Figure 3. In actual practice, the current flow is less than straightforward as many factors affect the actual flow of electrons and ions. Barriers can be created which cause a satellite to charge negatively when simple current considerations indicate it should buildup positive charge.

3. Differential Charging

For a high altitude satellite with purely conductive surfaces in sunlight, photoemission is the dominant current. As shown in Figure 4(a) the plasma ion and electron currents are incident on both the shadowed and illuminated surfaces. On the sunlit side photoemission is added to the current balance. As the current due to photoemission exceeds the difference between the ambient electron and ion currents the satellite charges to a positive potential until equilibrium is reached.

In practice most satellites are not built with purely conductive surfaces but consist of sections made of different materials (probes, solar panels). With this mosaic of insulating and conducting surfaces the current flow is unevenly distributed over the sunlit and the dark sides of the vehicle causing differential charging. Even spin-stabilized satellites have permanently shadowed areas that can charge differentially.

When a satellite is configured with conductive and insulating surfaces the charging problem becomes quite complicated. As can be seen in Figure 4(b) the charging equation on the sunlit side of the satellite is unchanged from before. However on the shadow side of the satellite, unlike before, the incident plasma

electron current is unable to conduct across to the sunlit side and be balanced by the photoemission current. The satellite surface will charge to a highly negative potential on the dark side. Solutions of Laplace's equations show a potential barrier must form adjacent to the sunlit side. An example of this potential barrier is seen in Figure 5 in which a computer model was used to calculate the effect of photoemission on a simulated spherical satellite experiencing differential charging. The sunlit side is the left side of the satellite which is at -1 kV with the rest of the satellite at -5 kV. The effect of this potential barrier is such that photoelectrons are not allowed to escape from the sunlit side and subsequently the whole spacecraft will charge negatively, in spite of the nominally large photocurrent.(Grard, *et al*, 1983)

C. Results of Charging

The build-up of charge on a satellite is a benign event in the absence of a discharge. The charge by itself has little effect on a satellite except for experimental satellites attempting to conduct low energy particle measurements. However, as the potential difference between parts of a satellite exceed a breakdown threshold ,a discharge or arcing will occur across these components.

Typically potential differences on the order of 500 V are needed to produce discharges that are significant to an operating system (JPL Report, 1989). It is this voltage differential and subsequent discharge that causes anomalous behavior on satellites. All discharges don't always cause anomalies. However, even a weak discharge can cause

- spurious electronic switch activity of components
- breakdown of vehicle thermal coating

- amplifier and solar cell degradation
- optical sensor degradation
- unplanned orbital maneuvers
- unplanned downlinking of telemetry

1. Timing of discharges by location

Different satellites will charge to different potential levels in the same environment depending on their surface materials, size, shape, and orientation to the sun (Gussenhoven and Mullen, 1983). Also, satellites will charge to different levels as magnetic activity varies.

During magnetic substorms, the removal and reinstatement of the photoelectric current caused by eclipse passage is observed to result in dramatic shifts in satellite potential (Purvis, *et al*, 1983). At geosynchronous altitude the electron temperature can reach 10^4 eV and as the spacecraft traverses out of sunlight the vehicle charges up to a negative potential roughly equal to the electron temperature, (KT/e) = 10 kV.

The dynamics of discharge have been observed to correlate with the build-up of spacecraft potential. As was seen in Figure 1 the timing of the discharge is also dependent on orbit location. During normal magnetic activity, discharge is more common between 0400 and 0600 local. This may be due to the quiet time injection events and the preferred drift for injected electrons (East). Early evening yields the minimum probability of a discharge event. (Deforest, 1972)

III. SPACECRAFT CHARGING CONTROL

The stimulus for investigating methods for changing and eventually controlling spacecraft potentials was the interfering effect of the satellite charge on low-energy particle and electric field experiments (Whipple, 1981). The concern related to the ability to use electron beams for experimental purposes. Ejection of an electron beam drives the spacecraft to a positive potential and thereby reduces the energy of the beam and can prevent the further escape of the electrons. As the problem of satellite discharges have become better understood the control of spacecraft charging was deemed important to control the occurrence of satellite anomalies associated with charging.

Spacecraft charging control is accomplished in two basic ways: 1) with passive techniques which involve the design of the satellite's materials and configuration, and 2) active techniques which involve the use of charged particle emitters to vary the charge of the spacecraft and its distribution on the spacecraft (Whipple, 1981).

A. PASSIVE CONTROL

The simplest method to control spacecraft charging is to employ proper design techniques that modify the characteristics of the charging equation term that is causing the charging. In addition, the judicial use of conducting surfaces wherever possible and proper grounding techniques will significantly reduce differential charging.

In practice complete elimination of insulators is practically impossible as any satellite requires certain isolated elements from the satellite ground such as

antennas, particle collectors, and solar arrays. Therefore the designer should carefully select satellite materials that have high secondary and photo-emission properties to reduce negative charging. Additionally the design should avoid cavities that contribute to shadows that accentuate differential charging. Further actions that have been tried is the coating of insulators with a conductive coating to provide a conduction path across the entire satellite. When nonconducting surfaces (solar panels) used on the GEOS series of geosynchronous satellites were coated with conducting indium oxide the satellite potential was successfully reduced. Unfortunately the procedure was quite expensive (Grard, *et al,* 1983). However, not all negative charging was eliminated requiring some form of active charge control on some satellites using conductive coatings.

To assist the satellite designer and experimenter, NASA has developed a computer program, the NASA Charging Analyzer Program (NASCAP), to evaluate a design for possible charging sites.

B. Active Control

Another method to modify and control spacecraft potential is to configure the spacecraft with a plasma source that artificially enhances ambient fluxes or creates new currents in the equilibrium charging balance. Utilizing a source emitting a neutral cloud of electrons and ions will effectively increase the charge density around the satellite and equalize the currents to the satellite body and surfaces.

1. Electron Emission

It has been suggested that the large variations in satellite potentials during eclipse passage could be eliminated by finding a suitable replacement for the photoelectron current. The operation of an electron source emitting a beam

of electrons would be an effective balance to the charging equation for the loss of the photoemission current. Though it may seem that adding an electron emitter would produce a current that would effectively reduce large negative potentials the resulting effect could be undesirable. In a hot plasma, the spacecraft's conducting and insulating surfaces will charge to a negative potential. The emission of electrons from the spacecraft frame can create large differential charging between the insulators which are at the unchanged plasma ground and the conducting surfaces at the new elevated spacecraft potential (Davis and Katz, 1989). This sudden increase of differential charging can accelerate or accentuate hazardous arcs.

As was seen previously with photoemission on a satellite experiencing differential charging, Figure 5 illustrates the same result of a potential barrier caused by the emission of electrons. The figure is a simulated spherical satellite with most surfaces at -5 kV. The NASCAP program was used to model an electron emitter on one side of the satellite driving the conducting surface to -1 kV. The potential barrier or saddle point in front of the conducting surface prevents electrons from leaving the satellite.

2. Ion Emission

Ion emission can be used to reduce positive potentials, or induce a negative charge on a satellite (Werner, 1988). In periods when the satellite is charged positively an ion emitter would be a useful method to reduce the satellite potential back to zero. For a low energy ion source, an additional effect would be a return flux of ions to the spacecraft to discharge the insulators which have charged differentially.

3. Neutral Plasma Emission

Neutral plasma sources provide the necessary currents to control and vary the satellite frame potential. While electron emission reduced potential on the ATS-5 satellite from several thousand to several hundred volts negative, the plasma sources on ATS-6 maintained the satellite at a near zero potential for all observed plasma conditions, both in sunlight and eclipse. (Purvis and Bartlett, 1980)

Experiments and spacecraft data show that a plasma source designed to control spacecraft charging must provide a sufficient current of thermal ions to hold the insulated surfaces at spacecraft ground and a sufficient current of thermal electrons to vary the spacecraft potential. The combination of electrons and ions being discharged by the satellite is shown in Figure 6. The addition of low energy ions that return to the satellite to discharge the insulated surfaces is paramount to effective control of satellite potentials. Modeling shows that electron currents of about 10 microamps should be sufficient to control the spacecraft potential (effectively replacing photoemission), with similar levels of ion current required to discharge the insulators. The control of spacecraft potential and the most optimum discharging of insulators is accomplished by biasing the plasma source relative to the spacecraft potential. (Olsen, 1981)

Additional research is needed to optimize the ion source with the goal of reducing power requirements, weight of the fuel and possible contamination of the spacecraft by the emitted material. A further step would be to devise a method to continuously emit an appropriate current to control satellite potential at all times (Purvis and Bartlett, 1980).

C. Results From Satellites and Rockets

Spacecraft charging affects most satellites but is most readily observed by plasma detectors such as those flown on the experimental satellites ATS-5, ATS-6, SCATHA, and ISEE. These satellites carried special instrumentation to measure spacecraft potential and the ATS, ISEE, and SCATHA satellites were additionally configured with onboard experiments that influenced this potential.

Experimentation on the relationship between charging and active plasma emission has been conducted since 1969 using sounding rockets and experimental satellites. Early work on beam experiments was done by Hess, et al while creating artificial auroras with an electron accelerator flown on a sounding rocket (Hess, *et al*, 1971). Additional work with poorly reported data are the ARAKS , a French and Russian project, and the EXCEDE rockets sponsored by the Air Force. The best documentation of active plasma emission effects on satellites was collected on the ECHO, PORCUPINE, and ARCS rockets, ATS and the SCATHA satellites.

1. Space Electric Rocket Test (SERT)

SERT 1 was a rocket-borne flight test of a mercury ion thruster to demonstrate thrust and beam neutralization. SERT 2 was a satellite flight test of the ion engine at low altitude orbit with limited instrumentation. The thruster successfully emitted a beam of ions that escaped from the spacecraft. The plasma bridge neutralizer neutralized the beam and demonstrated that it was able to vary the spacecraft potential by varying the neutralizer's potential relative to the spacecraft. (Olsen, 1980)

2. ECHO

Winkler conducted an extensive sounding rocket program in electron beam emission. This included an effort to study the charging problem on a sounding rocket. He found that the rocket does not charge to the voltage of the emitted beam in general but rather draws a substantial return current from the space plasma or locally generated plasma (Winkler, 1980).

3. Porcupine

The PORCUPINE project, comprised of two rockets launched in 1979, was conducted by researchers from Germany, France, the Soviet Union, and the United States. Two rockets were launched with multiple payloads of which one was configured with a 200 eV Xenon ion beam emitter capable of producing an approximate 4 amp beam. Detectors on the other sub-payloads determined that the beam carried a current across magnetic field lines after it propagated at least several meters from the source and a return current from the plasma was generated outside the beam. (Pollock, 1987)

4. Auroral Rocket for Controlled Release (ARCS)

The ARCS 1 rocket was launched in 1980 with a single Ar^+ ion gun capable of producing a 100 mA beam. At the initiation of the ion beam, evidence of transient payload charging was observed from a -1 V pre-experiment level to a level of approximately -5 V. (Pollock, 1987)

The ARCS 2 rocket was launched in November 1982 and differed from ARCS 1 in that it carried two ion beam generators on a separable payload from the diagnostic payload. Little information is available of the effects of the He^+ and Ar^+ ion beam on the spacecraft potential.

The ARCS 3 rocket, flown in February 1985, was a reflight of the ARCS 2 payload with some modification including both ion generators changed to only Ar^+ emission. Data collected during the numerous experiments indicate that the sub-payload was charged to at least 3 V negative during operation of the ion generator aimed perpendicular to the magnetic field.

5. Applied Technology Satellite (ATS)

a) ATS-4

The ATS-4 satellite was launched August 1968 but only entered into a low altitude orbit due to launch vehicle failure. The satellite carried a Cs^+ ion thruster which operated successfully. During beam operation the escaping current of 100-400 microamps nearly balanced the photoelectric and ambient plasma bombardment current leaving the spacecraft during sunlight. During eclipse the neutralizer emission current did not balance the charging equation and drove the spacecraft to a 100 V negative potential. (Hunter, *et al*, 1969)

b) ATS-5

The Applied Technology Satellite (ATS-5) was launched in August 1969 into a geosynchronous orbit. The satellite was cylindrical with solar arrays covering most of the exterior except for a bellyband containing instrumentation. Located at the endpoints were cavities containing a mixture of conducting and insulating surfaces. The satellite carried experimental cesium ion thrusters onboard with a separate electron beam filament for neutralizing the ion beam. The filament neutralizers on the ion engines were designed to emit thermal electrons in an attempt to discharge the -1 to -10 kV potential of the satellite during eclipse. The operation of the electron emitter did reduce the large

negative potentials but was unable to eliminate the spacecraft charge completely (Whipple, 1981).

Olsen showed that because of differential potentials on the order of 100 V, less than 1% of the emitted electron current escaped the spacecraft. The differential charging was sufficient to explain the equilibrium potentials seen and was evidence of the effect differential charging would have on spacecraft configured with insulators. (Olsen, 1985)

c) ATS-6

The ATS-6 satellite was launched to a geosynchronous orbit in May 1974. It was designed to carry two ion thruster engines to test their usefulness for station keeping. A hollow cathode plasma bridge neutralizer was incorporated to provide charge and current balance for the main ion beam. Particle data from ATS-6 showed that the satellite charged in eclipse up to the largest recorded potential to date, -19 kV, when the plasma sources were off (Olsen, 1987).

Considerable data was also obtained on the use of ion emission and electron emission on both spacecraft potential and differential charging. The operation of the ion thruster and plasma neutralizer in various environments had major effects on the spacecraft potential with respect to ambient plasma and on surface differential charging. The large spacecraft potential was reduced by operation of either the ion engines or the neutralizer. Differential charging was eliminated by operation of the ion engine and reduced by operation of the neutralizer when operated in ion mode. These tests carried out on ATS-6 showed that neutral plasma emission could be used to control spacecraft

charging and did not create surface differential charging as electron emission does.(Olsen, 1985)

6. Spacecraft Charging at High Altitude (SCATHA)

The SCATHA satellite was launched in 1979 to conduct a complete study of satellite charging effects at near-geosynchronous altitudes and test charge control procedures. The satellite carried thirteen experimental packages including a mixture of particle detectors and both electric field and magnetic field detectors. Additionally a Xe^+ ion gun capable of 1 - 2 keV emission and an electron gun capable of 50 eV to 3 keV were configured for active charge control experiments.

Review of SCATHA data indicates a clear linkage between satellite charging, discharge, and anomalous behavior (Koons, *et al*, 1988). In experiments with the electron gun, results similar to ATS-5 were observed when the electron emission discharged the satellite until a limiting point was reached caused by differential charging. The ion gun was very effective in controlling a differentially charged satellite when using a neutralized ion beam (Olsen, *et al*, 1988). Results from the SCATHA experiments indicate that not only was it possible to reduce large negative potentials but it was possible to charge the satellite to either negative or positive potentials by the appropriate combination of ion and electron beam currents (Whipple, 1981).

a) GEOS and ISEE series satellites

Both the GEOS and ISEE series satellites were launched in the late 1970's and were different than the ATS and SCATHA satellites in that they were specifically designed to avoid the problem of differential charging. Their surfaces

were made entirely of, or covered in conducting material such as indium oxide to better facilitate the study of magnetospheric plasmas (Norwood *et al*, 1988).

Accordingly, almost no differential charging was experienced and the spacecraft kept a positive potential in sunlight. The exception occurred when the spacecraft entered a relatively cold and dense electron environment where small negative potentials were observed (Grard, 1983).

IV. THEORY

Active control of spacecraft charging relies on the emission of plasma containing electrons and ions. The principle of thermionic emission has been known for many years and is the basis for any active emitter design that will deliver the required current for discharging spacecraft potentials. Ion emission, in particular, can be accomplished by numerous methods of which only a few meet the requirements of charge control. This technique of ion emission can be accomplished in various ways with two of these methods, gas discharge and surface ionization, discussed further.

A. ION EMISSION

1. Gas Discharge

Gas discharge systems have been shown to have several excellent tendencies for ion emission. The system is capable of long life and produces high ion densities by an electrical discharge through a gas vapor. Ion currents of 1 to 10 mA are easily obtained when a voltage is applied between the heated cathode and the anode (Moore, et al, 1983).

The gas discharge, or hollow cathode emitter, was used for the ion engine onboard the ATS-6 satellite and is shown schematically in Figure 7. The liquid Cs is heated and vaporized in both the cathode and anode tubes. The cathode tube is further heated and a potential is applied across the cathode and anode which causes an arc. After the arc is struck, the discharge is maintained by passing a current through the ionized gas. The stream of Cs^+ vapor is then

accelerated out of the discharge chamber by the accelerating grids. (Moore, 1983)

A similar hollow cathode system was used onboard the SCATHA satellite for experimental purposes and is illustrated in Figure 8. Designed to emit Xenon propellent at nominal currents of 0.3, 1.0 and 2.0 mA it is based on the same technology as the ATS-6 ion engine. (Werner, 1988)

Though the hollow cathode system has excellent properties for producing ion streams it has some severe drawbacks when it is considered for satellite charge control. Even though the hollow cathode emits relatively high ion currents it requires a high level of power, up to 20 watts, to achieve this steady output. Additionally the entire hollow cathode system is heavy and voluminous and as the liquid or gas bottles are discharged the satellite could experience problems with weight balance and stability, especially for a spin-stabilized satellite. Finally due to the arcing required for ionization the satellite can experience electromagnetic interference which can adversely affect the operation of some science instruments.

2. Surface Ionization

The technique for production of ions used here is based on the theory that when an impure material is placed on a heated filament, positive ions will evaporate (Cobine, 1958). Additionally, when the filament is heated in the presence of a vapor whose ions can escape from the metal of the filament a copious amount of ions are produced.

In a study of thermionic emission of positive ions Blewett and Jones observed that Lithium with a Beta-Eucryptite coating gave roughly twice the emission as the next best mixture (Blewett and Jones, 1936). It has been shown

that current densities of 1 to 5 mA per square centimeter of coated filament surface can be drawn continuously (Johnson, 1962).

Numerous designs have been employed utilizing this concept but the compact Lithium emitter described by Heinz and Reaves for low energy experiments is most useful for the design of a low energy spacecraft charge control device (Heinz and Reaves, 1968). This emitter is commercially produced by Spectra-Mat, Inc and is shown in Figure 9. It is further described in Spectra-Mat documents as:

> The emitter consists of an indirectly heated, highly porous, tungsten plug into which the emitter material has been fused. The molybdenum body holding the tungsten plug is machined with a solid partition for complete isolation between the emitter and the heater cavity. The three rhenium support struts are brazed at a 120° spacing with a moly/ruthenium eutectic at 2100°C in hydrogen, yielding a ductile and versatile mounting tripod. The heater is a noninductive wound bifilar coil with heliarc welded rhenium leads solidly potted into the body cavity. The high purity Al_2O_3 potting mix is H_2 fired at 1900(°C) which completely immobilizes the heater. The emitter matrix, a specially prepared, extremely porous, tungsten disc with a density of 30% (70% porosity) is heliarc welded to the moly body. (Spectra-Mat,Inc, 1980)

When this emitter is sufficiently heated in the presence of an electric field, the negative potential helps ions overcome the surface vapor pressure of the emitter and accelerates them outward. The observed total emission current versus filament power for a 0.6 inch diameter source is shown in Figure 10.

B. ELECTRON EMISSION

Electrons are emitted by surfaces at high temperature in a process called thermionic emission. Depending on the material properties and the temperature of the surface the electrons are emitted as a result of electron bombardment, ion bombardment, electric fields, chemical effects, or photoemission (Cobine, 1958).

It has been found that electropositive metals such as thorium emit much larger electron current than metals with larger work functions. Therefore a heated filament of thorium in the presence of a very high electric field is very effective at producing large electron currents in the mA range. Since tungsten is a stronger material than thorium a practical method of fabricating an electron source is to mix tungsten and thorium together to form a filament.

V. Design of the Device

Active spacecraft charge control has been experimentally tested by the use of ion engines and neutralizers onboard satellites and sounding rockets. To date an operational active charge control device has not been flown though they are being built for the upcoming NASA/POLAR and ESA/Cluster mission. The NASA design is an extension of the successful ion engine results from the ATS-6 and SCATHA satellites. However, the hollow cathode technology used to date has limitations and improvement in its parameters would provide a more effective and feasible charge control device.

A. Ion Source

The ion source of the active charge control device was the principal design challenge with the other components designed around it. The ion source has certain design requirements and other properties that are desirable. The ion source must emit a minimum of about 10 microamps at no greater than 20 watts power. Any improvement of these parameters, higher current or lower power, is highly desired. Additionally the emitter should have a long operational life to provide control for the entire life of the satellite.

As discussed previously, the hollow cathode system achieves these requirements but at a cost of weight, volume, and power. A different ion source that incorporates the output of the hollow cathode but with lower requirements was desired. The basic ion source described by Heinz and Reaves and commercially produced by Spectra-Mat, Inc was chosen. It is a 1/4" diameter Lithium or Potassium impregnated tungsten plug and a slight variation of the

surface ionization emitter previously discussed and shown in Figure 9. Note that the emitter to be used is 1/2 the size shown.

This ion source has been investigated in depth by Gant (1991) for current and lifetime parameters for different impregnate material; Lithium, Cesium, and Potassium. His results indicate that either Lithium or Potassium hold promise for our purpose of achieving high current output at low power input. The 1/4" Li emitter tested by Gant produced currents of 10 microamps at 27 watts and achieved a lifetime of 93 hours. The K emitter produced currents of 10 microamps at 15 watts and achieved a lifetime of 44 hours. (Gant, 1991)

In the design of an active charge control device each component; the ion source, ion extraction system, and electron source must be optimized to provide the required plasma at the least power. The basic layout of the components is shown in Figure 11. Disregarding the electrical connections for now the design uses the ion source (b) as the foundation of the charge control device with the extraction grid (c) mounted above it and the deceleration grid (d) mounted in-line with the emitter and extraction grid. The electron source (e) is the final component of the charge control device and is mounted above the grid and emitter system so as not to interfere with them.

Using this basic concept a flight prototype was designed and is shown in the engineering drawing in Figure 12. This is a side view of the charge control device and includes 3 extra copper plates at the base to assist in the connection of the various electrical leads. The actual charge control device measured 1.6 inches in diameter and 2 inches tall and is shown at 3 different angles of view in Figures 13 through 15. Additionally an experimental thermocouple was imbedded in the heater potting for accurate temperature measurements.

In an attempt to reduce power requirements a new method of placing a reentrant thin-wall heat shield around the ion source to reduce heat loss was attempted. The emitter surface is in the same plane as the plate of the heat shield to prevent space charge effects from the heat shield itself. The ion source is designed with 4 leads, 2 for power leads to the moly bifilar heater and 2 other leads for the thermocouple imbedded in the heater potting. The ion source, heat shield, and support plate are welded together and must be replaced as a single unit. They are situated in the charge control device as the fourth plate from the base plate as shown in Figures 12 through 15.

B. Extraction Grids

The extraction grids provide for acceleration and deceleration of the ions once they are emitted. Each grid is electrically isolated and its potential can be independently varied to provide for optimum extraction and then deceleration to the required ion energy level. The deceleration grid is added to test the effectiveness of slowing the ions down to lower energy levels.

The design of the grid's apperture, wire mesh and spacing was a result of reviewing previous experiments with extraction grids (Rovang and Wilbur, 1982), (Homa and Wilbur, 1982), and (Haskell, *et al,* 1966) and from additional work done (Appendix C) with the experimental setup that was used by Gant. The spacing of the grids between each other and to the ion emitter will influence the electric field needed to extract ions and the transparency of the grid will determine the current through the grids and out to the plasma.

Both of the grids are similar and situated exactly in-line with each other as can be seen in Figures 12 through 15 as the top 2 plates of the charge control device. The grids are manufactured from molybdenum with HT moly wire

interspersed at 0.078 inches in the 1/4" inch diameter center hole. Spacing between the acceleration and deceleration grids and between the acceleration grid and the ion emitter can be varied by using various combinations of ceramic spacers.

C. Electron Source

The electron source is an integral part of the spacecraft charge control device and provides for a neutral plasma discharge from the spacecraft. A 0.010 inch diameter thoriated (1.5%) tungsten wire is used for this purpose. The filament was further treated with a mixture of barium carbonate from RCA to test its emission properties. The electron source design has 2 filaments that can be interchanged if 1 filament was to burn out. The filaments are positioned at the top of the charge control device and above both extraction and deceleration grids. During operation the high energy electrons will boil off and discharge to the space plasma to assist in discharging the spacecraft frame.

VI. EXPERIMENT

The spacecraft charge control device was tested in a simulated space environment with different modifications to determine the optimum design. Space was simulated by a vacuum chamber with a copper mesh screen and collection plate biased by a variable power supply. The experimental setup is completed by various power supplies, potential and current measuring equipment, and an optical pyrometer to accurately measure emitter temperature.

A. VACUUM CHAMBER

The vacuum system used to simulate the space environment consists of a large (22" tall by 18" diameter) cylindrical glass bell jar with electrical connections through vacuum feedthroughs on the bottom base-plate and the glass top plate. The chamber was maintained at an experimental vacuum of 10^{-7} torr by a combination of turbo and mechanical pumps. The spacecraft charge control device was mounted horizontally in the bell jar facing the cylindrical wall. In addition to the charge control device the experimental setup consisted of a copper wire mesh screen wrapped around the internal sidewalls of the chamber and isolated from all other components. Additionally a 4 by 6 inch copper plate was connected to a BNC feedthrough at the top of the chamber and positioned 10 inches in front of the emitter face on the charge control device and electrically isolated from all other components. The copper plate was added during the experiment to provide a clean surface for current collection.

B. Electrical Setup

On the spacecraft charge control device, the extraction and deceleration grids are electrically isolated from both the ion and electron emitters. Extra ceramic spacers allow the varying of grid spacing to the emitter to measure the effect of spacing on plasma emission.

A power supply is assigned to each emitter, both extraction and deceleration grids, and the copper mesh screen and collection plate. The electrical circuits are shown schematically in Figure 11. Components labeled (a) and (b) are the copper mesh screen and collection plate respectively and are used to simulate space and collect the emitted current. Components (c) through (g) make up the charge control device and are the electron emitter, deceleration grid, extraction grid, ion emitter, and the thermocouple respectively.

To ease power supply requirements all voltages are applied relative to ground. As verified previously, the same results could have been obtained by varying the emitter voltage relative to the extraction grid which would be at spacecraft ground on an actual spacecraft.

C. Experimental Procedure

Experimental measurements were made on various configurations of the spacecraft charge control device for both a Lithium and Potassium ion emitter. Changes were made to the initial design of the charge control device after experimental results indicated modifications might improve the operation of the charge control device. The initial design of the charge control device was operated at various configurations of power and biasing of the grids. Only pertinent data that indicated design modifications were warranted are presented. Additionally, since more Lithium ion sources were available than Potassium for

testing, the majority of early experiments were conducted with the Lithium ion source.

1. Initial Design

The initial design of the charge control device is as described previously and shown schematically in Figure 11 without any modifications except for the addition of a copper collection plate for some experiments. The extraction grid was spaced 0.10 inches from the ion emitter face and the deceleration grid was positioned another 0.05 inches from the extraction grid.

This design was operated with two different Lithium ion sources in the charge control device for comparison of the ion sources and verification of the design.

a) Power Sweep

After calibration of the thermocouple, using an optical pyrometer, a power and temperature sweep was conducted on the first Lithium ion source. The extraction grid was biased to -100 V, the deceleration grid was biased to -50 V, and the screen was biased to -100 V. In principle, this should give approximately <50 eV ions (emitted kinetic energy) leaving the deceleration grid and being attracted to a surface 50 V negative with respect to the deceleration grid. Figures 16 and 17 show the results of these sweeps. The current is measured from the extraction grid, the deceleration grid, and the screen. The total emitted current is also plotted for comparison. In Figures 16 and 17 it can be seen that the emitter produces a total current of 10 microamps at 1100 °C and 23 watts. However, the ion current that is emitted from the charge control device is only about 2 microamps.

A second Lithium source was installed into the charge control device after a full range of experiments was conducted on the first Lithium source and similar results were obtained. After the first series of experiments a 4 by 6 inch copper plate was positioned 10 inches in front of the charge control device emitter face to provide a clean collection point for current measurement. The extraction grid was biased to -150 V, the deceleration grid was biased to -100 V, the copper plate was biased to -150 V, and the screen was biased to -15 V.

A representative temperature and power sweep for this source is shown in Figures 18 and 19. This ion source emitted 10 microamps total current at 1050 °C and 24 watts. With this chamber configuration, however, the current out of the charge control device is the sum of the current to the plate and the screen and is approximately 6 microamps.

The first Lithium ion source was unable to achieve 10 microamps output current to the screen while the second Lithium ion source achieved 10 microamps out of the charge control device at 28 watts power. Unfortunately this power level is much too high.

b) Extraction Sweep

To measure the effect that the extraction grid potential had on emitted current the extraction grid was varied from 0 to -200 V and the current was measured. For the first Lithium ion source, the deceleration grid was biased to -100 V, the screen was biased to -100 V, and the ion source was heated to 1100 °C. This means there is no further acceleration of the ions leaving the deceleration grid with a nominal kinetic energy of 100 eV. As shown in Figure 20 the total current emitted rose exponentially until the extraction grid was -15 V and then steadily rose while the magnitude of the extraction voltage was

increased. The screen current stabilized at 3 microamps after the extraction voltage reached -8 V. The excess current was collected by the extraction grid on the charge control device.

With the second Lithium ion source the only difference in setup from the previous example was that the plate was biased to -150 V and the screen was biased to -15 V. As can be seen in Figure 21 the total current emitted again rose exponentially until extraction voltage was -40 V and then rose steadily as before. The majority of the excess current was collected on the extraction grid as the magnitude of the voltage was increased beyond 40 V. Higher extraction voltages significantly increase the total emitted current, but the current collected by the grids on the charge control device collect the majority of any marginal current increase.

c) Deceleration Sweep

The next series of experiments was meant to measure the influence of the deceleration grid. The deceleration grid was designed to manipulate the energy of the emitted ions leaving the charge control device.

The first Lithium ion source was setup for a sweep of deceleration grid voltage from 0 to -200 V with the extraction grid biased at -100 V, the screen biased to -150 V, and the source heated to a temperature of 1100 °C. Figure 22 shows that the deceleration voltage does not determine the total ion production of the source. As the deceleration grid voltage is decreased the current to the deceleration grid increases at practically the same level as the current to the extraction grid decreases. The current out of the charge control device is approximately 5 microamps for negative deceleration voltages, but for potentials

> -20 V little or no ion current leaves the source. This means that the ions must be emitted to the screen with at least 20 eV energy.

The second Lithium ion source was again configured similarly as the first source except that the plate was biased to -150 V and the screen was biased to -25 V. As shown in Figure 23 the same general pattern can be seen except the currents measured are significantly lower than with the first ion source. This experiment on the second Lithium source was one of the first experiments run on the ion source and the emitted current rose significantly after several experimental runs. This is not considered important for this comparison since the nature of the ratio of the currents was of interest and not the initial amplitude.

d) Plate Sweep

To measure the effect of source potential versus plasma potential a sweep of plate potential from 0 to -200 V was conducted on the 2 Lithium ion sources. The first Lithium was heated to 1100 °C with the copper collection plate installed and the extraction grid biased to -100 V, the deceleration grid biased to -50 V, and the screen biased to -50 V. Figure 24 shows the total emitted current was constant at 12 microamps while the plate current increased in step with a decrease in extraction grid and deceleration grid current as the plate voltage was driven more negative.

When a similar experiment was run on the second Lithium ion source at the same temperature with the extraction grid biased to -150 V, the deceleration grid biased to -100 V, and the screen biased to -15 V similar results were obtained as shown in Figure 25. Again total emitted current was constant with plate current increasing as plate voltage was decreased to -200 V.

e) Comparison of Deceleration Grid Voltages

To determine the effect of the deceleration grid potential on the extraction of ions a series of extraction grid sweeps of the 2 Lithium sources were conducted with different deceleration voltages applied. The first Lithium source was heated to 1100 °C with the screen biased at -100 V and the deceleration grid potential biased at -10, -50, and -100 V while the extraction grid was varied from 0 to -200 V. Figure 26 shows the comparison of these 3 sweeps. The total emitted current and the current leaving the charge control device increased as deceleration voltage and extraction voltage decreased. However the increase between -50 V and -100 V on the deceleration grid is very small.

The same setup was used with the 2 sweeps of the second Lithium source except that the plate was biased to -150 V and the screen was biased to -25 V. Again Figure 27 shows that the results are similar to the first Lithium ion source with total current emitted and the current leaving the charge control device (plate and screen current) both increasing as the extraction voltage decreases.

f) Results

The initial design charge control device was configured with a deceleration grid to control the energy level of the ions leaving the spacecraft. However the results of these experiments indicate that controlling the kinetic energy of the emitted ions would be difficult and the deceleration grid reduced the net ion emission in most cases. Since the goal was to reach 10 microamps current out of the charge control device at the minimum possible power level, the collection of a large percentage of the current by the deceleration grid was

deemed a hindrance and the advantage of having control of the emitted ion energy was unwarranted. The deceleration grid was therefore removed for further testing.

2. Removal Of Deceleration Grid

A series of experiments were run on the second Lithium ion source and a new potassium ion source to gauge the effect of the removal of the deceleration grid on the total emission and the emission that leaves the charge control device. A direct comparison between the charge control device with deceleration grid and then without can be made using the second Lithium ion source.

a) Power Sweep

The second Lithium ion source with deceleration grid reached 10 microamps total current at about 23 watts as shown previously in Figure 19 and the total emission does not change upon removal of the deceleration grid. The Lithium source was setup as for the previous power sweep (section 1,a) discussed with the extraction grid biased to -150 V, the plate biased to -150 V, and the screen biased to -15 V. As can be seen in Figure 28, the source still emits 10 microamps at about 23 watts. However, a comparison of Figures 19 and 28 shows that without the deceleration grid the current from the extraction grid increases by the amount that the deceleration grid contributed previously. The current out of the charge control device increases with power until it steadies at about 7 microamps at 24 watts.

The Potassium ion source was installed in the charge control device and a power sweep was conducted with the extraction grid biased to -100 V, the plate biased to -110 V, and the screen biased to -100 V. The results of the power sweep are shown in Figure 29 and differ significantly from the Lithium ion

source. Almost all of the total emitted current is concentrated in current collected by the extraction grid. The current out of the charge control device steadies out at approximately 3 microamps at 17 watts power.

b) Extraction Sweep

An extraction sweep of the charge control device was conducted with the plate biased to -150 V and the screen biased to -15 V. With the deceleration grid removed the second Lithium source had an increase of total current but extraction grid current increased to 10 microamps then steadily decreased as extraction voltage was decreased to -200 V as shown in Figure 30. With this decrease in extraction voltage the current out of the charge control device increased steadily.

Compared to the results with the deceleration grid in place, the second Lithium source showed an increase of total current and an increase of extraction current as the voltage was varied to -200 V as shown in Figures 21 and 30. Current out of the charge control device steadied out at about 8 microamps after -40 V extraction voltage.

The Potassium ion source also exhibited an increase of total current as the magnitude of extraction voltage was increased. However the increase was almost totally due to an increase in extraction current as can be seen in Figure 31. The current out of the charge control device remained constant at about 5 microamps throughout the power sweep.

c) Plate Sweep

A plate sweep was conducted with the extraction voltage biased to -150 V and the screen biased to -15 V. The second Lithium ion source was operated at 1100 °C. Figure 32 shows that while total current remained steady

at 18 microamps, the current moved from the extraction grid to the plate as the plate voltage was adjusted from 0 to -100 V. While similar results occur in the experiment with the deceleration grid in place the gradient of the decrease in extraction current was not as great as shown in Figure 25. This result is roughly what is wanted for application on differentially charged satellites.

With the Potassium ion source very different results were obtained as all currents remain essentially unchanged. The total current is steady at 70 microamps with the extraction grid current encompassing 65 microamps of the total as shown in Figure 33.

d) Results

With the removal of the deceleration grid it was not entirely clear that more current is being emitted by the charge control device. It appears that the majority of the current previously collected by the deceleration grid is now collected by the extraction grid, at least for Lithium. To improve the net current out of the charge control device a way must be found to increase the transparency of the extraction grid while maintaining the electric field for extraction of ions. Before pursuing this problem the effect of grid spacing was researched.

3. Grid Spacing Effects

To measure the influence that extraction grid spacing has on the extraction of ions the Potassium ion source was set up with the extraction grid set at 0.05, 0.18, and 0.31 inches distance between grid mesh and ion emitter face. The ion source was varied in power with the extraction grid biased to -100 V, the plate biased to -110 V, and the screen biased to -100 V. The result of changing the grid spacing can be seen in Figure 34 which shows the plot of total

current emitted and current out of the charge control device for the 3 different grid spacings. As the plot shows, for power settings up to about 12 watts the total current and current out of the charge control device have similar gradients but above 12 watts the currents steady out at significantly different current levels.

The closer that the extraction grid is positioned to the emitter the greater the total current emitted but the less net current emitted from the charge control device. At a spacing of 0.18 inches and above 12 watts the total current is between the 0.05 and 0.31 inch currents but the current emitted from the charge control device is maximized and is a greater percentage of the total current than at the other spacings.

4. Modified Extraction Grid

As a result of the large percentage of total current being collected by the extraction grid a modification was attempted to reduce this current and increase the current out of the charge control device. It was thought that too much current was being collected by the wire mesh of the grid so in place of the extraction grid previously described, a new extraction grid was fabricated that did not have any wire mesh, and the center hole diameter was increased by 50 % to 7/16". Even though the wires helped provide a more even electric field, it appears that the net current improved. The new extraction grid was configured on the charge control device without the deceleration grid. The Potassium ion source was used and the spacing of the extraction grid from the emitter face was adjusted for 3 different spacings; 0.10, 0.18, and 0.31 inches.

a) Grid Spacing at 0.10 inches

The new grid was spaced 0.10 inches from the emitter and was biased to -140 V with the plate biased to -150 V and the screen biased to -140 V.

A power sweep was conducted and the results are plotted in Figure 35. As the power to the ion source is increased the extraction current remains at zero until 12 watts and then rises slowly. However the current out of the charge control device rises steadily until 15 watts and then becomes constant at about 13 microamps. Current out of the charge control device reaches 10 microamps at 13 watts which is a significant improvement over the previous designs with the old grid.

When compared to previous results of the Potassium ion source with the original extraction grid installed as plotted in Figure 29 the current out of the charge control device has increased dramatically. The current collected by the extraction grid has dropped significantly and the total current at the same power setting has improved. Note that the difference in overall current levels could be a little misleading since Figure 29 is based on a very early sweep of the Potassium source. Ion emission from these sources increased gradually over time.

This success motivated a look at how the device would behave in the desired mode of satellite operation; emitting ions to space or differentially charged satellite surfaces. A combination sweep of the charge control device was conducted that varied the potential of the extraction grid, the plate, and the screen in tandem. The screen (space plasma) and the extraction grid (satellite ground) were biased to the same potential and the plate (a differentially charged surface) was biased 10 V below them while the source was powered at 11 watts.

The results of the combination sweep are shown in Figure 36 which indicates an increase in total current as the potentials are decreased relative to the ion source. The current out of the charge control device increased steadily

and is a larger percentage of total current as the potentials are decreased. Surprisingly the extraction current rises until the extraction grid is biased at -50 V and then falls off to zero.

b) Grid Spacing at 0.31 inches

The modified extraction grid was next configured at a spacing of 0.31 inches from the ion emitter face. In this series of sweeps however the extraction grid was biased to -100 V, the plate was biased to -110 V, and the screen was biased to -100 V (midpoint settings for previous sequence). A sweep of current was conducted as the power to the ion source was increased and the results are plotted in Figure 37. As previously seen, the majority of the current is now emitted out of the charge control device except at higher power settings. The extraction current makes up a much smaller percentage of total emitted current at this spacing than was seen at 0.10 inches but the total current emitted overall is also reduced from 10 microamps to 3.5 microamps at 14 watts.

To test the influence of the new extraction grid potential on current out of the charge control device the extraction grid was biased from 0 to -150 V while the Potassium ion source was set to 15 watts power. As can be seen in Figure 38 the extraction grid potential has an almost linear effect on the total current produced and the current out of the charge control device. Even as the extraction grid is biased to -150 V the current collected by the new extraction grid does not increase very much beyond zero.

c) Grid Spacing at 0.18 inches

Since a spacing of 0.18 inches between the extraction grid and the emitter face was previously found to maximize current out of the charge control device with the old extraction grid the charge control device was configured with

the new extraction grid at this spacing for a power sweep. The new extraction grid was biased to -140 V, the plate biased to -150 V, and the screen biased to -140 V with the results of the sweep plotted in Figure 39. As in previous sweeps with the new extraction grid the majority of total current was current that was able to leave the charge control device. The goal of 10 microamps current out of the charge control device is reached at 14 watts. The extraction current increases more than was seen at 0.31 inches spacing and less than at 0.10 inches spacing.

A combination sweep of the extraction grid, plate, and screen was conducted as previously described with the ion source powered at 15 watts. The results are plotted in Figure 40 and show that as potentials are decreased the current out of the charge control device increases linearly. Extraction current drops steadily and plate current steadies out at -120 V. The increasing screen current is the only contribution to current out of the charge control device after -120 V which is different from the results found at the 0.10 inches spacing combination sweep shown in Figure 36.

d) Comparison of Spacing with New Extraction Grid

The total current emitted is affected significantly by the spacing of the extraction grid from the emitter face. As shown in Figure 41 the total current increases as the extraction grid is moved closer to the emitter. However, the movement of the extraction grid does not appear to linearly affect the total current. As the plot shows the current change from 0.10 to 0.18 is not as dramatic as from 0.18 to 0.31.

Even more important than total current is the current emitted out of the charge control device. A comparison of this current at the 3 different grid

spacings is shown in Figure 42. Again the current does not appear to follow the spacing linearly but falls off sharply as grid distance from the emitter face is increased.

5. Electron Source

The electron filament source was tested for current emitted to the screen. The electron source was initially brought up to a temperature of 2500 °C for 2 minutes to flash the thoriated tungsten filament. The results after flashing were not as dramatic as expected so a second filament was treated with a barium carbonate mixture to increase thermionic emission. The results for this filament configured on the initial charge control device and heated to 1700 °C are shown in Figure 43. The screen was biased to +50 V, the plate was biased to +150 V, and the deceleration grid was biased from 0 to +100 V. The current off the electron source is in the milliamp range and the required 1 milliamp of current out of the charge control device is easily obtained. The only problem is a fairly substantial power requirement (2.5 V, 6.4 A, and 16 watts).

VII. Discussion

The purpose of the experiments conducted was to optimize the charge control device to achieve 10 microamps current out at the lowest possible power. The experiments were designed to test incremental design modifications to the charge control device and as results were analyzed the charge control device was modified and the next set of experiments were conducted. Results of these various experiments raise a variety of interesting points.

The initial design of the charge control device was tested using 2 different Lithium ion sources. A plate was added to the experimental setup after it was felt a clean collection surface was needed directly in front of the charge control device to provide a clear electric field and clearer measurements for emitted current. Though the 2 Lithium sources were found to require different power settings to reach the same temperature, the emission of 10 microamps was found to be at the same power for both emitters. In the case of both Lithium emitters the deceleration and extraction grids took too large a percentage of total current and the goal of 10 microamps out of the charge control device was not possible at a reasonable power. The benefit of having the deceleration grid available for precise control of emitted ions was felt to be too costly in terms of diverting too much current to the grids and the deceleration grid was removed from the design.

When the deceleration grid was removed for a series of experiments on a Lithium and Potassium ion source the results were not what was expected. The current that was previously collected by the deceleration grid did not all go out of

the charge control device, rather a sizable percentage was collected by the extraction grid. It appears that the removal of the deceleration grid affected the electric field sufficiently that the majority of the ions that used to collect on the deceleration grid did not have the energy to exit the charge control device and collected on the extraction grid instead. Though the removal of the deceleration grid improved the results of current out of the charge control device the increase is insufficient to achieve 10 microamps at low power.

An interesting result was obtained with the removal of the deceleration grid on the Potassium ion source. While the Potassium source emitted a much larger total current than the Lithium source the current emitted by the Potassium source went predominantly to the extraction grid. The current out of the charge control device with the Potassium source never exceeded 5 microamps even though total current consistently reached 70 microamps. This result can be related to the relative masses of the Lithium and Potassium atoms. The extraction of the ions appears to depend to some degree on their masses. The Potassium atom is larger than the Lithium atom and it is possible that the larger Potassium atom encounters more difficulty in being extracted from the lattice structure of the Beta-Eucryptite. The extraction of ions through the Potassium salt is helped by higher extraction voltages. This is an important result as emission from the Potassium ion source can be significantly improved with higher extraction voltages at no cost of higher power to the ion source.

The variation of the spacing between the extraction grid and the emitter is found to affect the current emitted. The strength of the electric field formed by the extraction grid and the emitter is determined by a factor of 1/d. As the grid is moved closer the electric field strengthened and ion extraction is increased.

However, the current out of the charge control device does not clearly follow this relationship. As the grid is moved closer a greater percentage of the new current extracted is collected by the extraction grid. The effect of the grid plate on the electric field at very close distances must divert more of the ions to the plate than before. It was found that a spacing of 0.18 inches maximized current out of the charge control device even though total current would be higher if the grid was moved closer.

When the new wire-less extraction grid was installed in the charge control device the percentage of total current that exited the charge control device improved dramatically. The removal of the wires and enlarging the center hole had dramatic effects that superseded much of the previous results found. The electric field formed by the new grid diverged out of the emitter and through the charge control device and as the grid was moved closer to the emitter an increasingly greater percentage of the total current went to the extraction grid. At a spacing of 0.10 inches the current collected by the extraction grid was significantly greater than at the other spacings. However, at this spacing the total current increased more significantly over the other distances such that the current out of the charge control device was still greater than at the other 2 spacings. Therefore the charge control device configured without the deceleration grid and with the extraction grid spaced at 0.10 inches from the emitter face provides the greatest current out which can be used for charge control.

The electron source exhibited the required output for charge control purposes and was operated for some experiments in tandem with the ion source

without any adverse effects. The electron source requires a coating or needs to be carburized at manufacture to provide the necessary emission currents for active charge control.

VIII. Conclusion

The experiments conducted on the charge control device were to determine its suitability as a replacement spacecraft charge control device. The initial charge control device design was modified in succeeding steps to optimize the current out at 10 microamps at low power.

The extraction and deceleration grid design was determined to be inadequate given the purpose of maximizing current out. The deceleration grid was removed and the extraction grid was modified. The final design achieved the required current out of the charge control device by manipulating the extraction grid's center hole and the spacing to the emitter face. A current out of the charge control device of 10 microamps was achieved at a power of 13 watts which is a significant improvement over our initial design and is competitive with hollow cathode designs. Additional improvements over other designs is the low weight and volume of the charge control device and the elimination of possible electromagnetic interference.

The problem of lifetime remains however, and further reductions in power consumption should be possible with this device. The lifetime can be improved by further improvements in the ratio of current emitted versus current collected on the extraction grid. An operational design for a charge control device would be provided by mounting multiple ion sources in a matrix, with 20 - 100 of the compact sources mounted in an array. A second alternative would provide a method to replenish Lithium or Potassium by diffusion from the back end of the emitter.

The radiated power (σT^4) of the ion source is on the order of 6 watts and only accounts for about 1/2 of the power used. The remaining power of 7 watts is therefore lost in the production of ions. A review of the charge control device design provides some recommendations on reducing this loss factor. The ion emitter appears to lose substantial heat out of the bottom of the emitter-heat shield unit. If a method could be devised to hold this heat in, such as a ceramic plug, the power requirements should drop. Additional heat loss from the side of the emitter could be reduced by the addition of more heat shielding which could reduce the power requirements by 10 - 20 %.

Additional improvements to the design of the charge control device would be movement of the electron filaments and their posts further away from the extraction grids. This would preclude the emission from the electron filament from coating the ceramics on the filament posts and providing a conduction path to the extraction grid.

The present method of connecting leads to the various components needs further improvement. For testing purposes a solid but quick method of connection is required. Instead of the 3 copper plates at the base of the charge control device for connecting to the emitter 1 plate separated into 3 isolated sections would ease connections and lower the weight and volume further. For actual connection to the leads from the emitter a quick connect tab with attachment point for emitter leads would ease change-out of the emitter and removal of the charge control device from the test chamber.

The charge control device with design modifications met the required goal of 10 microamps at low power and further enhancements would improve the device considerably.

APPENDIX A

Table 1
Summary of some known anomalies (JPL Report, 1989)

Satellite	Anomaly
Voyager 1	Power-on resets
SCATHA	34 Pulses detected
DSP	False flag from star sensor Thermal control degradation Sensor data noise Control circuit switching
DSCS II	Spin up Power system failure (#1)
GPS	Clock shift False command
INTELSAT III and IV	Unexplained spin up
Skynet 2B	Telemetry problems
ANIK	Power downs
CTS	Short circuit noise bursts and power inverter shutdown
Meteostat	Status changes
GEOS 4 and 5	Upsets and loss of GEOS 4
Solar Max mission	10 upsets/year
Navstar 1	Solar array hold mode
Telesat	Telemetry logic switching

APPENDIX B

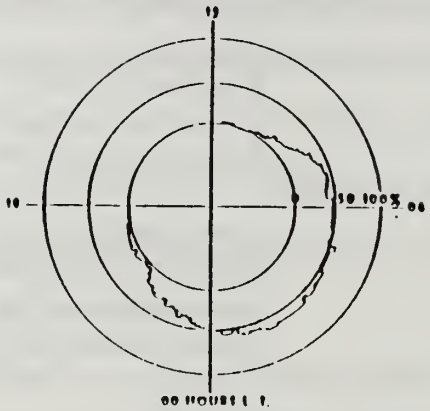

local time distribution of ATS-6 spacecraft charging events.

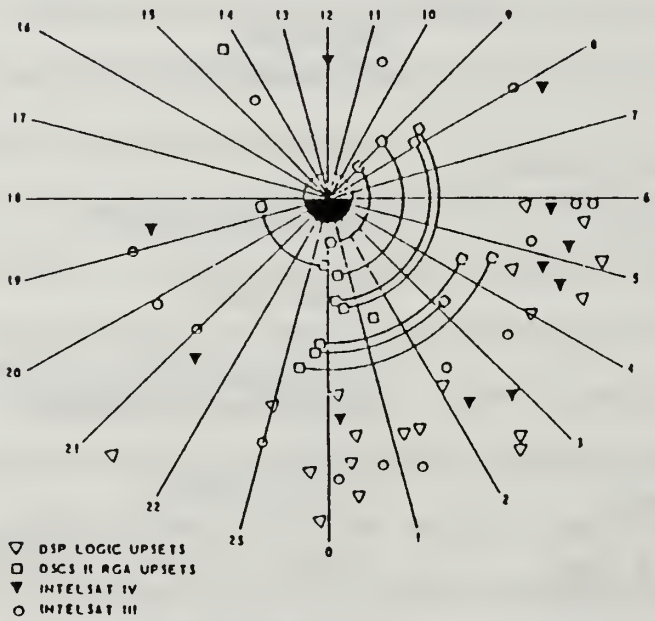

Occurrences of satellite operational anomalies plotted as function of local time in the geostationary orbit (McPherson and Schober, 1976). The radial distance has no significance.

Figure 1. **Correlation between charging events and satellite anomalies (McPherson and Schober, 1976).**

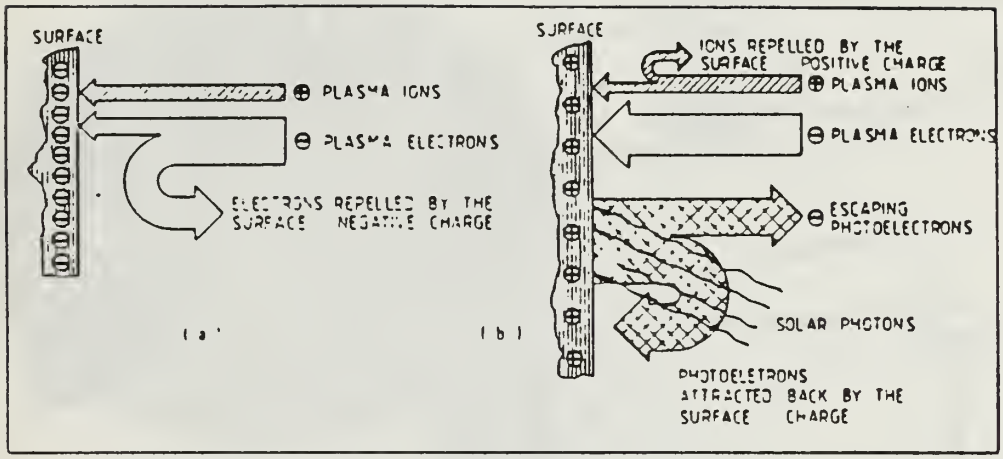

Qualitative illustration of the charging of a surface by a plasma. The width of the arrows is proportional to the flux of each particle species; the equilibrium potential is reached when the sum of the currents collected and emitted by a surface element is zero. (a) Surface in shadow: the current balance requires equality between the flow of the plasma ions and that of the plasma electrons impinging on the surface. (b) Surface in sunlight: equilibrium is achieved when the flow of escaping photoelectrons is equal to the difference between the incoming flows of plasma electrons and ions.

Figure 2. **Charging of a satellite by ambient plasma and photoemission (Grard, *et al*, 1983).**

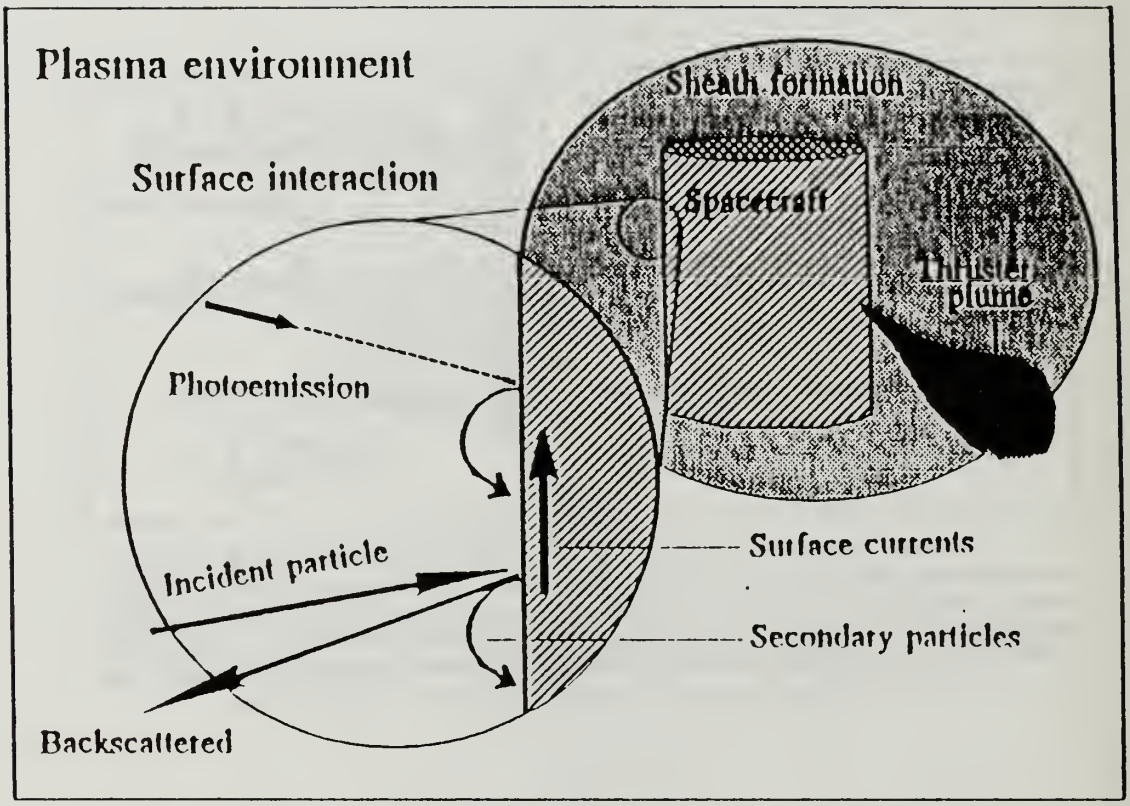

Figure 1. In surface charging, currents from the movement of ambient electrons, ions, secondary electrons, and photoelectrons result in a net current on the external surface of the satellite body. (after Robinson, 1989)

Figure 3. **Illustration of current flow to a satellite (JPL Report, 1989).**

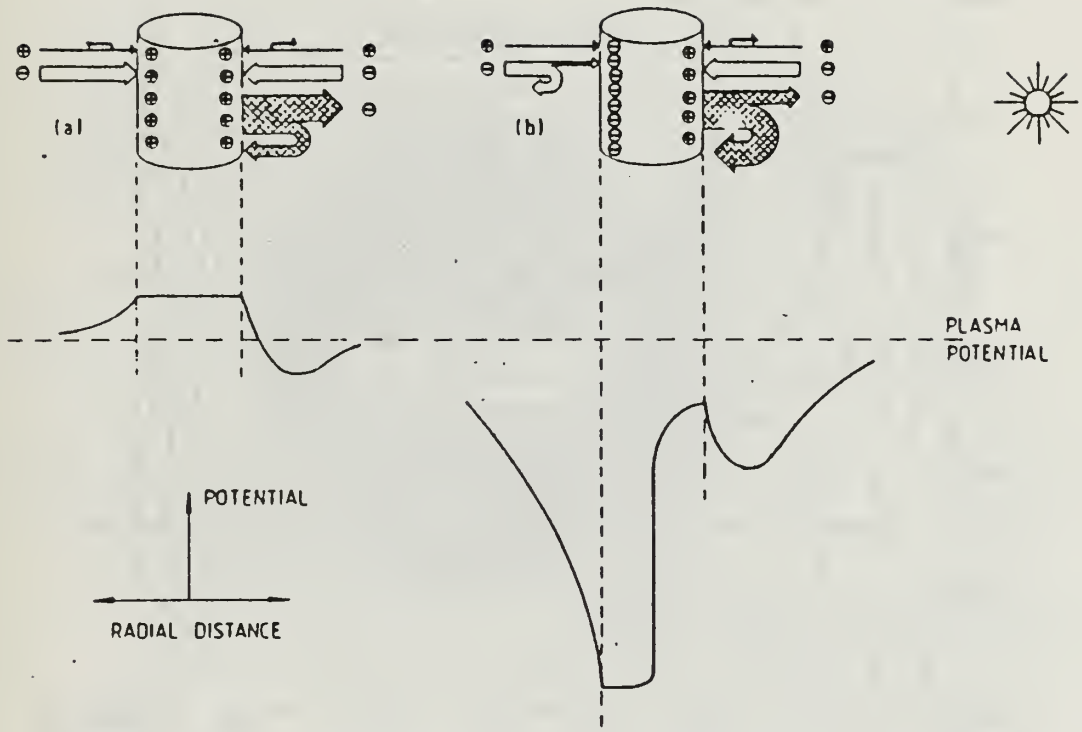

Schematic representation of particle flows to and from a satellite for the case of (a) a conductive surface and (b) an insulator surface. The lower portion gives a qualitative plot of the associated potential profiles in a hot plasma.

Figure 4. **Illustration of current flow to a satellite experiencing differential charging (Grard, 1983).**

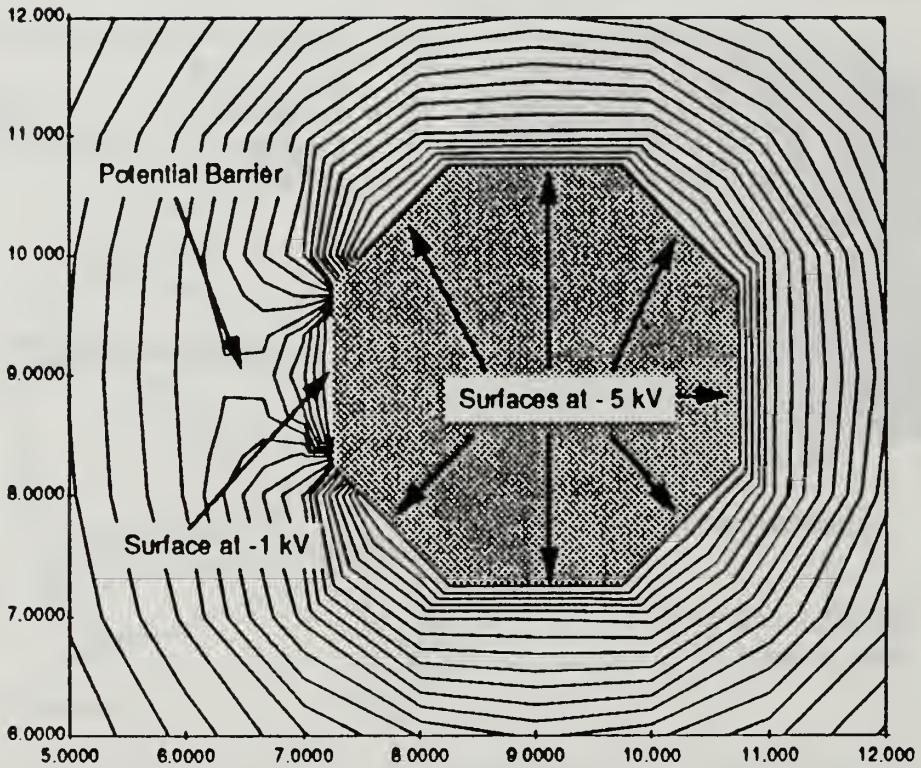

Figure 5. **Potential barrier developed by differential charging on a satellite (Davis and Katz, 1989).**

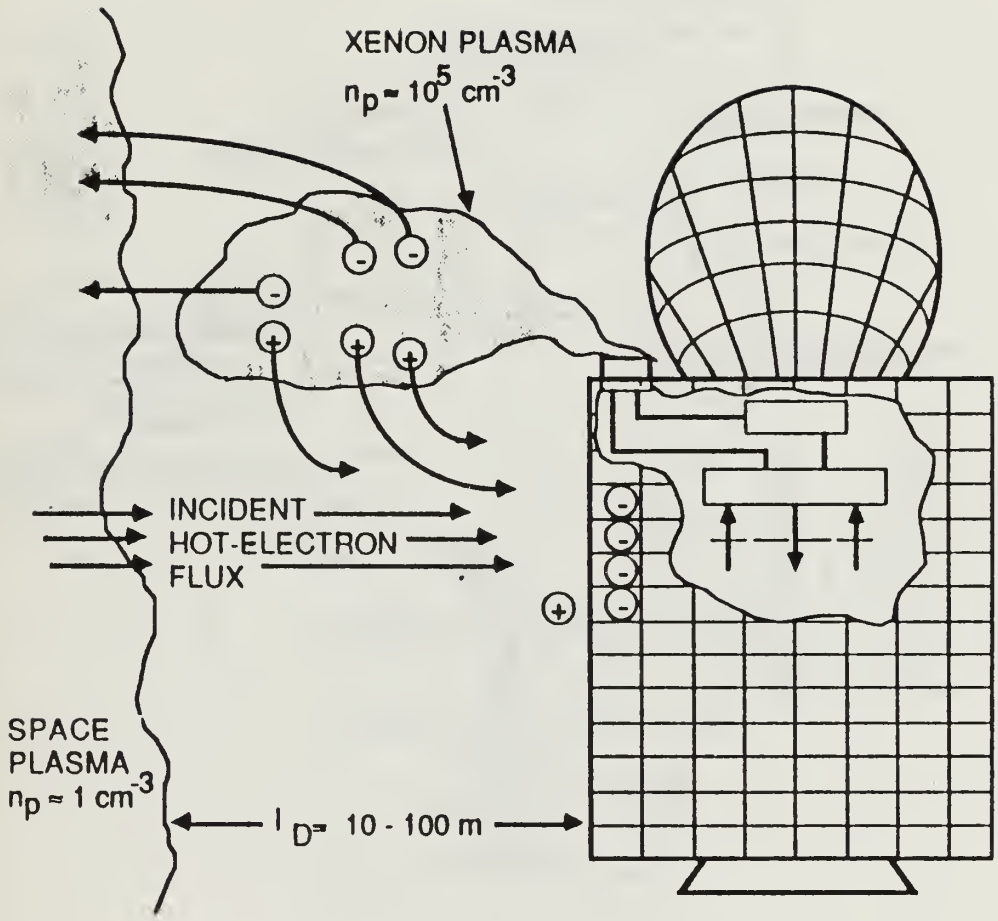

Figure 6. **Emission of a neutral plasma to control differential charging (JPL Report, 1989).**

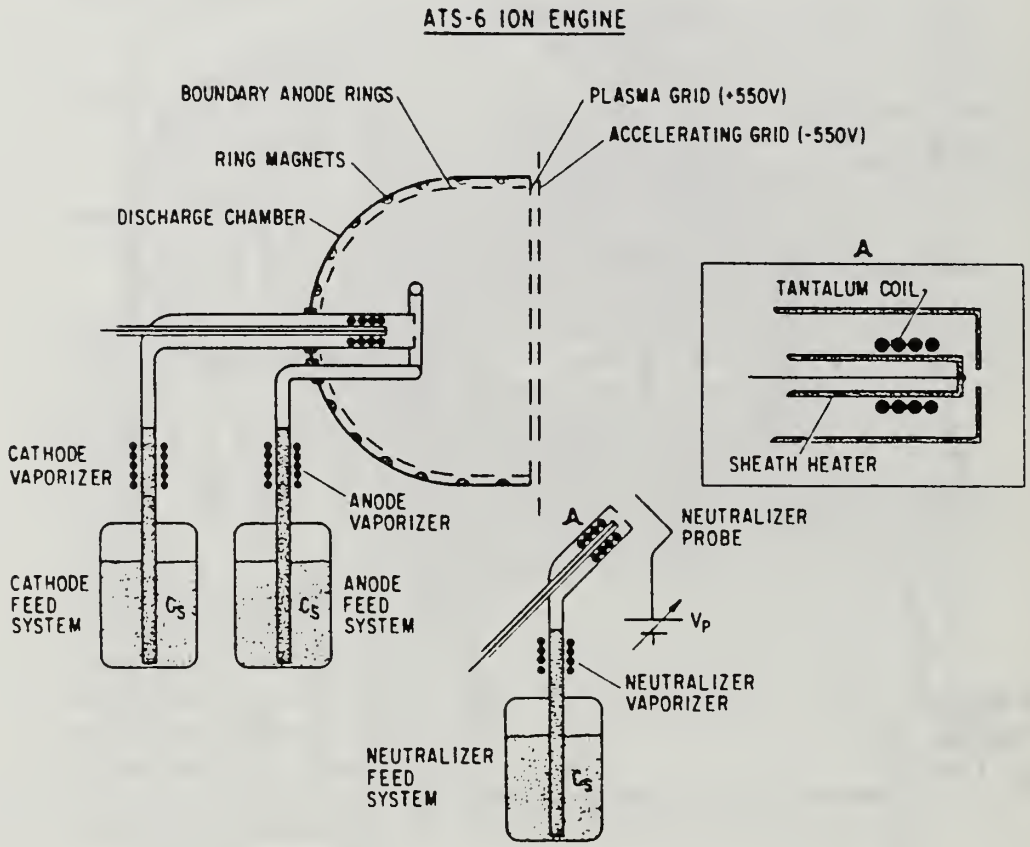

Figure 7. **ATS-6 hollow cathode ion engine (Olsen and Whipple, 1978).**

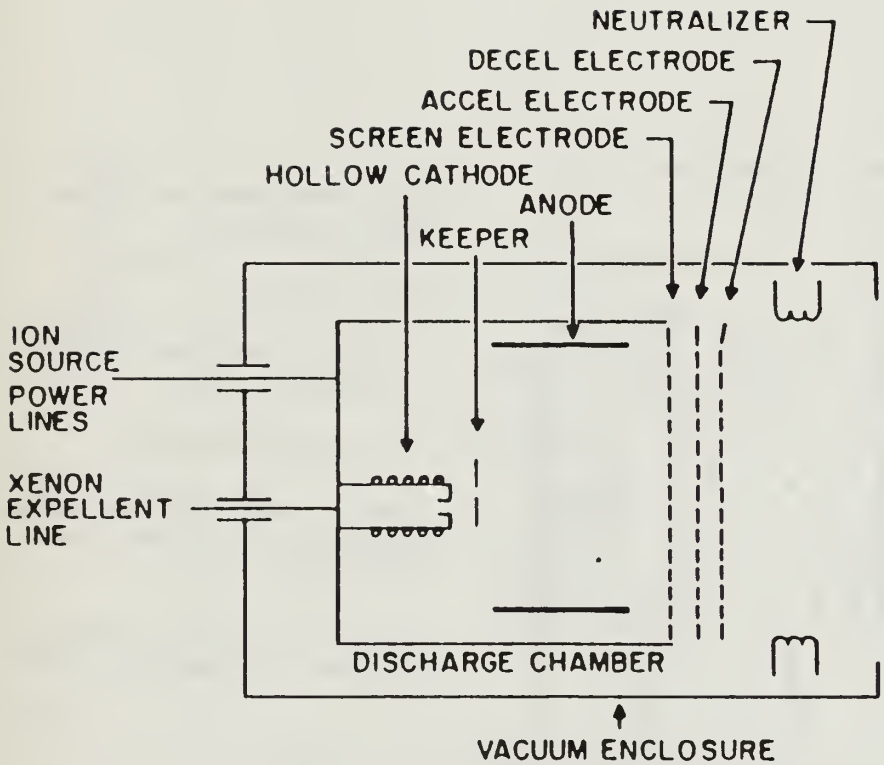

Ion gun block diagram.

Figure 8. **SCATHA hollow cathode ion engine (Olsen, *et al*, 1990).**

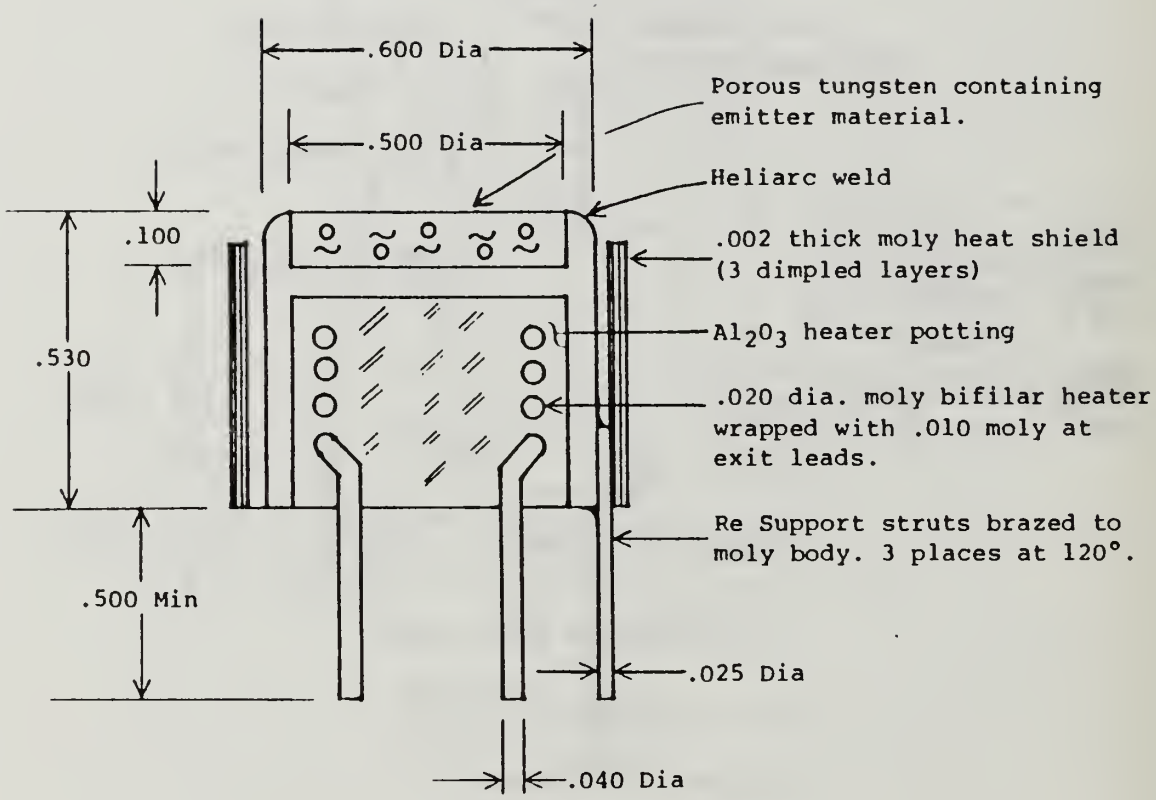

Figure 9. **Solid state ion source (Spectra-Mat, 1980).**

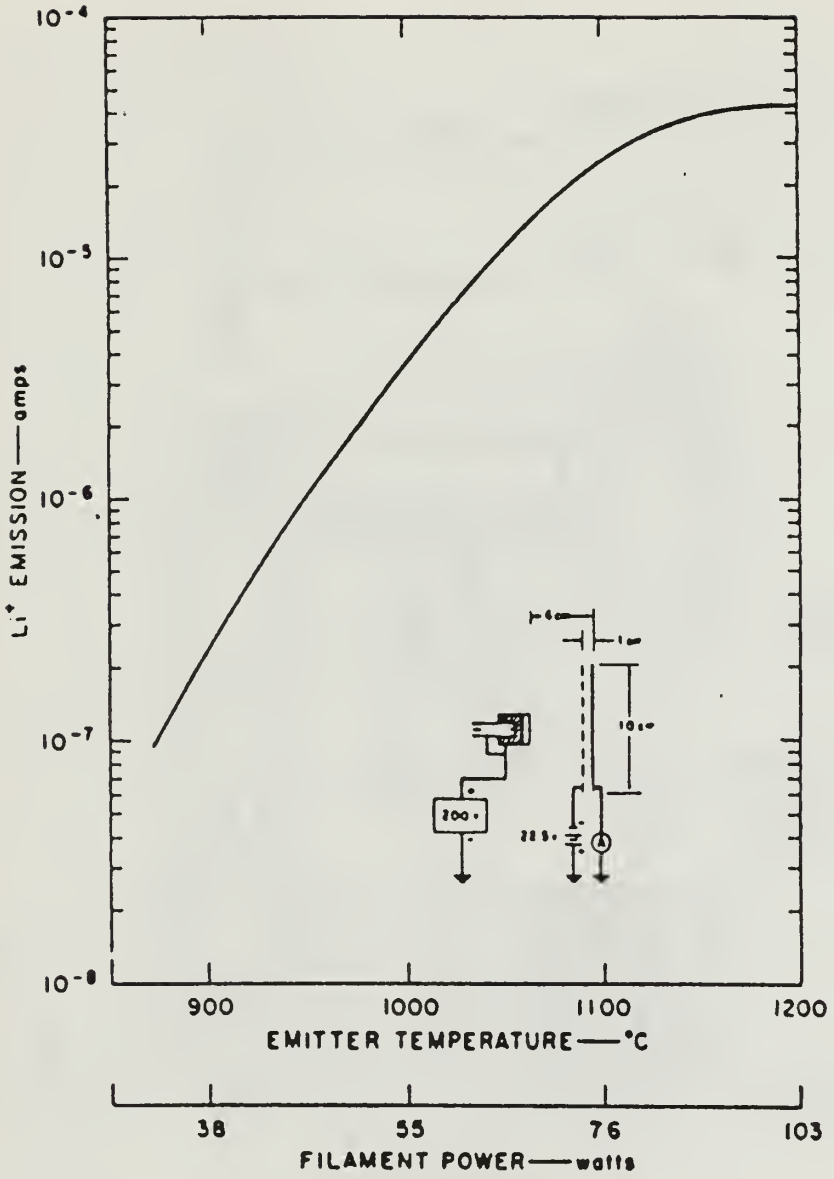

Total emission current as a function of power and temperature: Insert shows experimental arrangement.

Figure 10. **Solid state ion source emitter current versus filament power (Heinz and Reaves. 1968).**

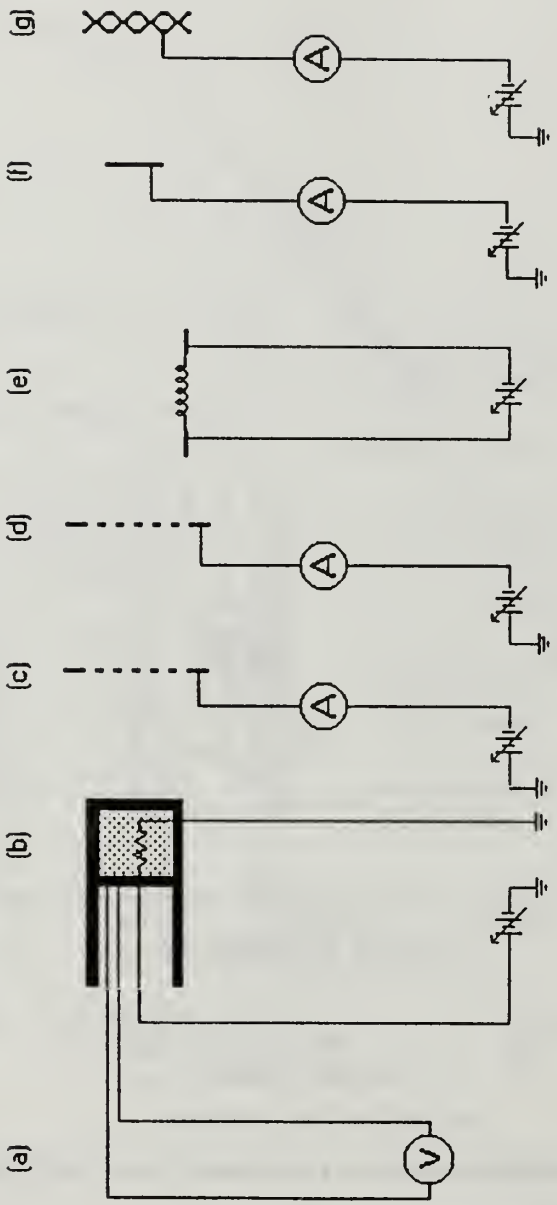

Figure 11. **Electrical setup of charge control device in vacuum chamber. Components of device: (a) thermocouple, (b) ion source, (c) extraction grid, (d) deceleration grid, (e) electron source, (f) collection plate, (g) screen.**

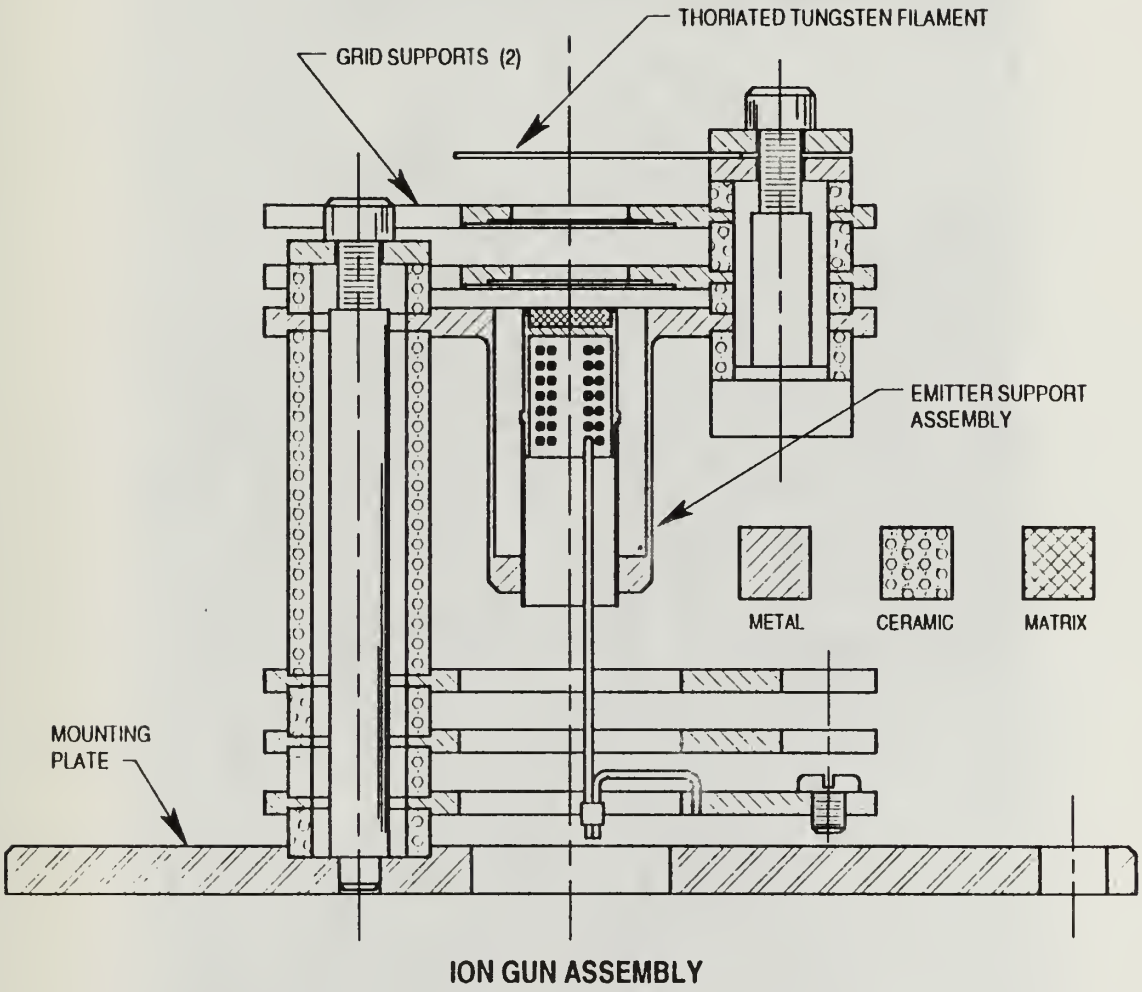

Figure 12. **Engineering drawing of charge control device (Bob Berggren, Spectra-Mat,Inc).**

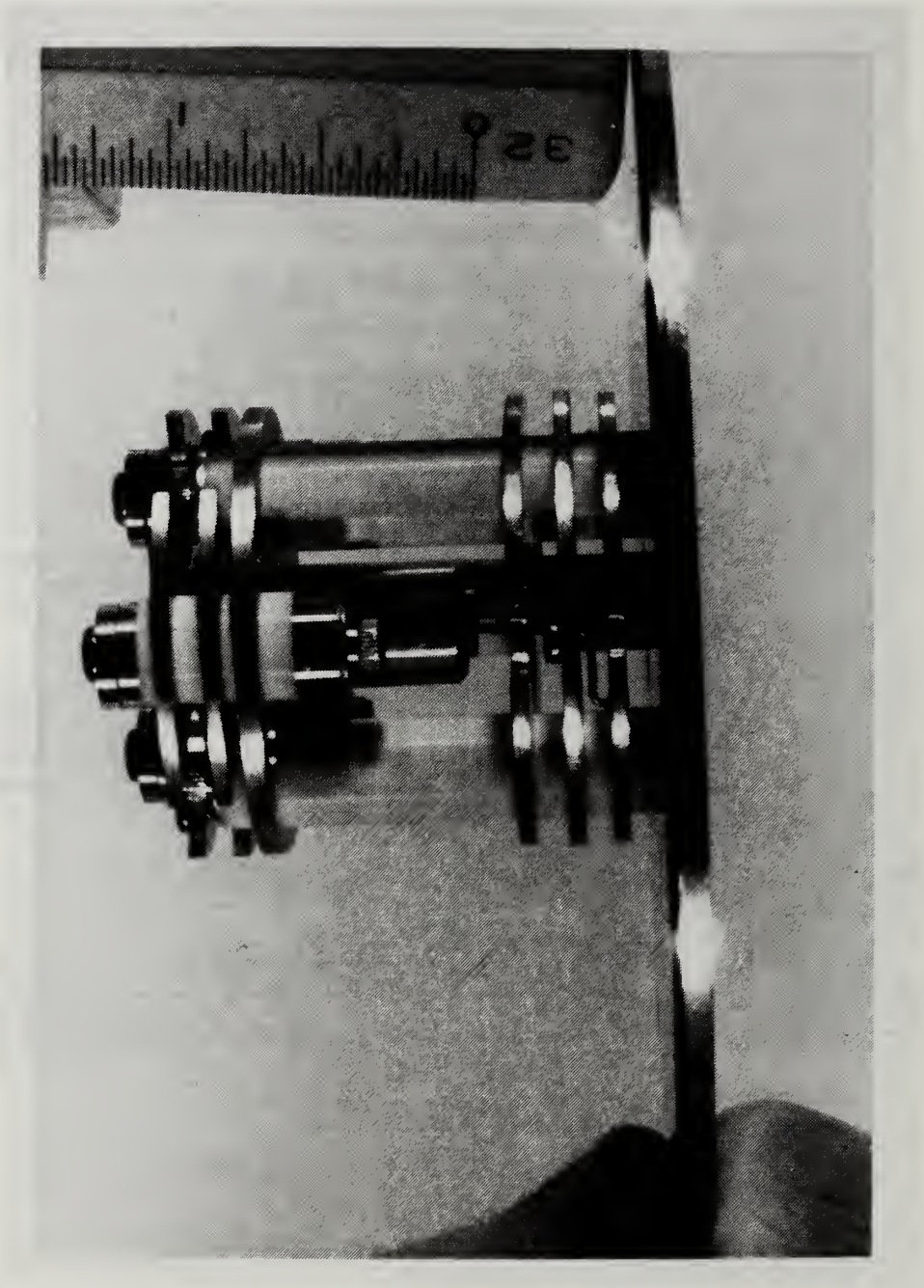

Figure 13. **Charge control device, side view.**

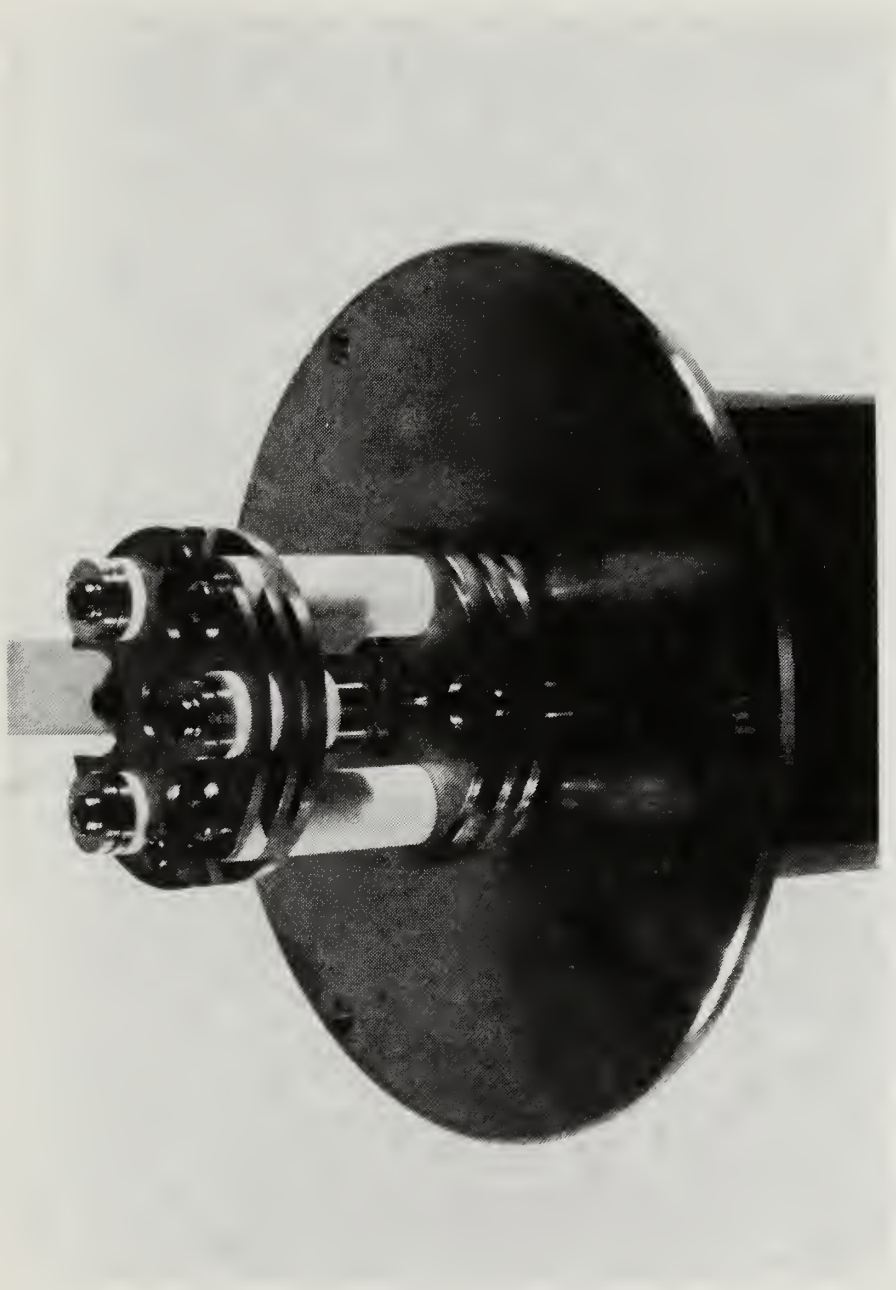

Figure 14. **Charge control device, oblique view.**

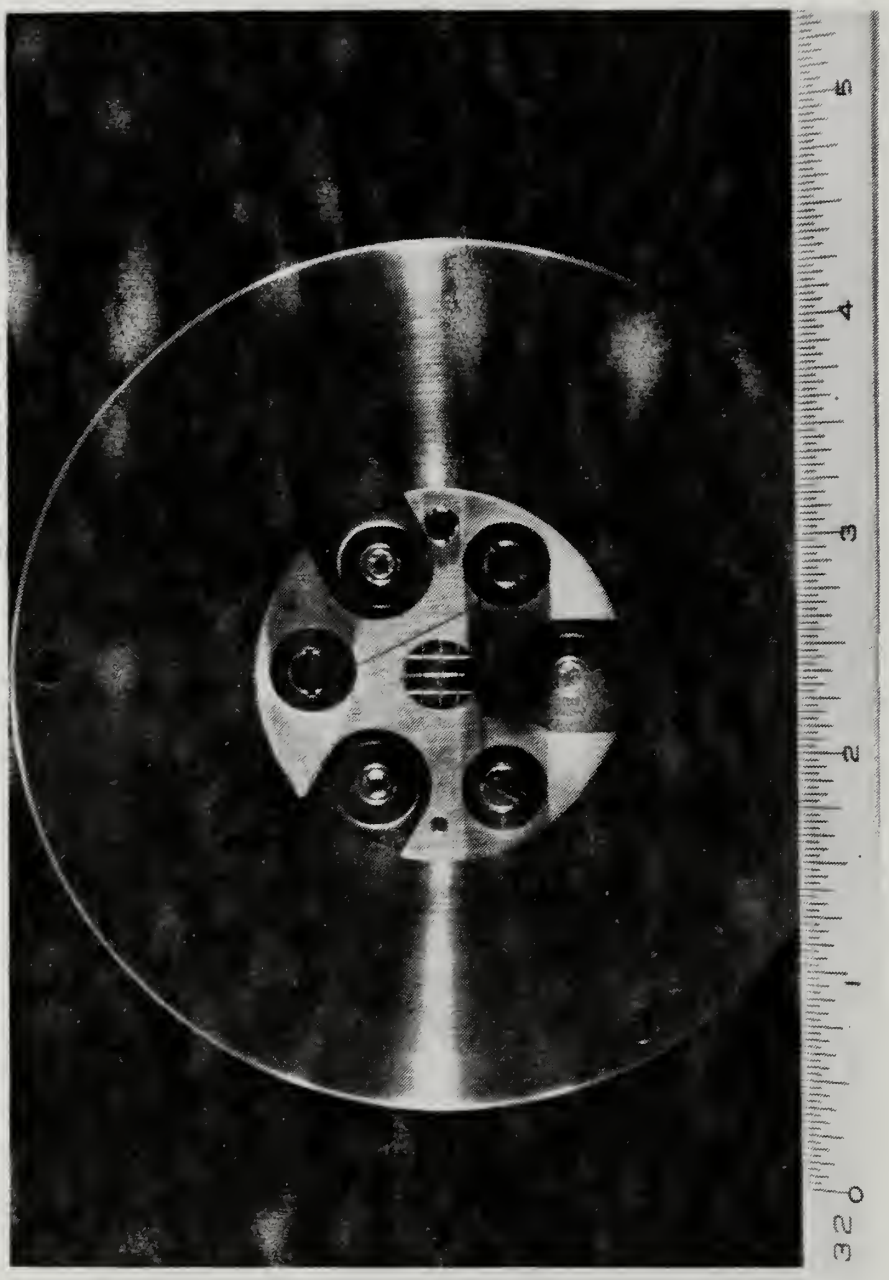

Figure 15. **Charge control device, top view.**

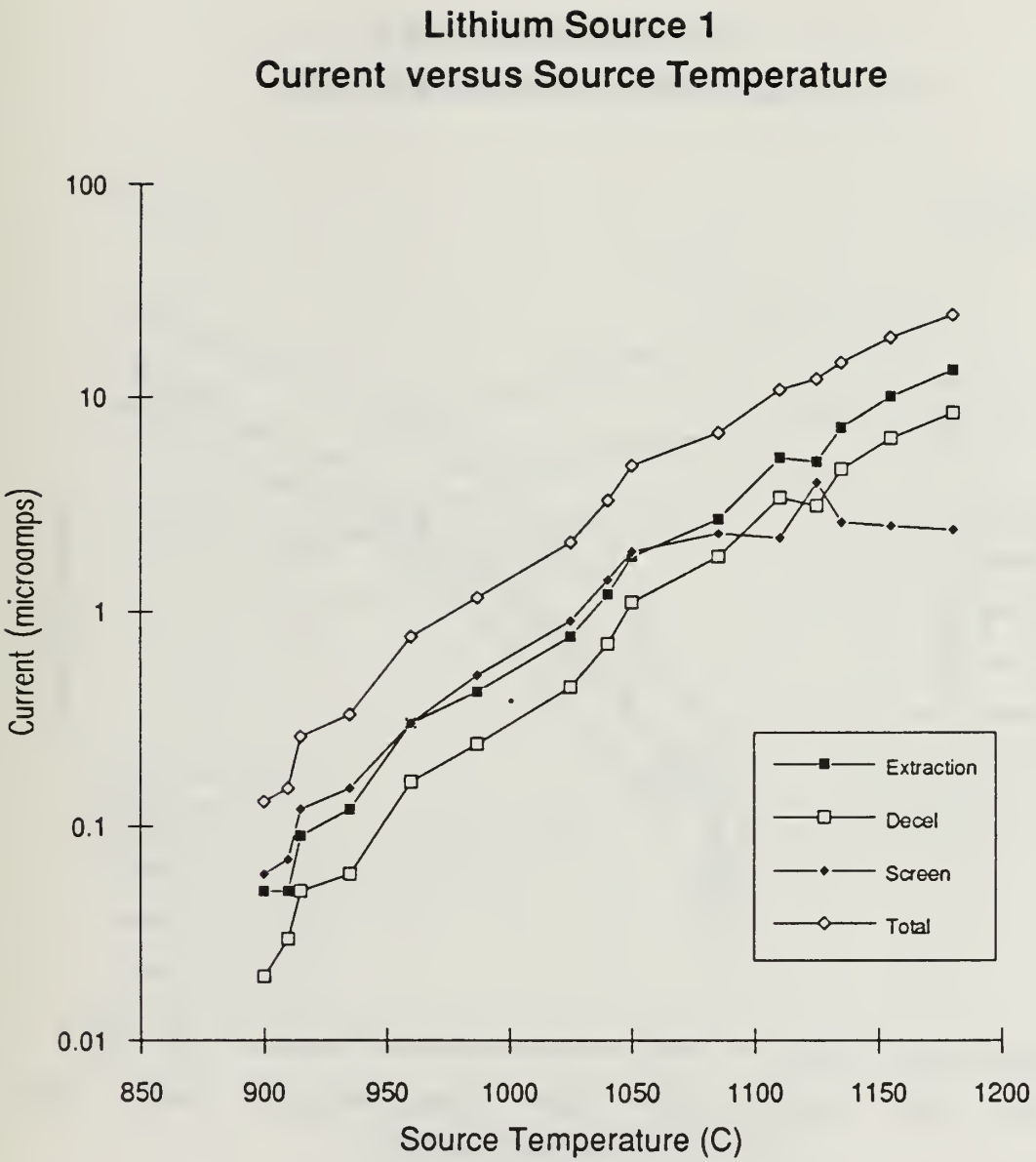

Figure 16. **Lithium ion source 1, current versus source temperature, initial design.**

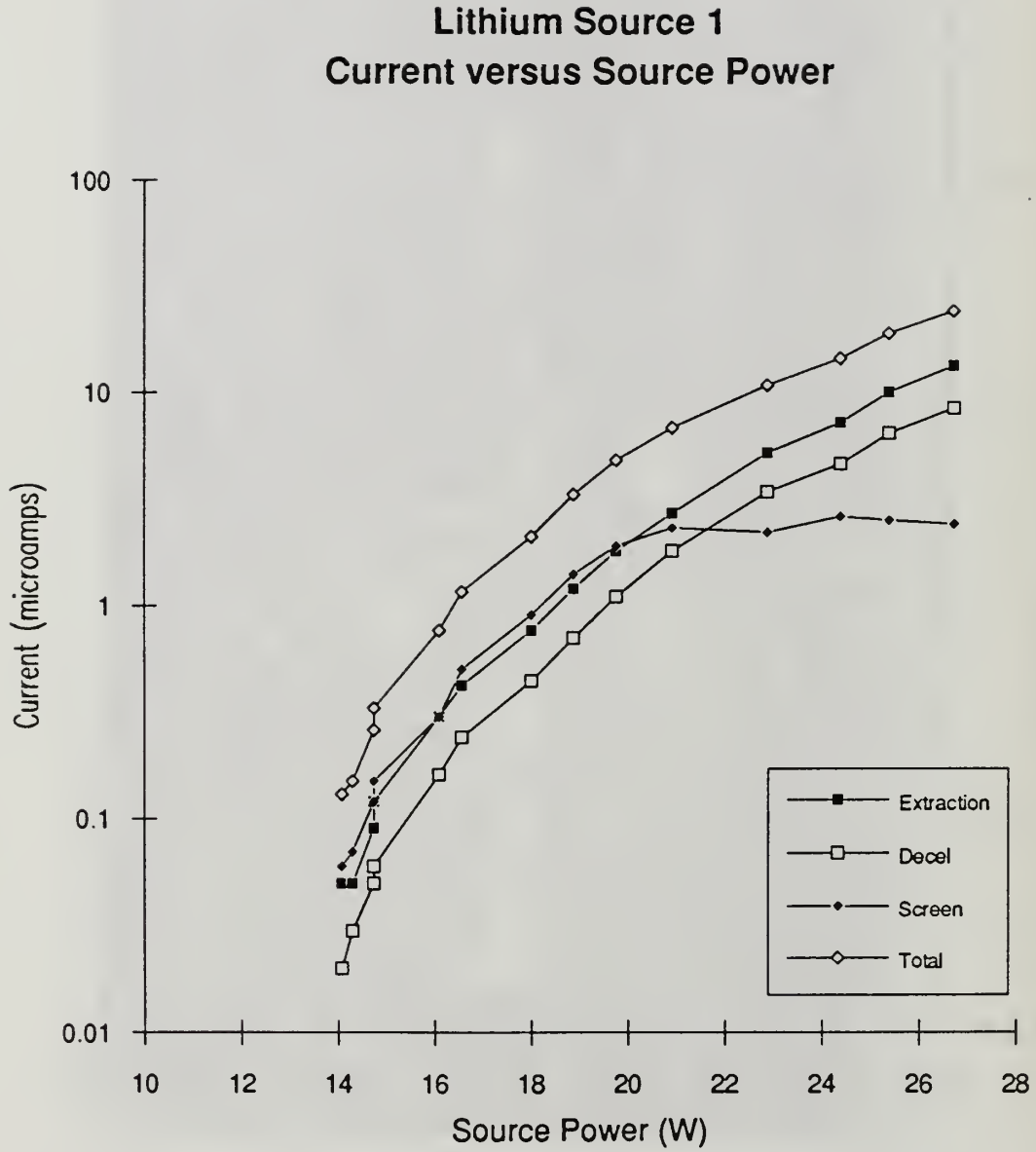

Figure 17. **Lithium ion source 1, current versus source power, initial design.**

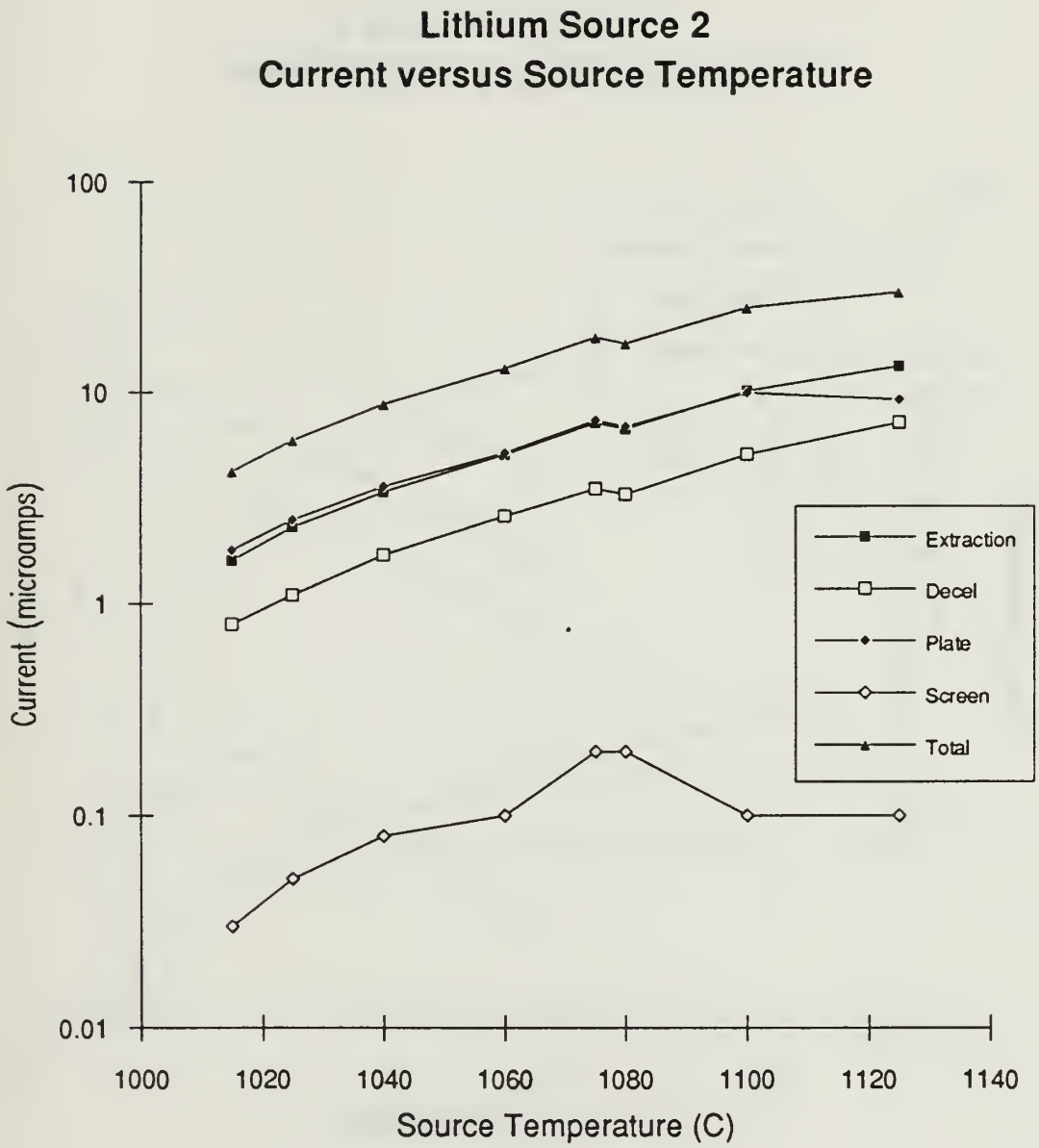

Figure 18. **Lithium ion source 2, current versus source temperature, initial design.**

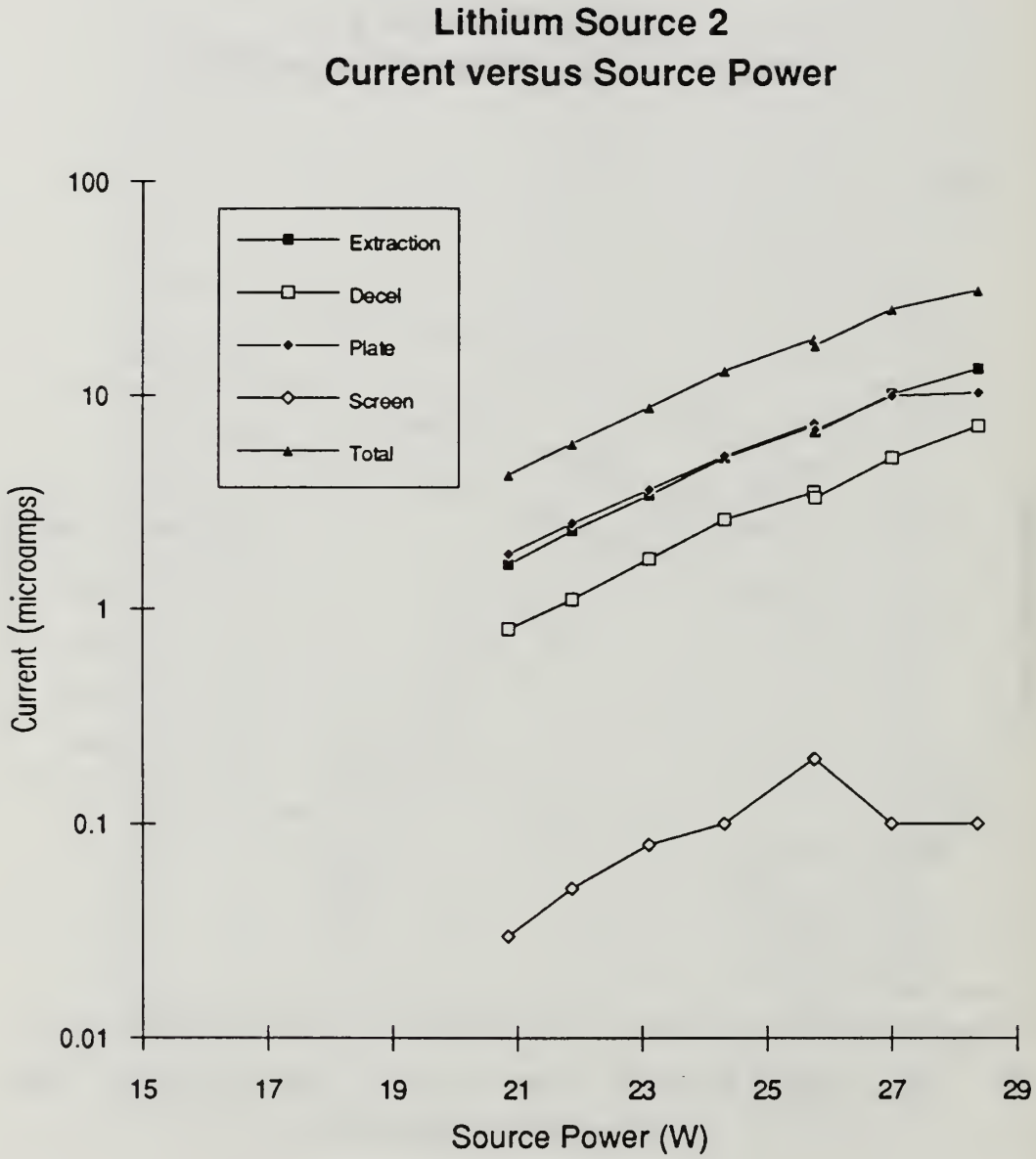

Figure 19. **Lithium ion source 2, current versus source power, initial design.**

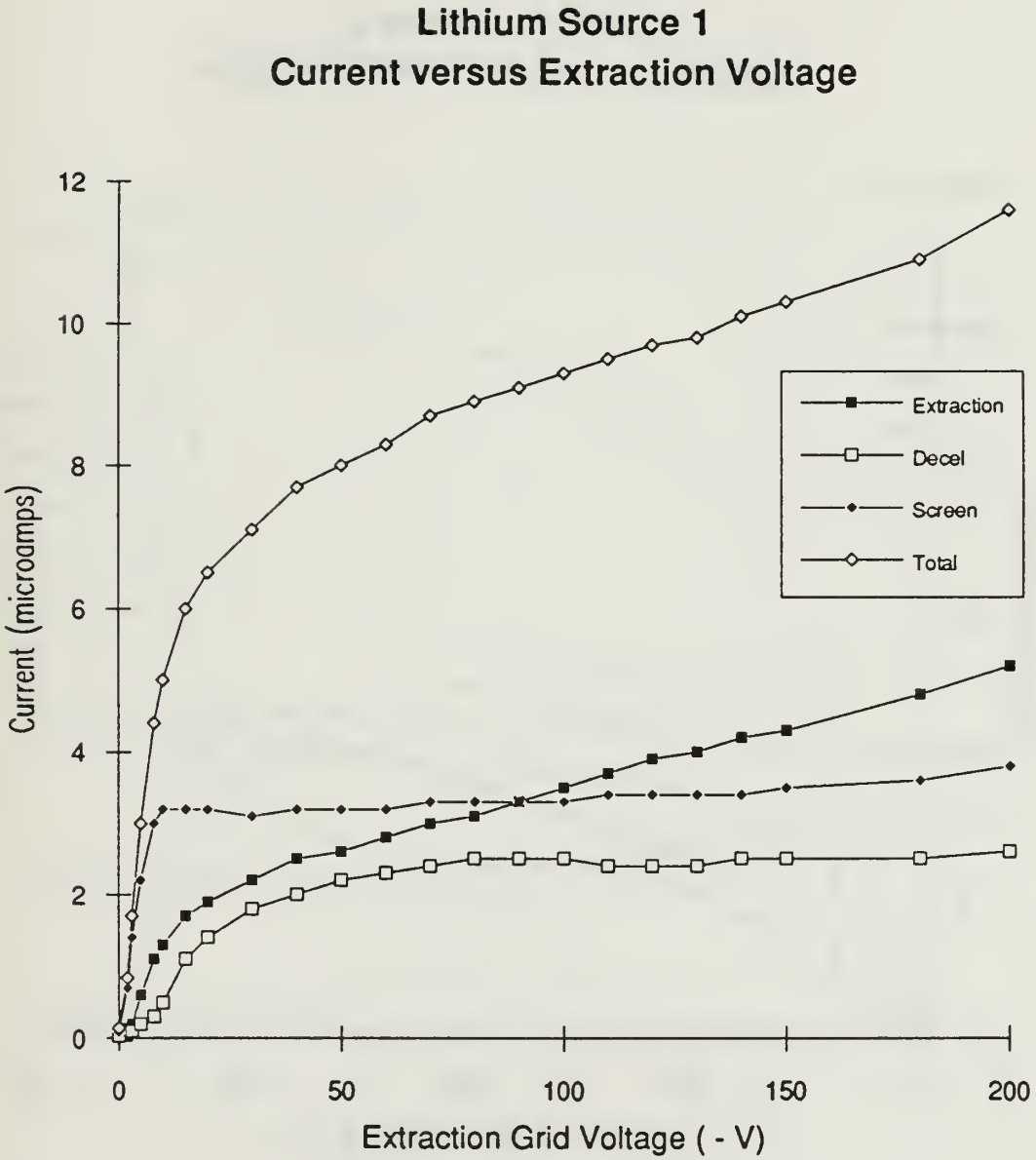

Figure 20. **Lithium ion source 1, current versus extraction voltage, initial design.**

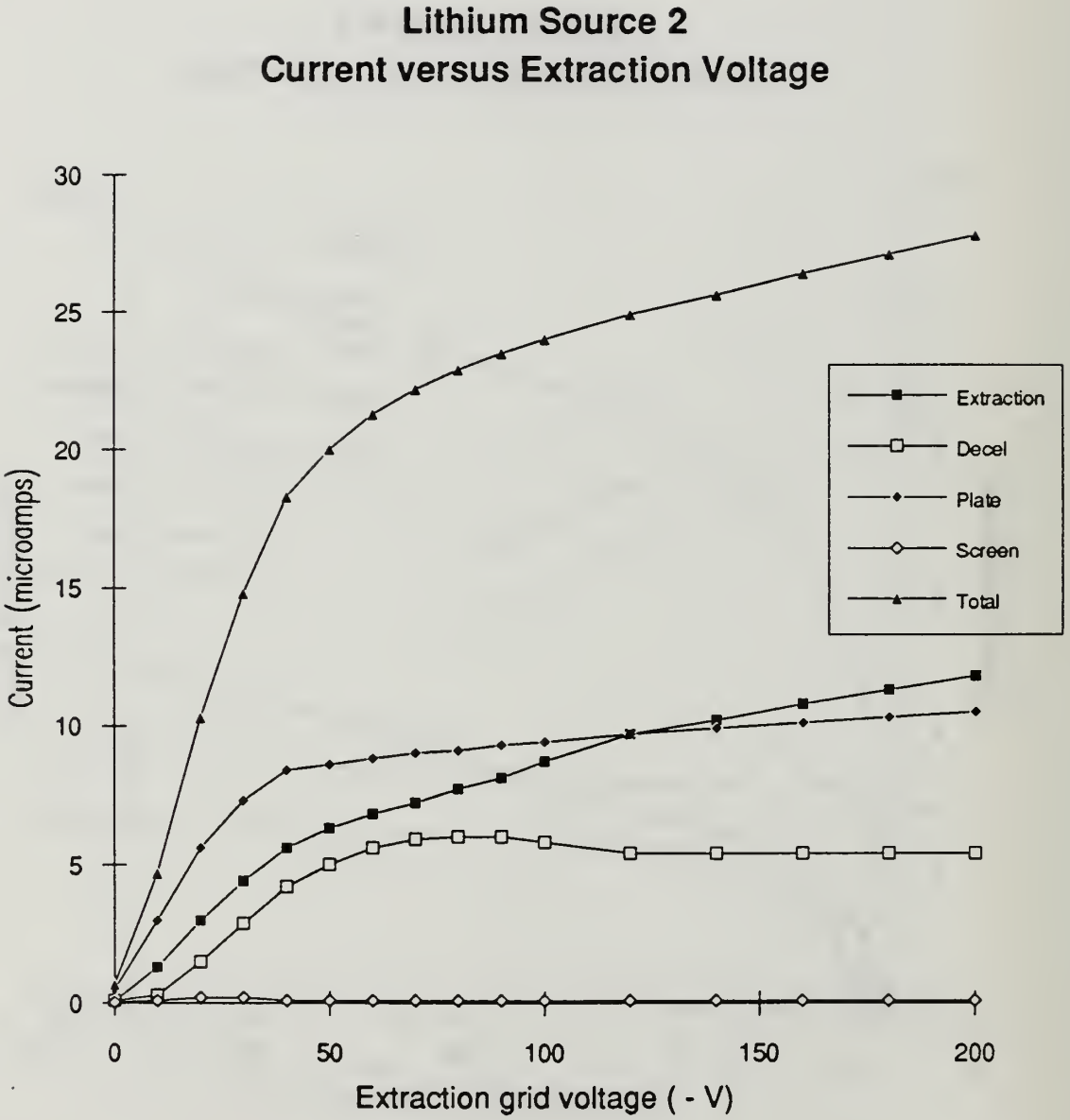

Figure 21. **Lithium ion source 2, current versus extraction voltage, initial design.**

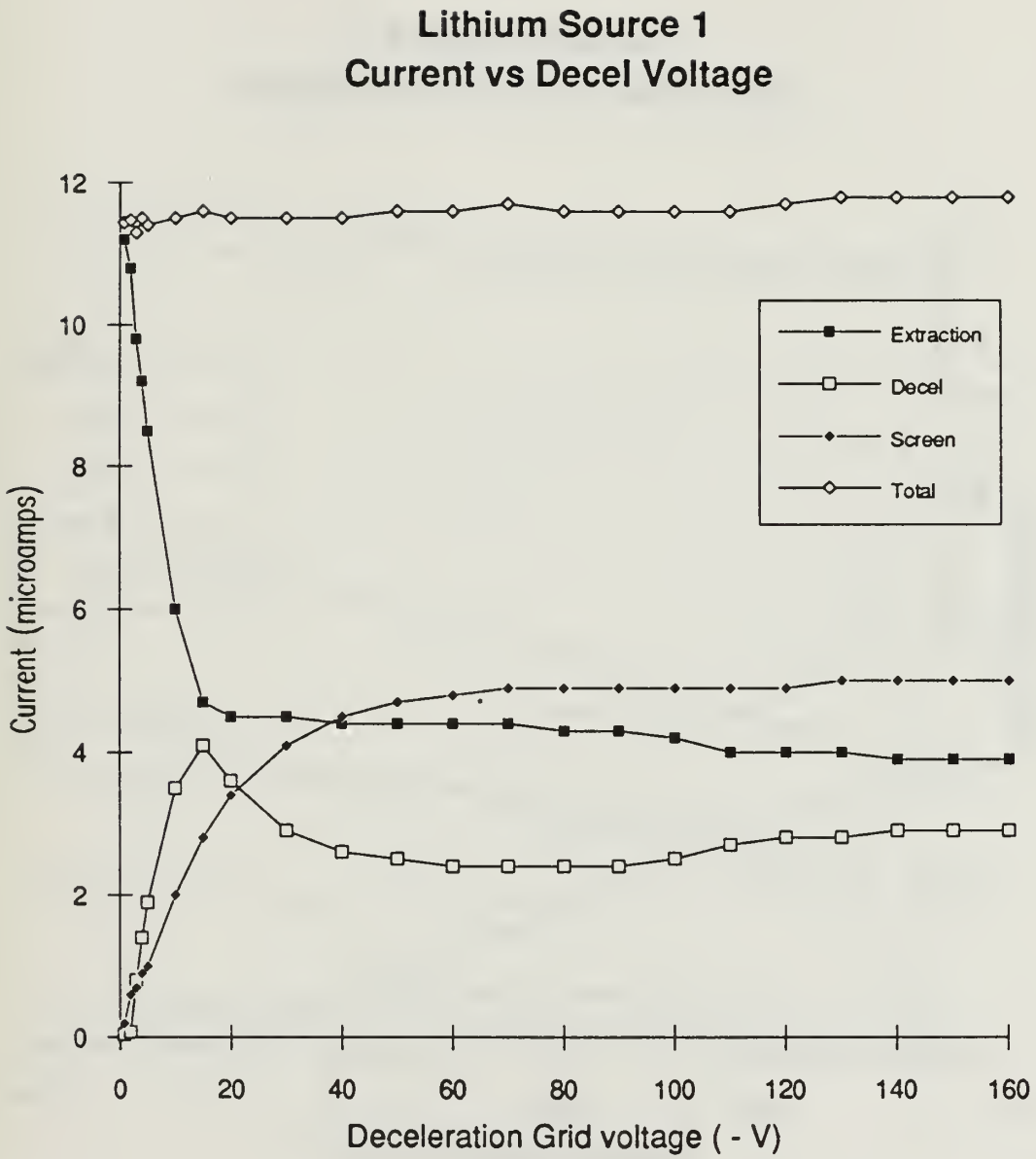

Figure 22. Lithium ion source 1, current versus deceleration voltage, initial design.

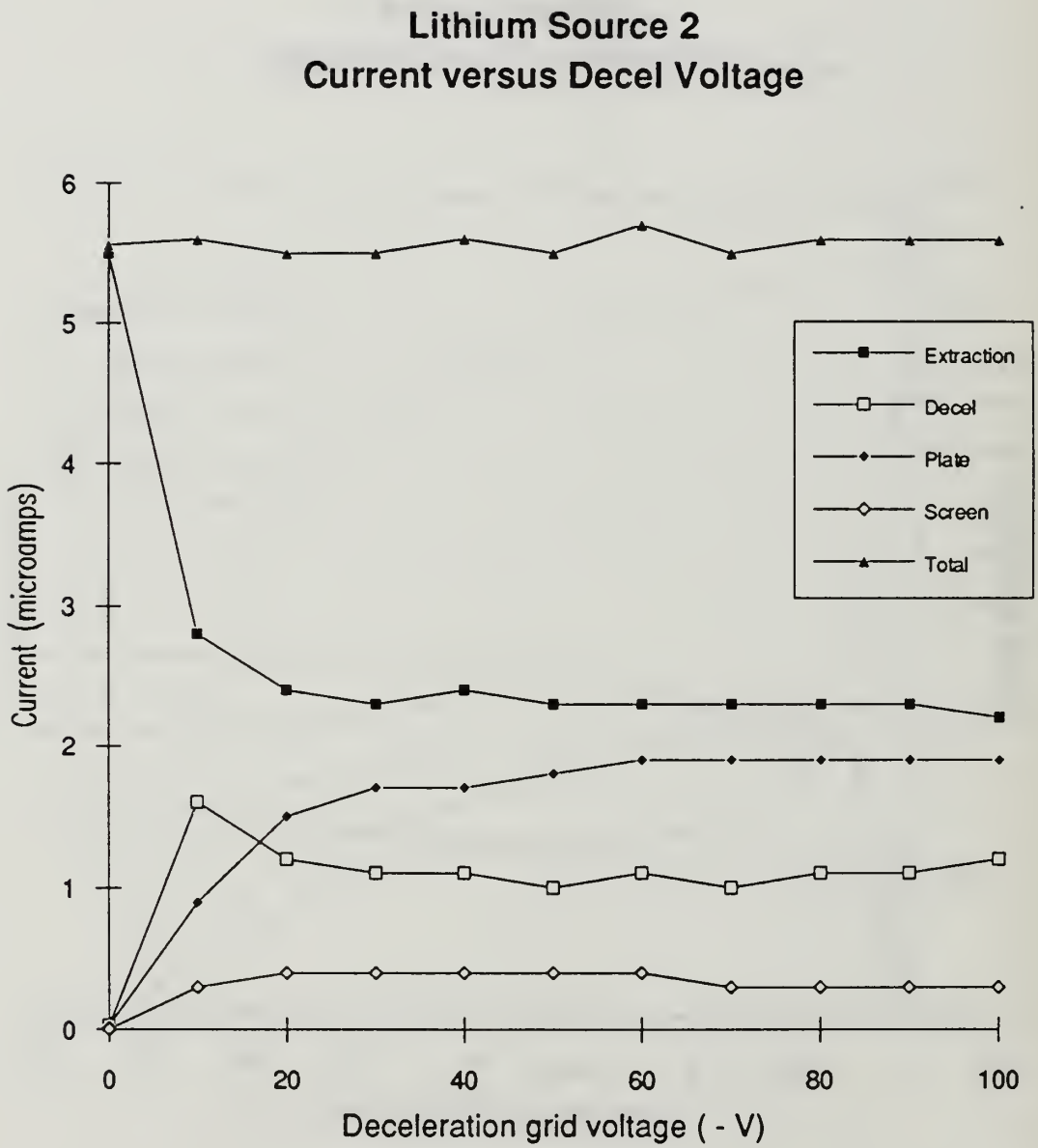

Figure 23. **Lithium ion source 2, current versus deceleration voltage, initial design.**

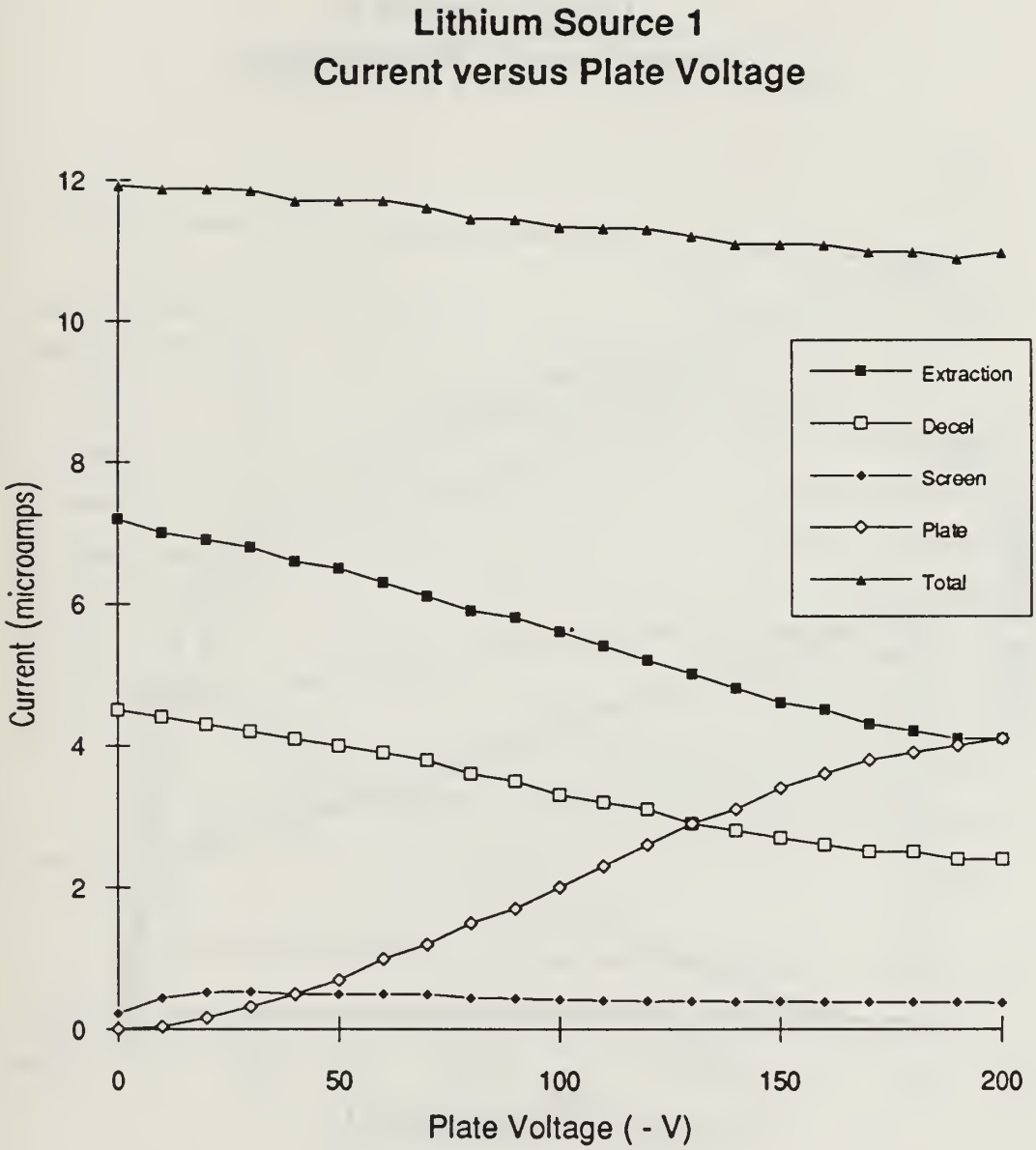

Figure 24. Lithium ion source 1, current versus plate voltage, initial design.

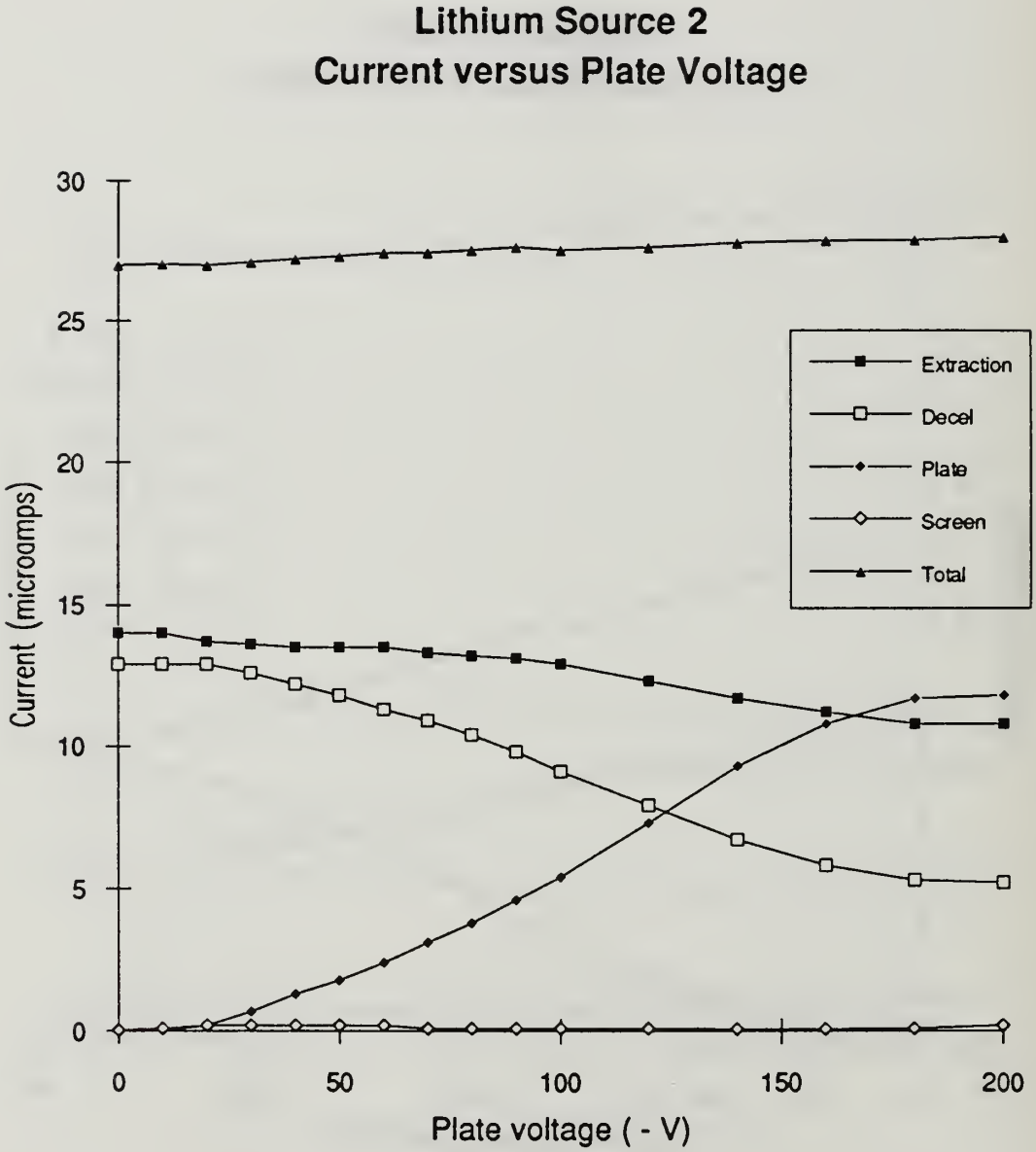

Figure 25. **Lithium ion source 2, current versus plate voltage, initial design.**

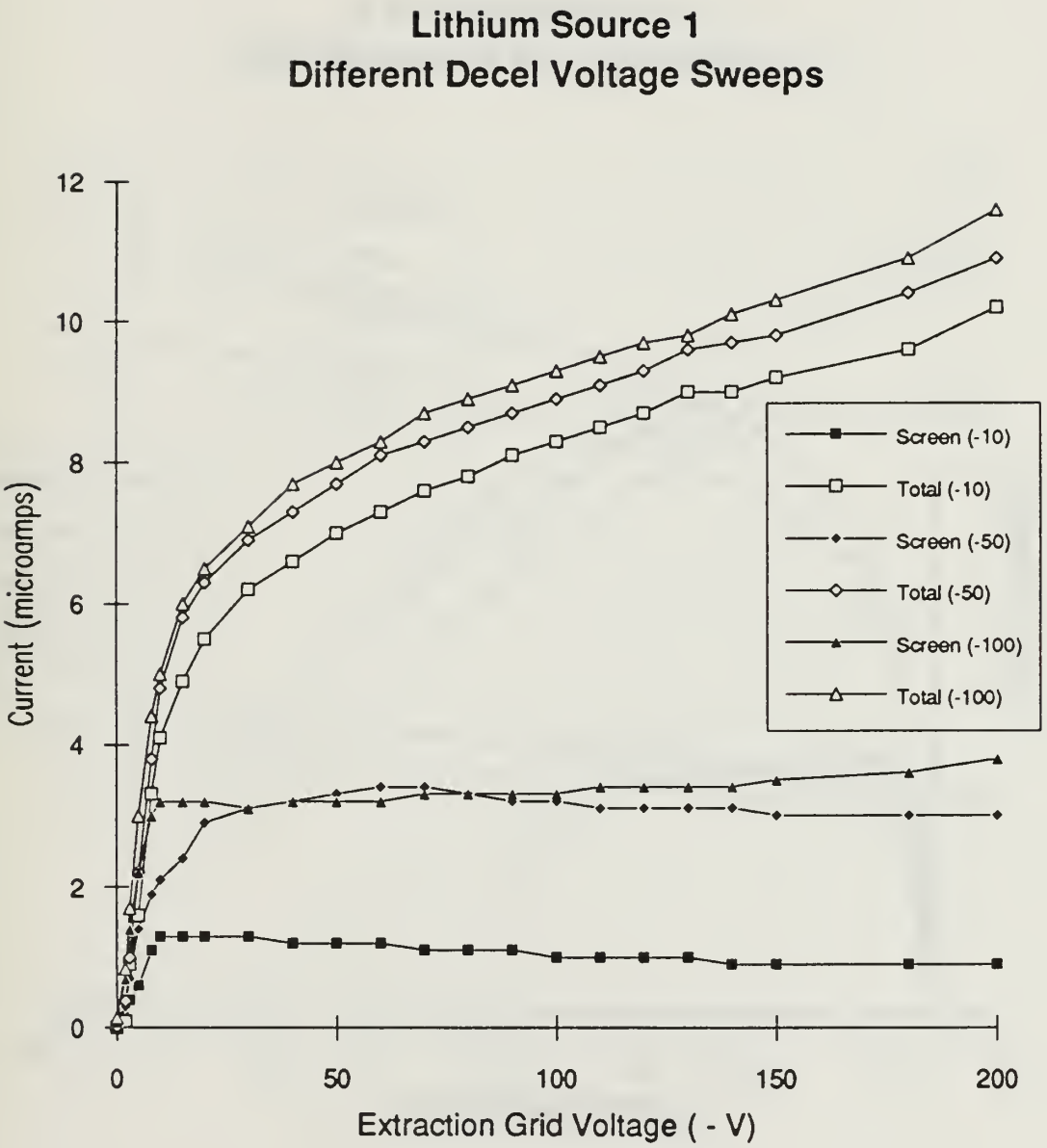

Figure 26. **Lithium ion source 1, comparison of current versus extraction voltage for 3 different deceleration voltages, initial design.**

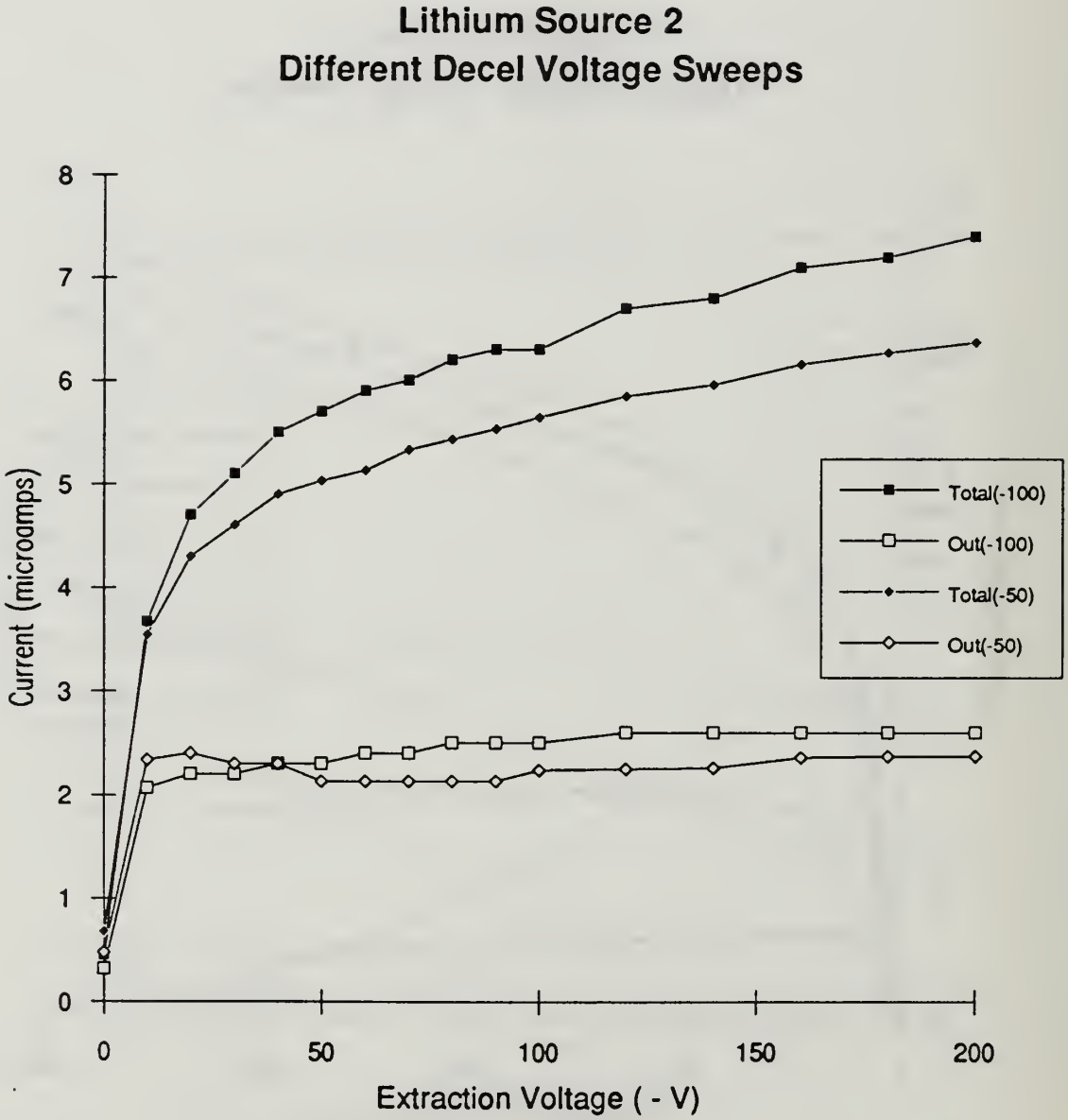

Figure 27. **Lithium ion source 2, comparison of current versus extraction voltage for 2 different deceleration voltages, initial design.**

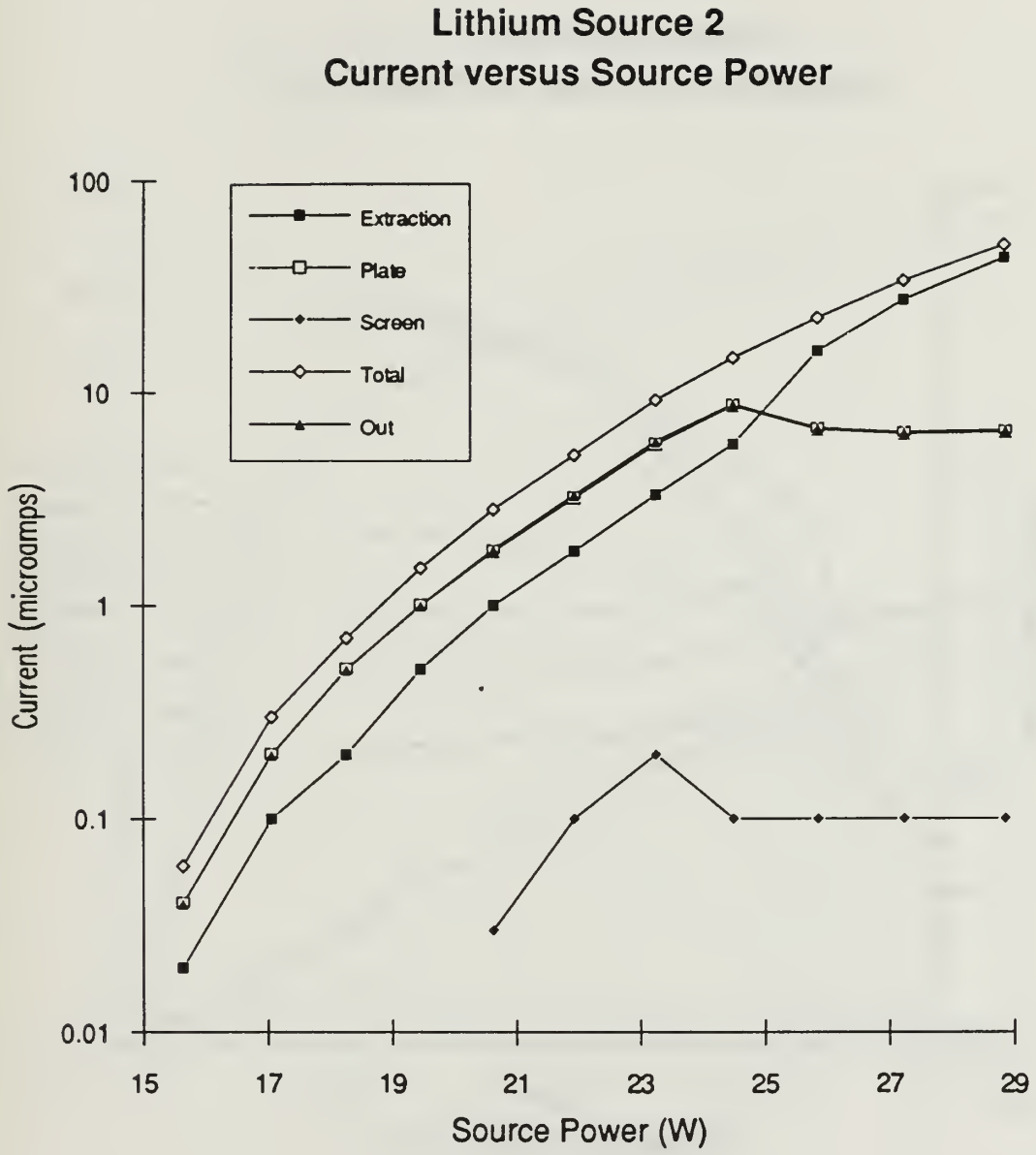

Figure 28. **Lithium ion source 2, current versus ion source power, deceleration grid removed.**

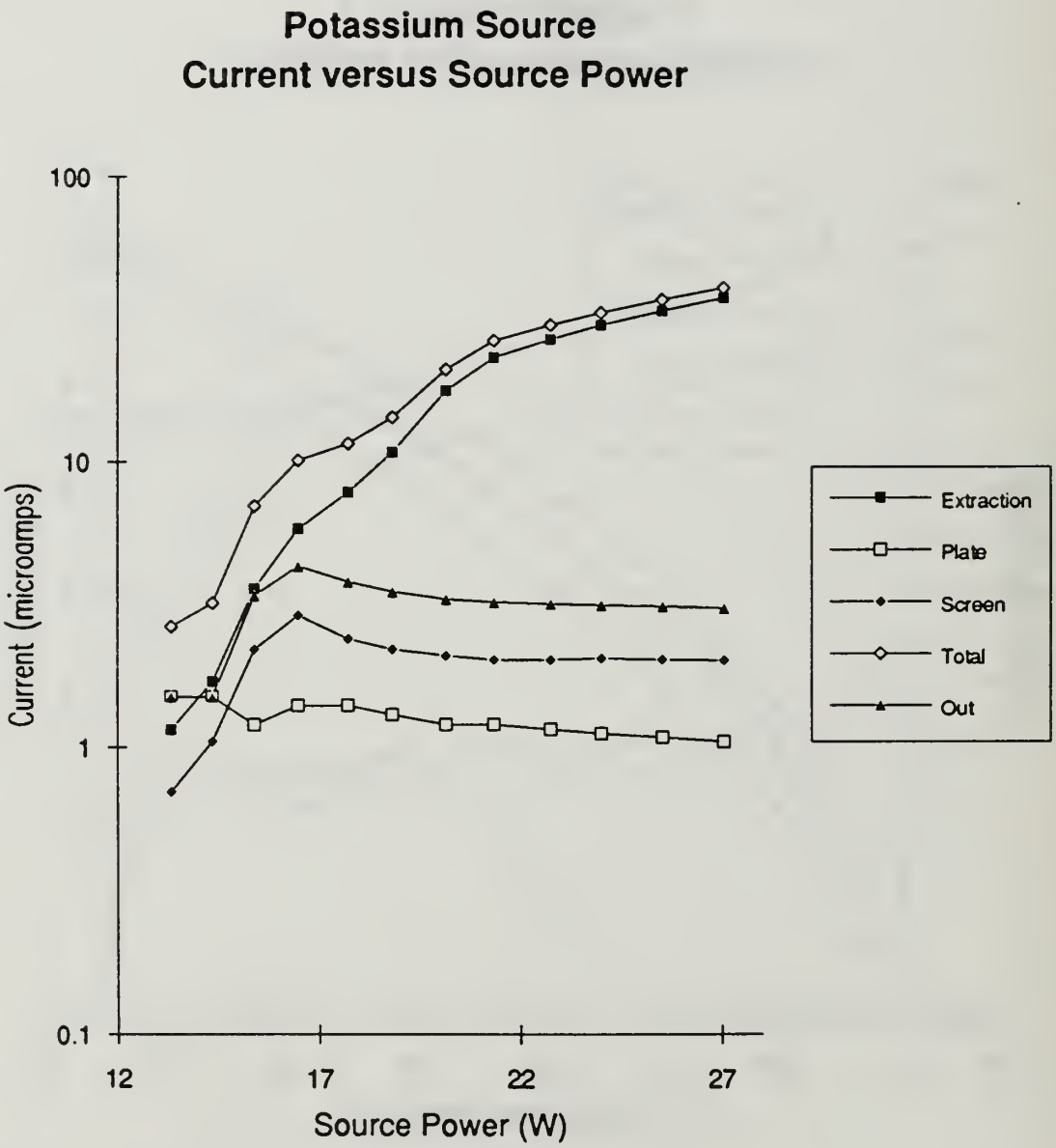

Figure 29. **Potassium ion source, current versus ion source power, deceleration grid removed.**

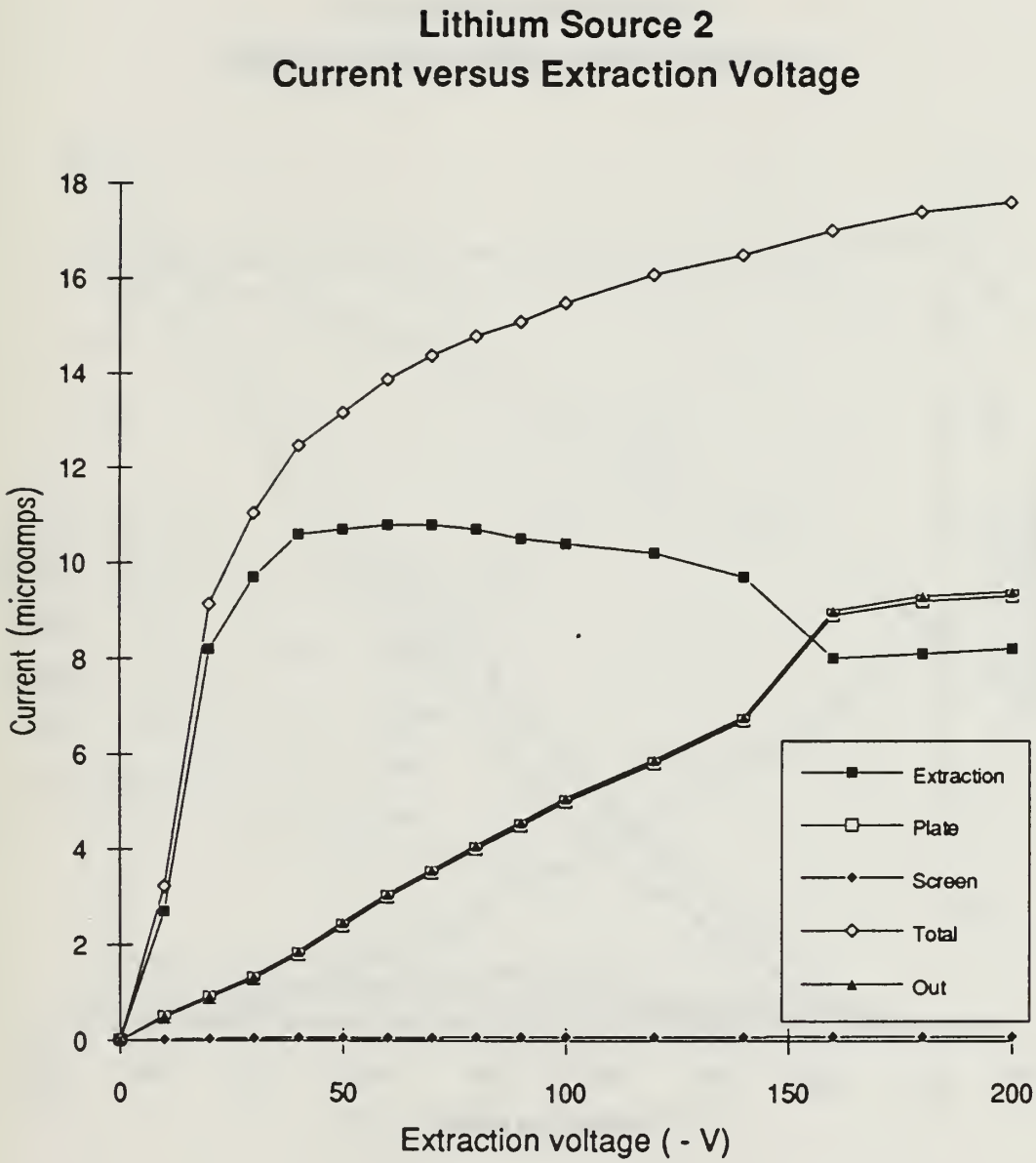

Figure 30. **Lithium ion source 2, current versus extraction voltage, deceleration grid removed.**

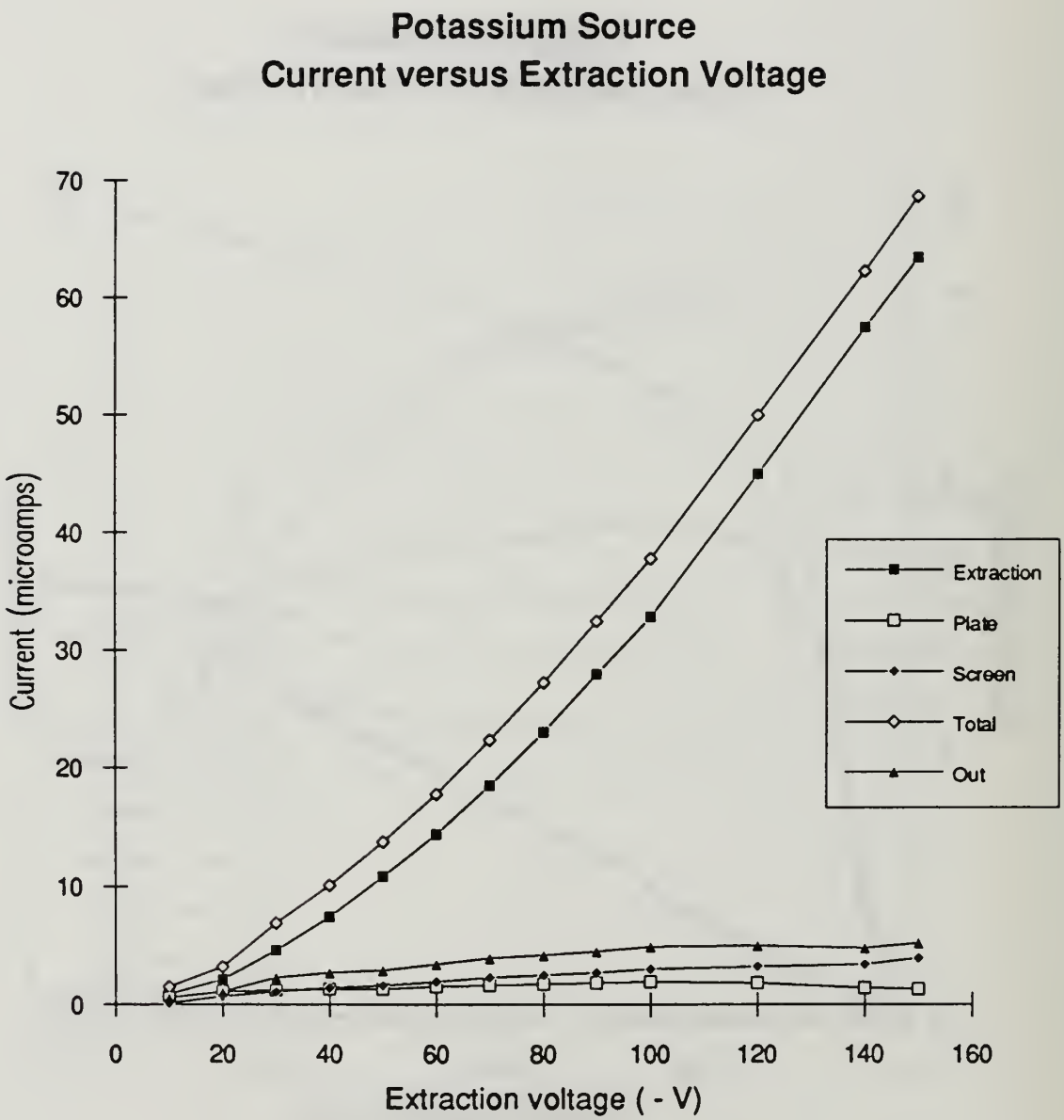

Figure 31. **Potassium ion source, current versus extraction voltage, deceleration grid removed.**

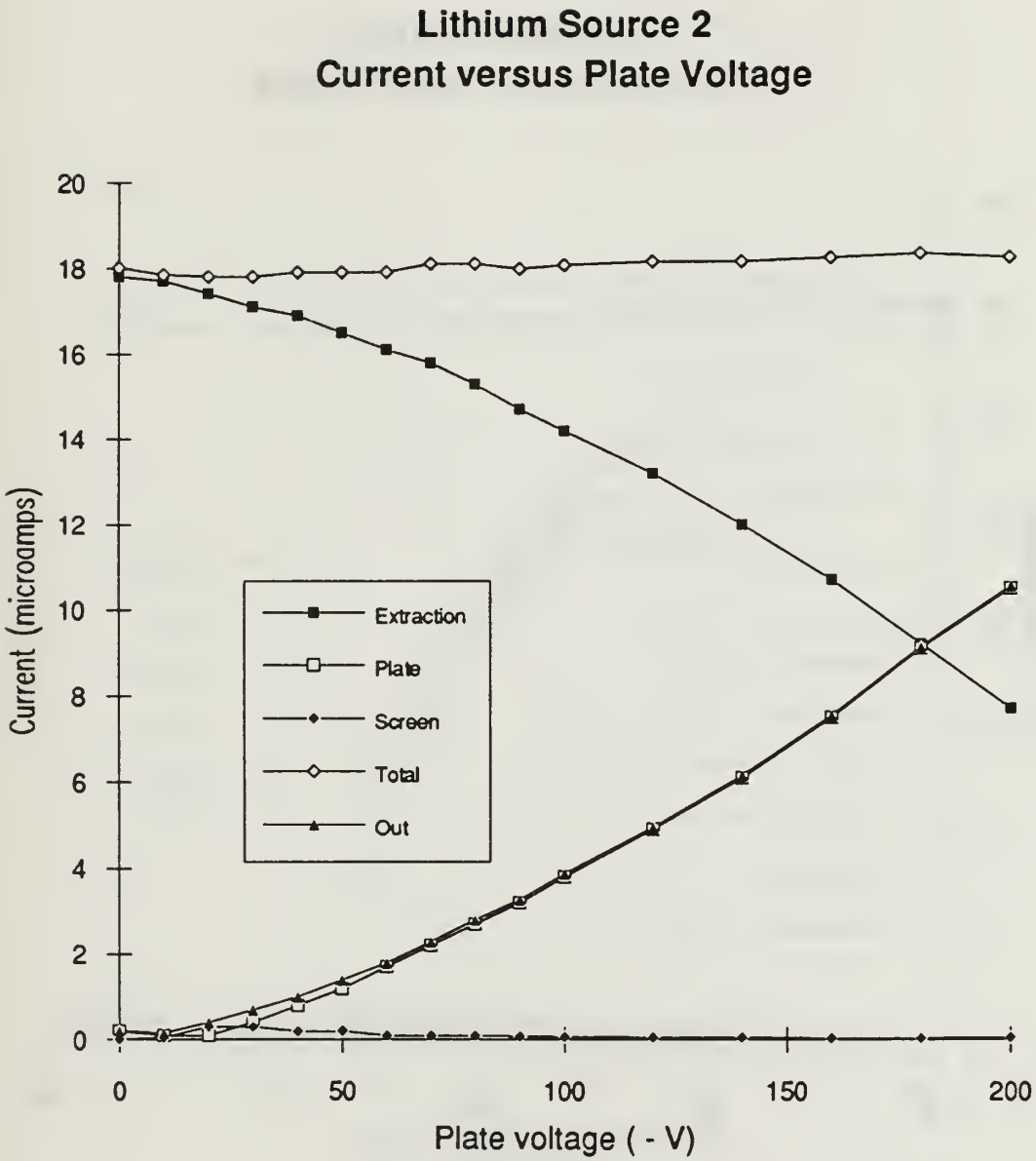

Figure 32. **Lithium ion source 2, current versus plate voltage, deceleration grid removed.**

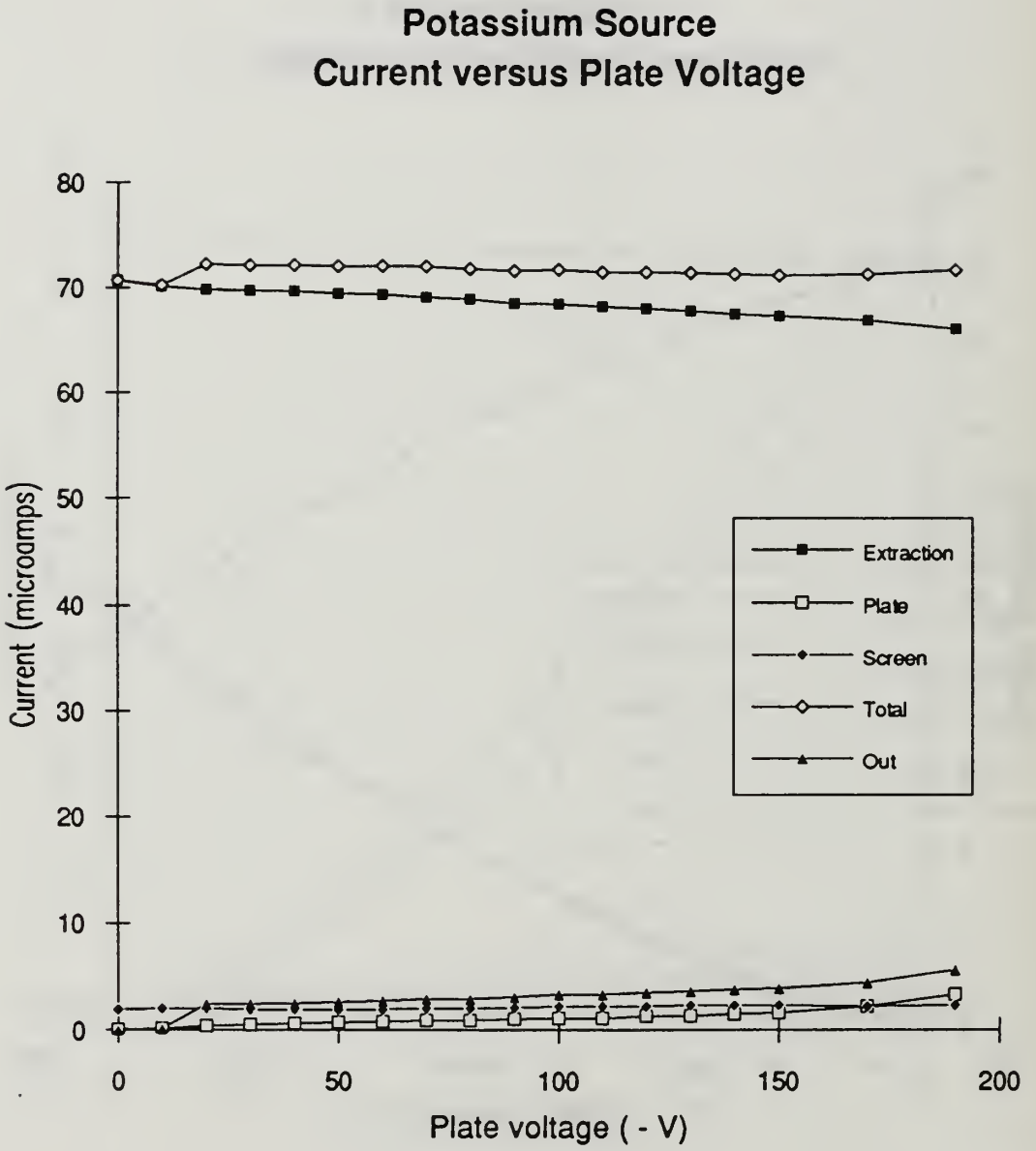

Figure 33. **Potassium ion source, current versus plate voltage, deceleration grid removed.**

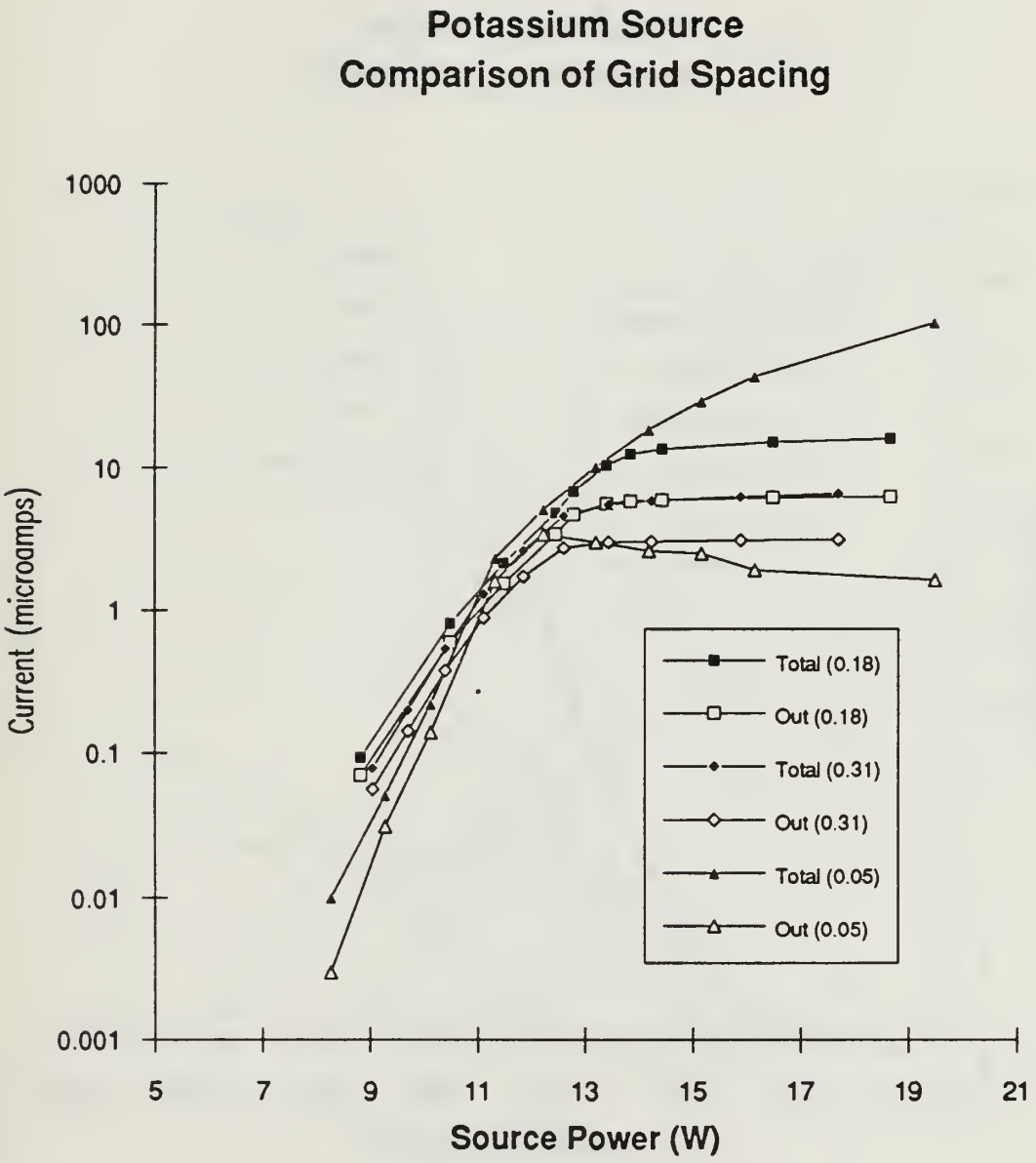

Figure 34. Potassium ion source, comparison of current versus ion source power for different extraction grid spacings, deceleration grid removed.

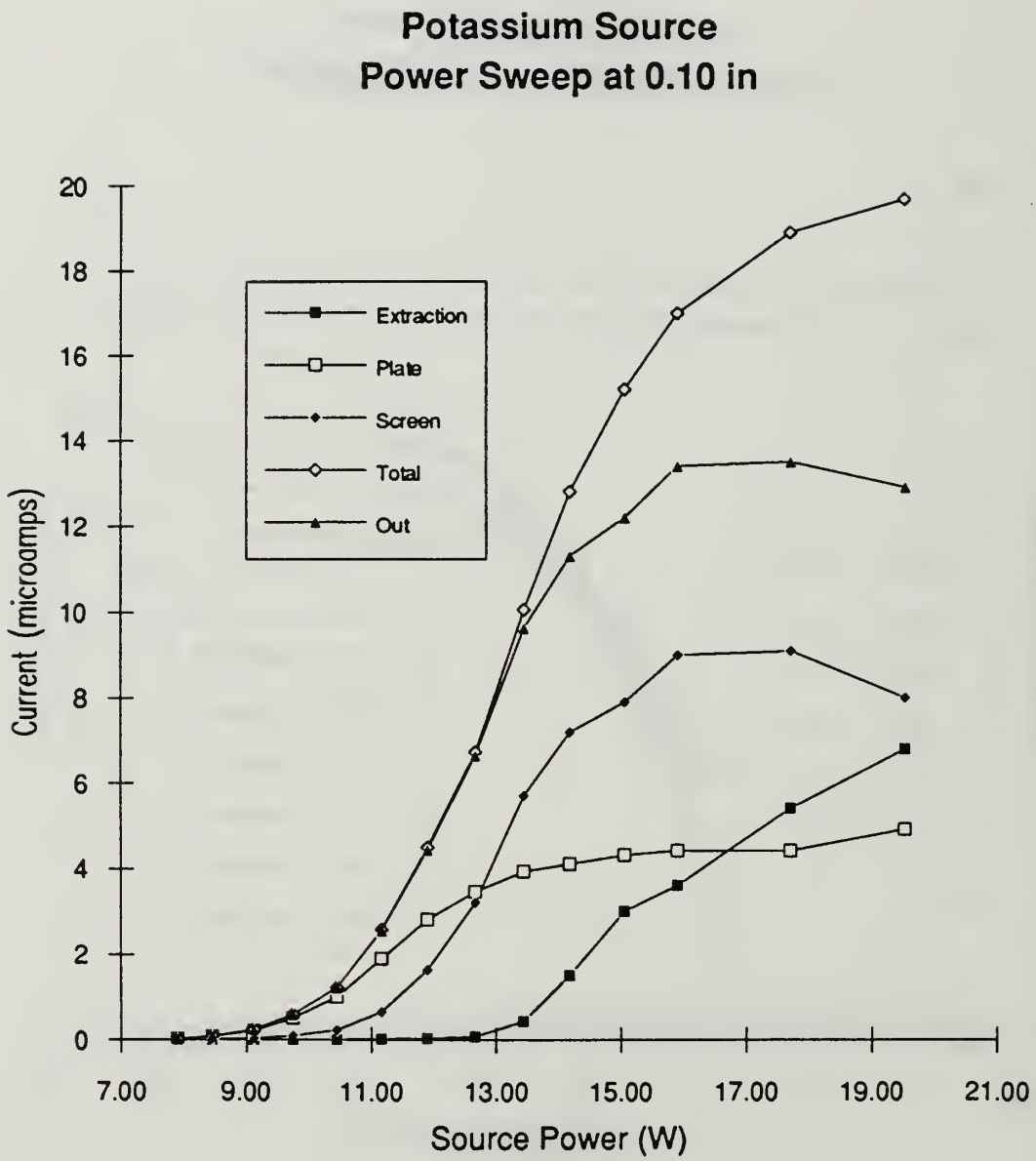

Figure 35. **Potassium ion source, current versus ion source power with new extraction grid at spacing of 0.10 inches.**

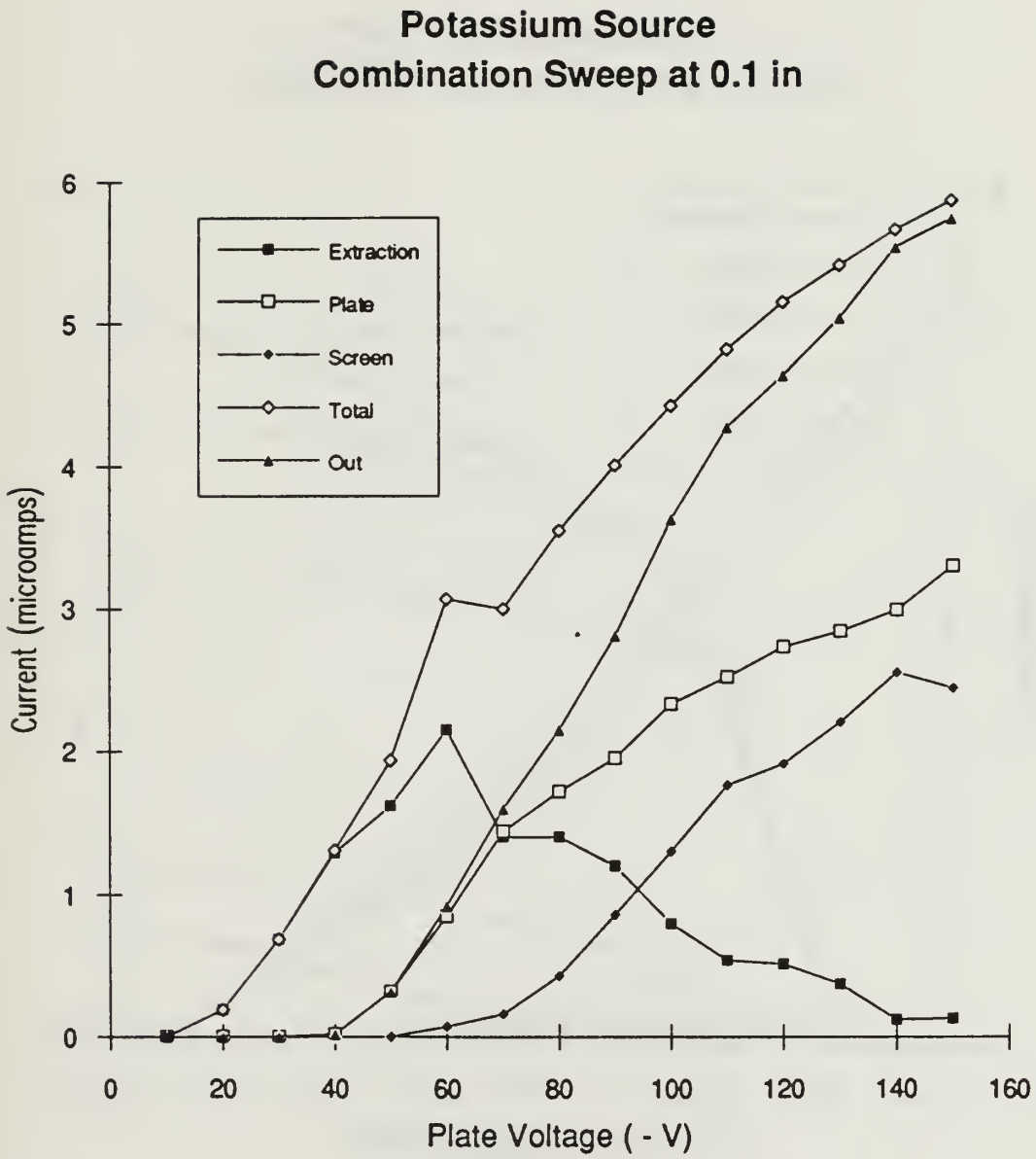

Figure 36. **Potassium ion source, current versus ion source power while varying voltages in tandem, new extraction grid at spacing of 0.10 inches.**

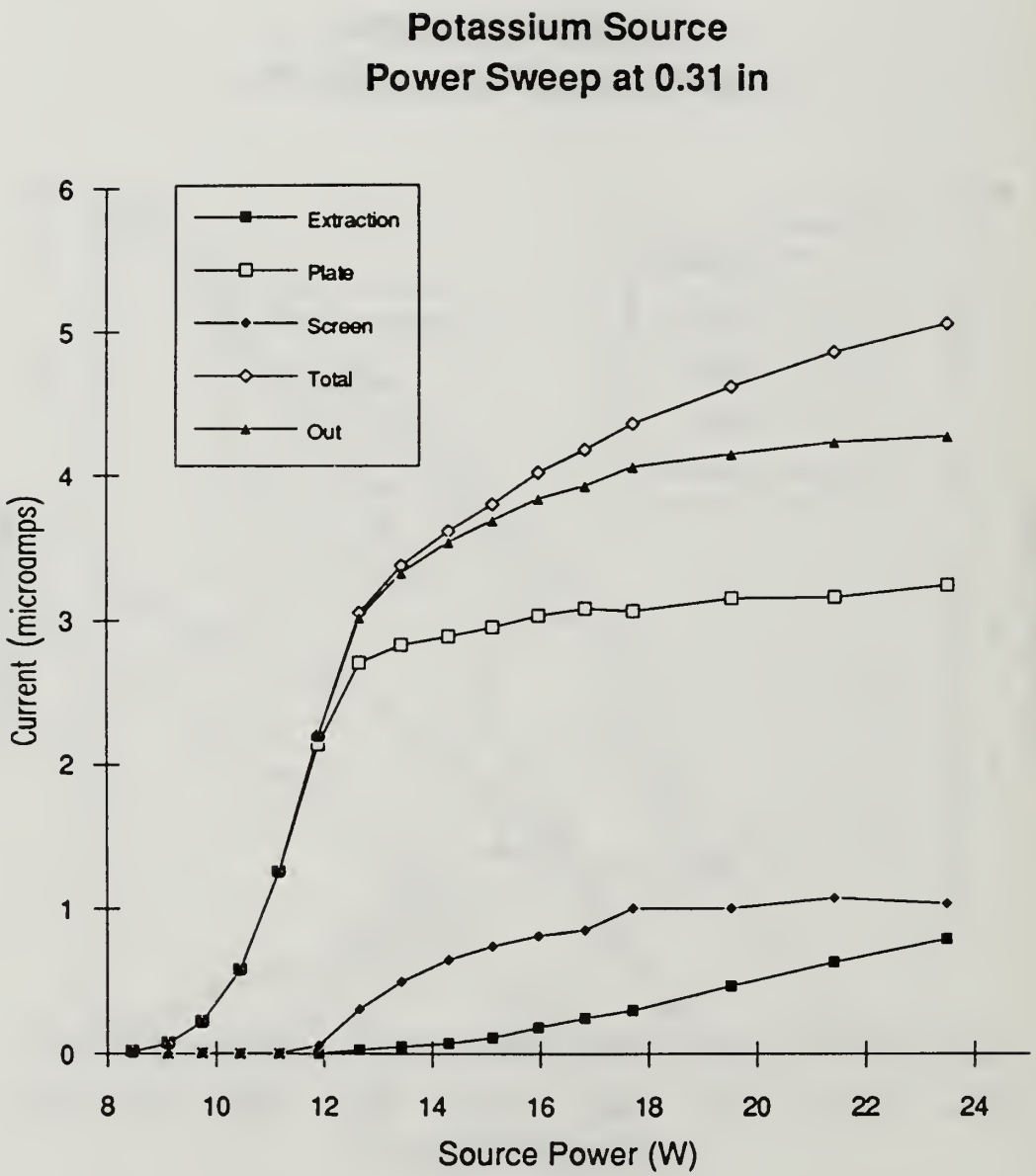

Figure 37. **Potassium ion source, current versus ion source power with new extraction grid at spacing of 0.31 inches.**

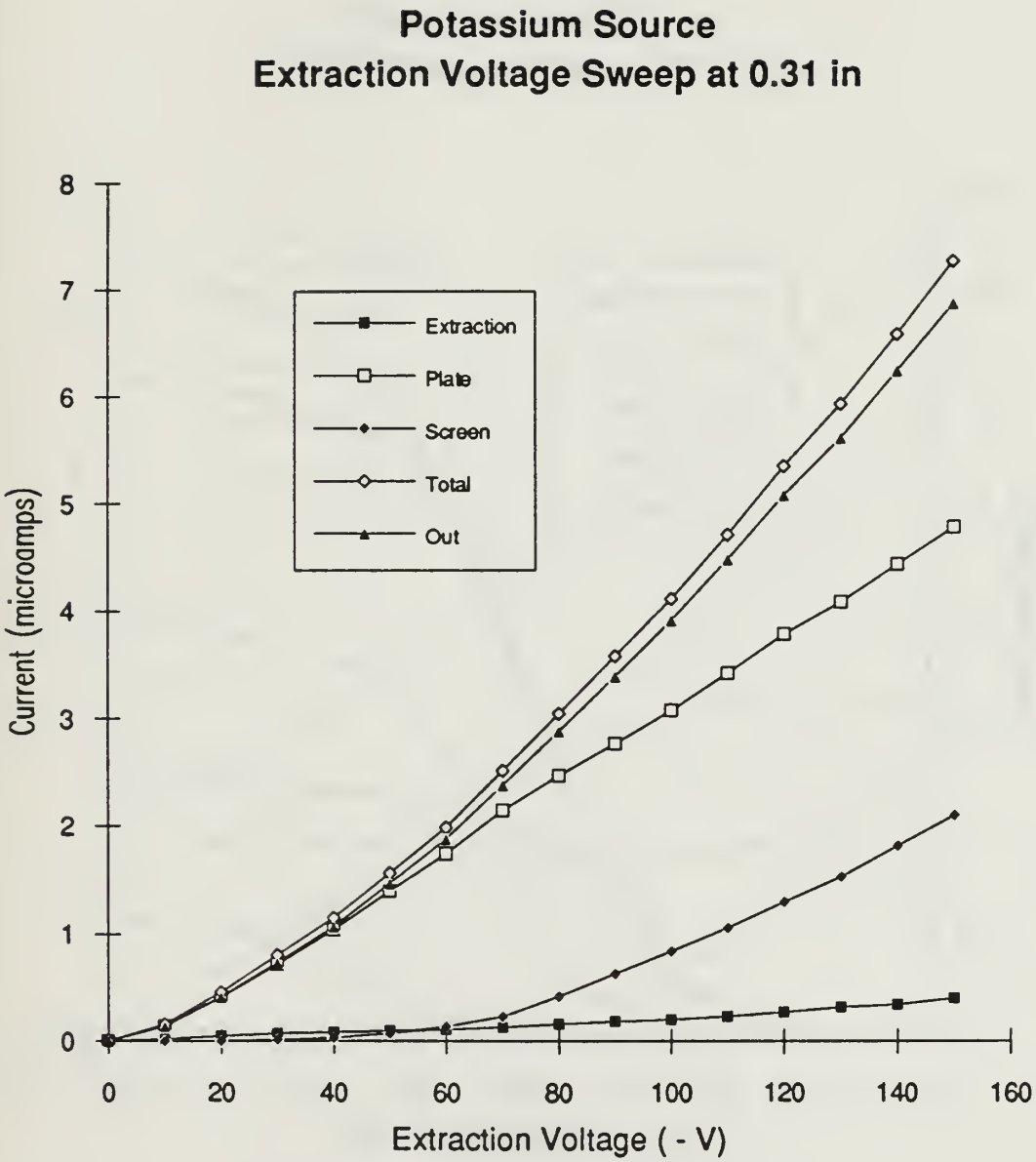

Figure 38. **Potassium ion source, current versus extraction voltage, new extraction grid at spacing of 0.31 inches.**

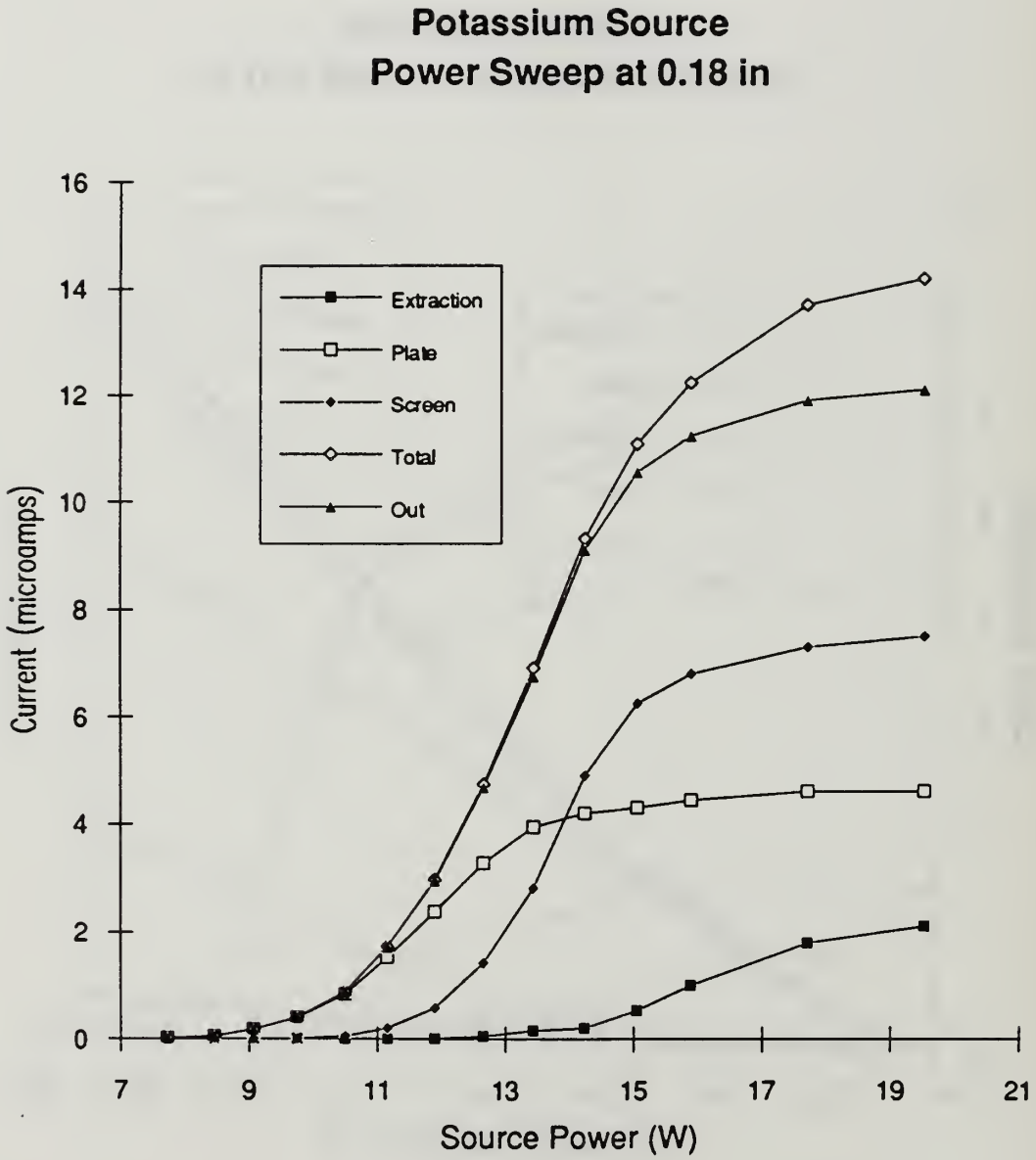

Figure 39. **Potassium ion source, current versus ion source power with new extraction grid at spacing of 0.18 inches.**

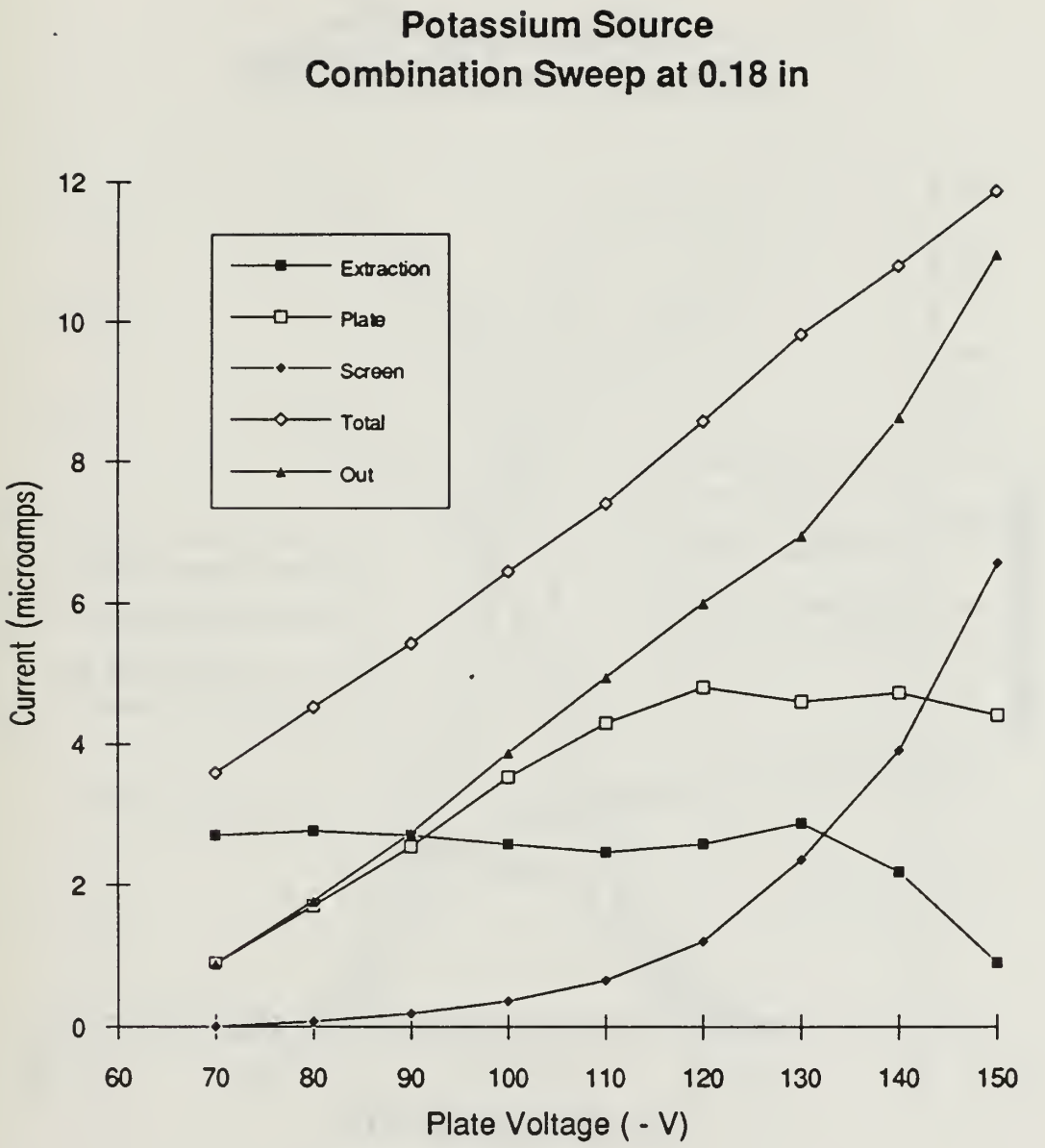

Figure 40. **Potassium ion source, current versus ion source power while varying voltages in tandem, new extraction grid at spacing of 0.18 inches.**

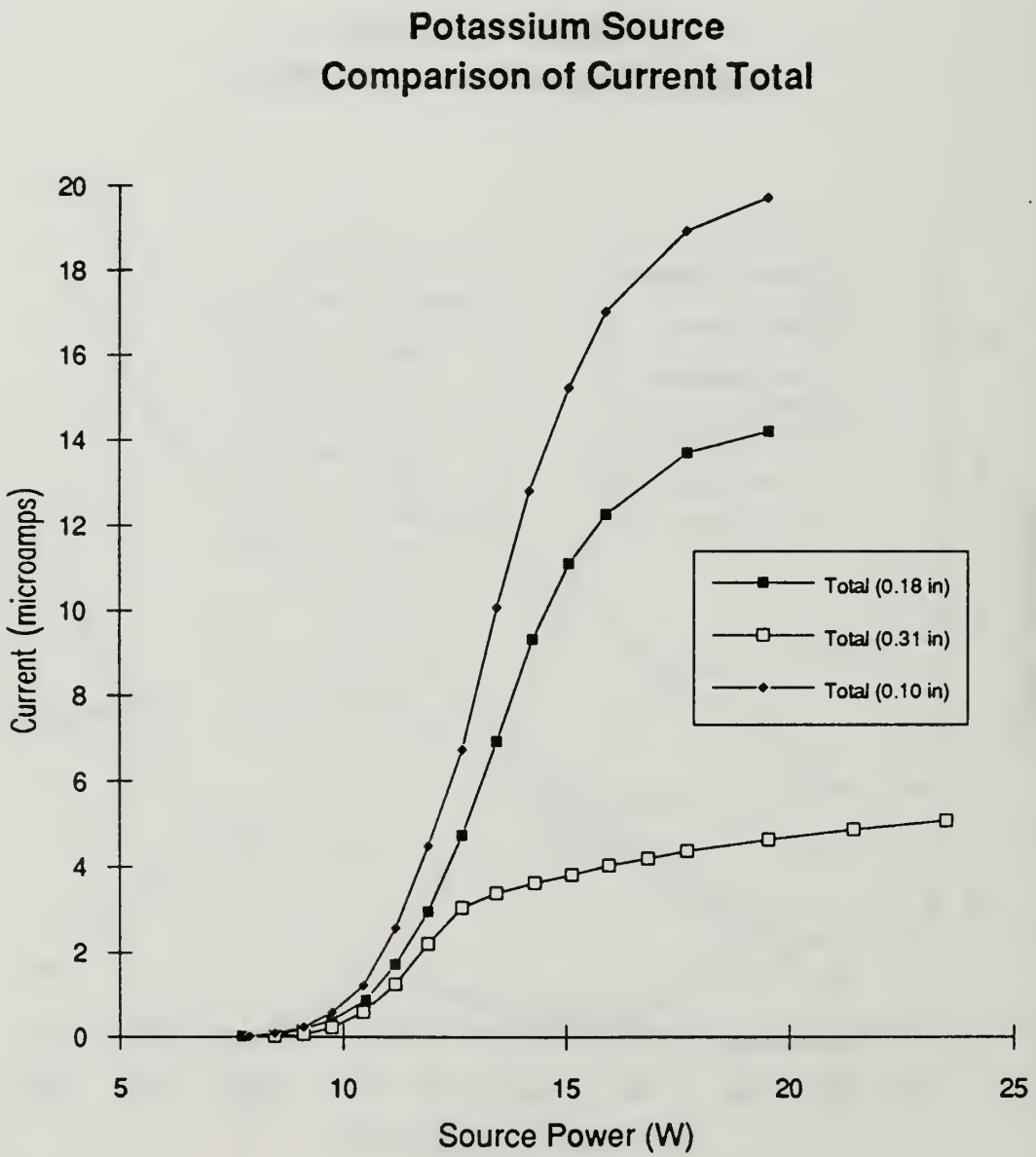

Figure 41. **Potassium ion source, total current versus ion source power for new extraction grid at 3 different spacings.**

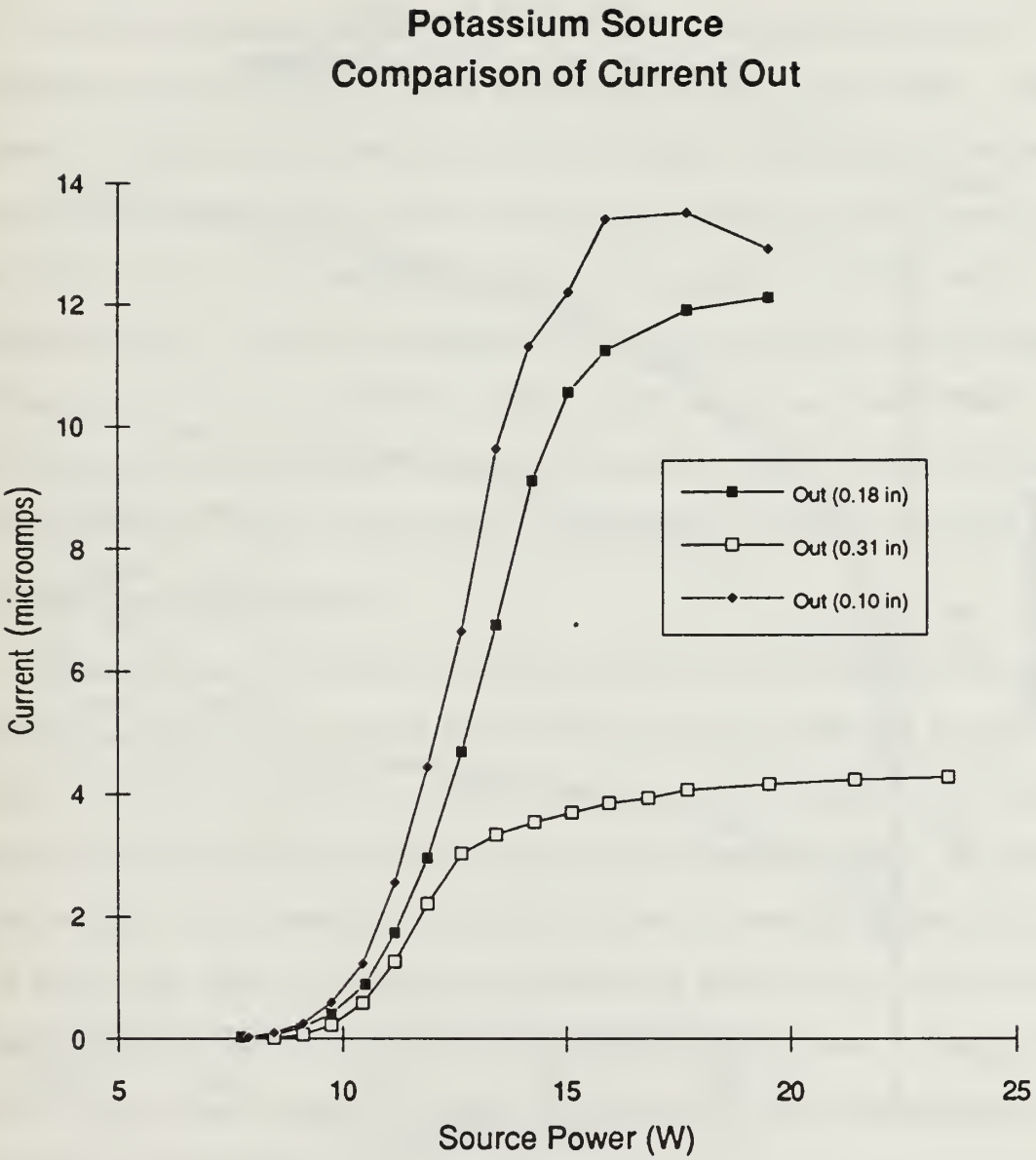

Figure 42. Potassium ion source, current out of the charge control device versus ion source power for new extraction grid at 3 different spacings.

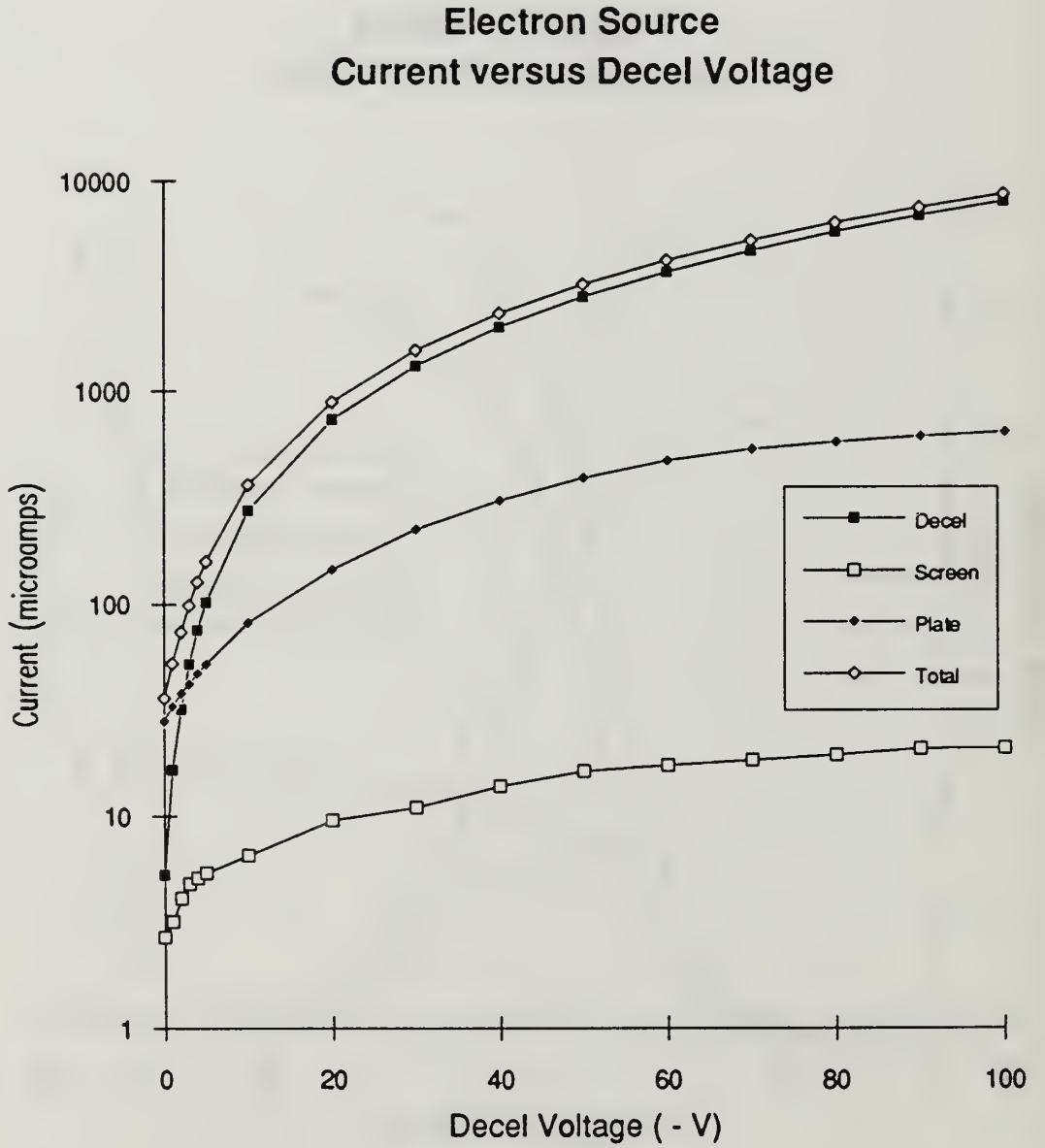

Figure 43. **Electron source, current versus filament power.**

APPENDIX C

To facilitate the design of the charge control device to be used in this experiment, previous designs were investigated (Rovang and Wilbur, 1982), (Homa and Wilbur, 1982), and (Haskell, *et al,* 1966). These designs varied in the utilization of the ion source and used different methods to pull the ions off of the emitter face. In our preliminary design the question is raised as to what effect the type of grid, the transparency of the grid, and the actual spacing between the extraction grid and the emitter face has on the overall results. A preliminary test was conducted to answer these questions to finalize the design of the final charge control device and the test program to optimize its output.

A. GRID TRANSPARENCY

The device used by Gant in his experiments was modified for these tests. A Lithium ion source was installed and heated to 1100 °C while the screen was biased to -200 V. A grid was manufactured with a removable plate around the center hole. On this plate a set of crossing grooves were machined. By placing equal length stainless steel wire in different grooves a mesh pattern was formed. The plate and groove arrangement allowed the movement of the wires to different spacings between the wires giving various transparency to the grid. An extraction grid sweep was then conducted at these different transparencies and the results are plotted in Figure C-1.

B. GRID SPACING

A set of 2 different sized ceramic spacers allowed the extraction grid to be spaced at a distance of 0.25 or 0.41 inches from the emitter face. A sweep of

the extraction voltage was conducted with the ion source heated to 1100 °C and the results are plotted in Figure C-2.

C. Results

The results of Figure C-1 indicate that grid transparency influences the current out of the emitter and to the screen. As transparency increases the current out of the emitter-grid assembly to the screen also increases.

Figure B-2 indicates that spacing has an effect on the current emitted but not as great as the transparency. The differences in current out of the emitter when the extraction grid is moved closer is about 10 % of total current produced.

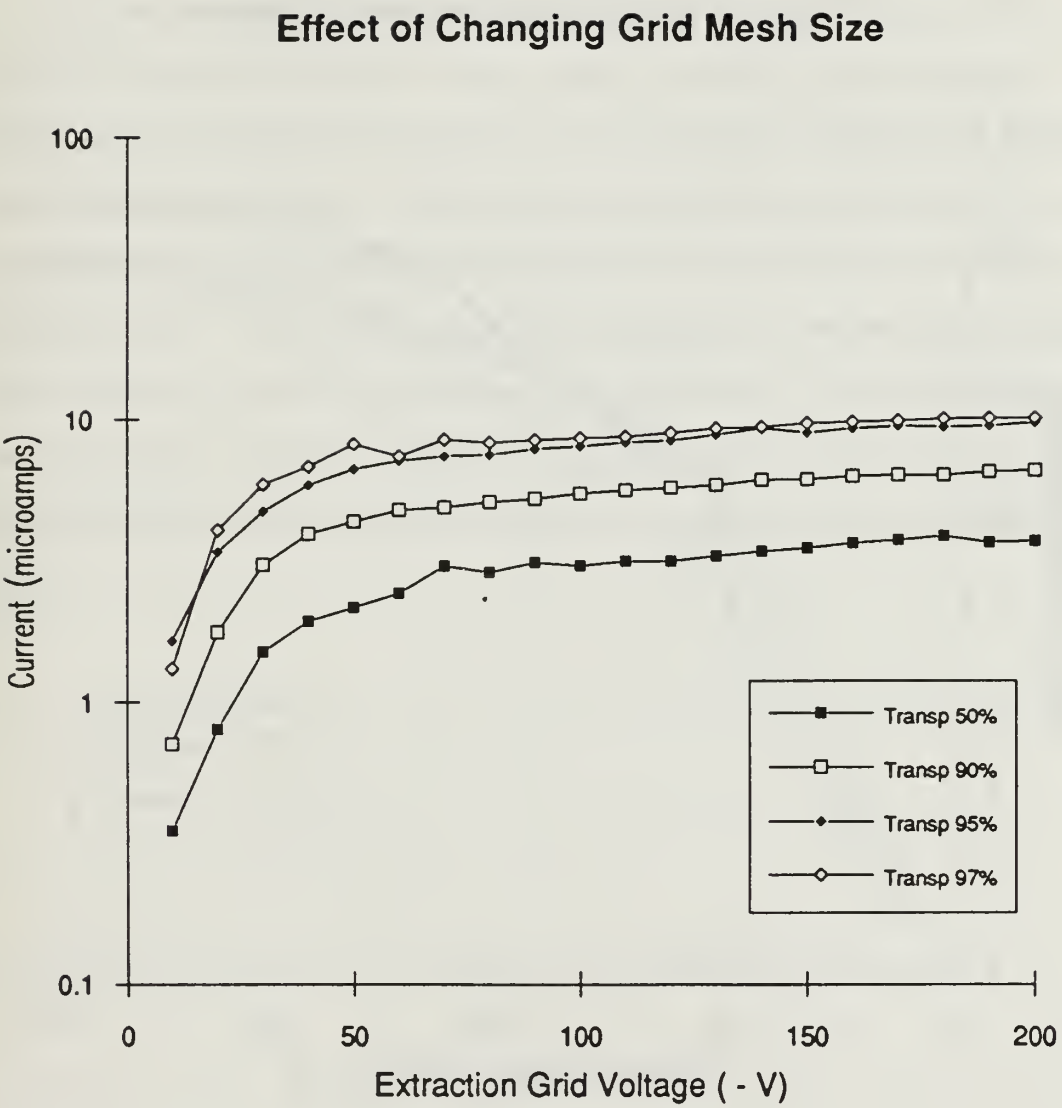

Figure C-1. **Current versus extraction voltage for different extraction grid transparencies.**

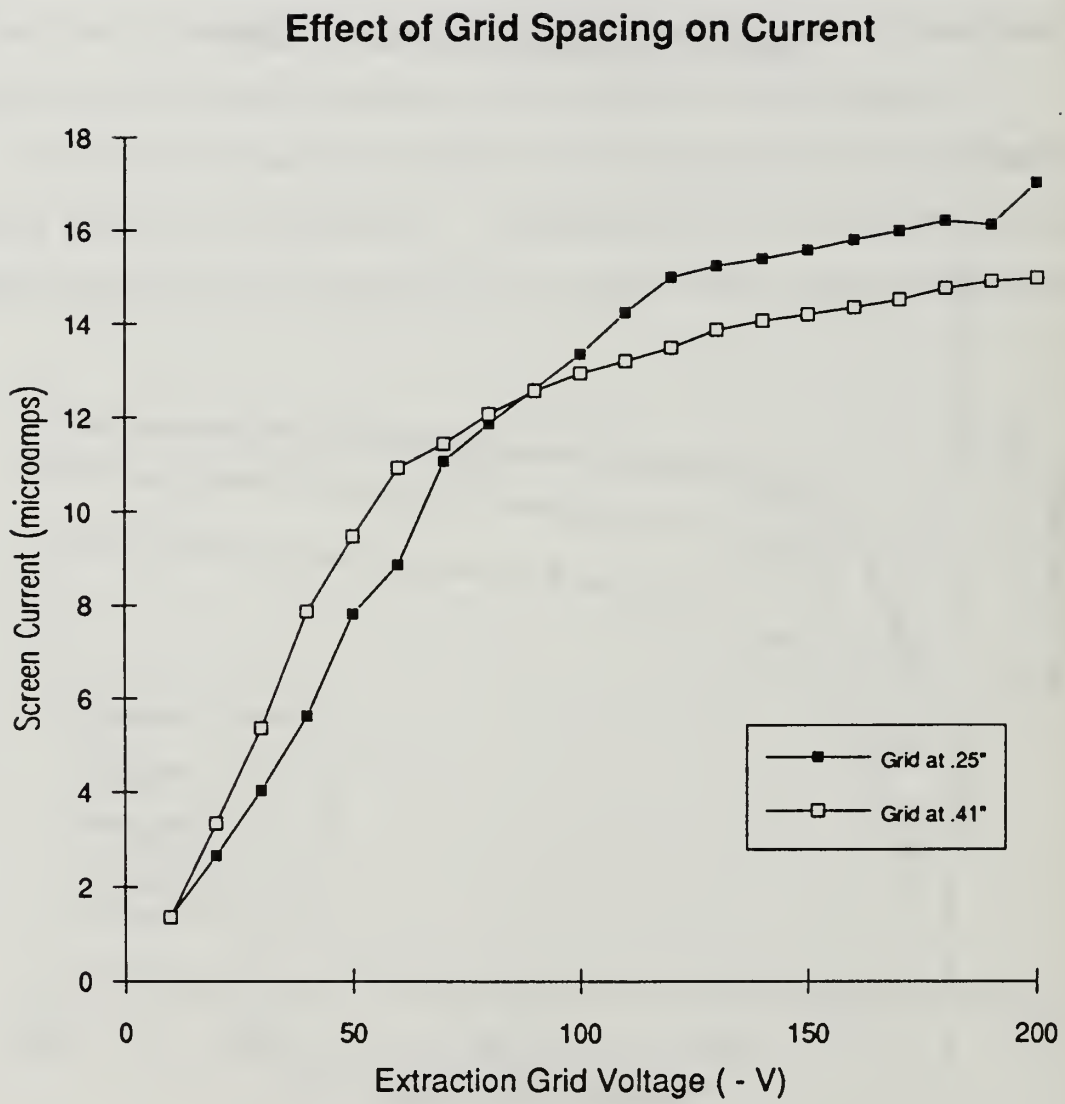

Figure C-2. **Screen current versus extraction voltage for 2 different extraction grid spacings.**

APPENDIX D

A. THERMOCOUPLE

An experimental thermocouple made of Tungsten and Rhenium (5%) was imbedded in each ion source's heater potting to assist in data collection. The thermocouple was calibrated against the ion source's temperature readings using an optical pyrometer. The thermocouple reading was found to be very accurate and when used with the calibration table the temperature was quickly and easily found. Each ion source was calibrated for thermocouple voltage versus temperature prior to conducting any experiments. Output voltage for a given temperature varies by ~10% from source to source. Figure D-1 is a plot of the thermocouple voltage versus measured temperature for the first Lithium ion source.

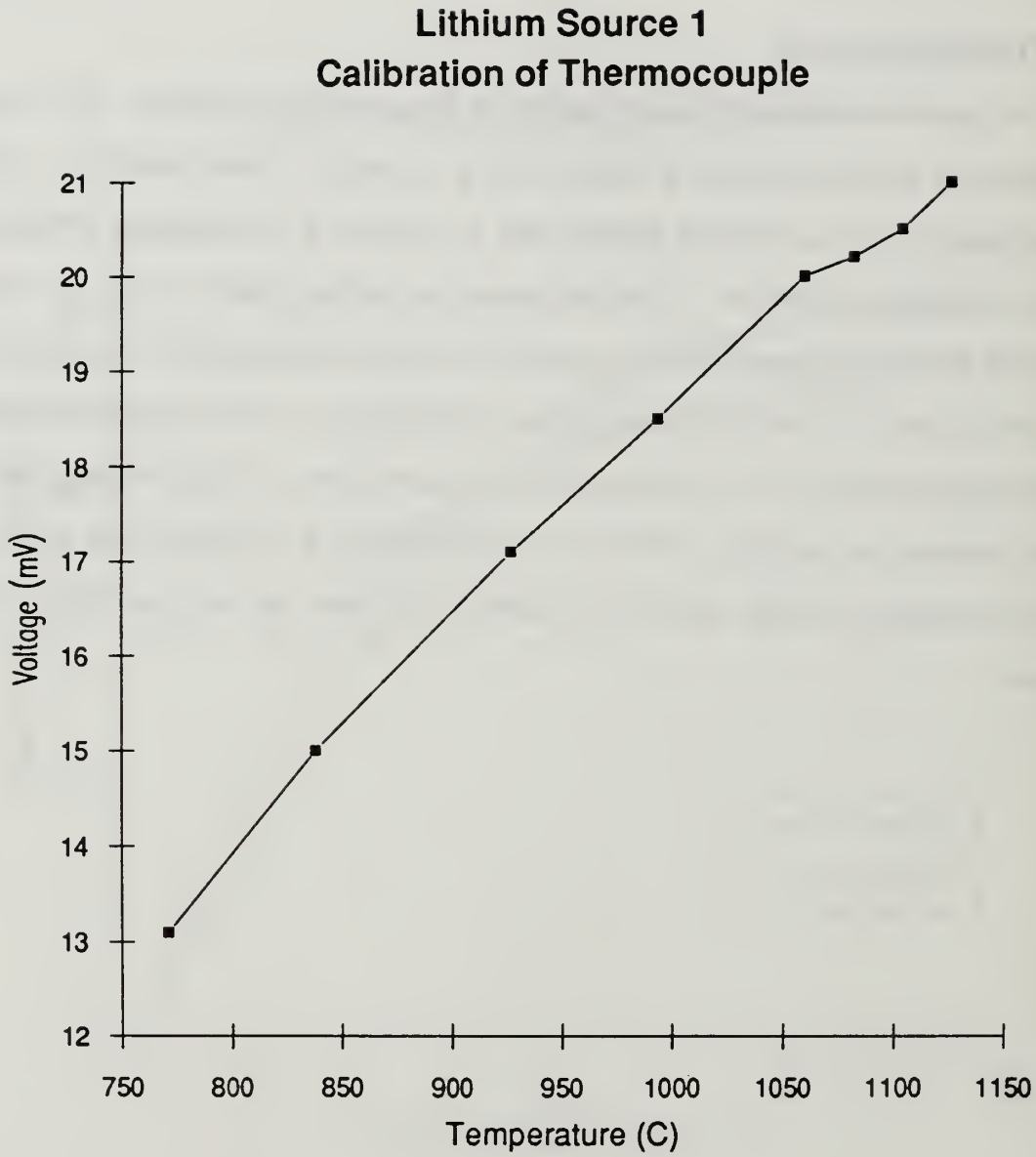

Figure D-1. Calibration of thermocouple, thermocouple voltage versus source temperature.

LIST OF REFERENCES

Blewett, J. P.,and Jones, E. J.,"Filament Sources of Positive Ions," *Physical Review*, v.50, pp.464-468, 1936.

Cobine, J.D., *Gaseous Conductors (Theory and Engineering Applications)*, pp. 123-128, Dover Publishing Inc., 1958.

Craven, P.D, and others, "Potential Modulation on the SCATHA Spacecraft," *Journal of Spacecraft and Rockets,* v. 24, pp. 150-157, 1987.

Davis, V.A., and Katz,I., "Plasma Sources for Active Charge Control," Proceedings of the Spacecraft Charging Technology Conference, Monterey, California, 31 October - 3 November, 1989.

DeForest, S.E., and McIlwain, C.E., "Plasma Clouds in the Magnetosphere," *Journal of Geophysical Research,* v. 76, 1971.

DeForest, S.E., "Spacecraft Charging at Synchronous Orbit," *Journal of Geophysical Research,* v. 77, p. 651,1972.

Gant, D.A., *Comparison of Alkali Ion Emitters*, Master's Thesis, Naval Postgraduate School, Monterey, California, December 1991.

Garrett, H.B., and Pike, C.P., "Space Systems and Their Interactions with Earth's Space Environment; Spacecraft Charging: A Review," *Progress in Astronautics and Aeronautics,* v. 71, pp. 167-226, 1980.

Grard,R., Knott, K., and Pederson, A., Spacecraft Charging Effects, *Space Science Reviews,* v.34, pp.289-303, 1983.

Gussenhoven, M. S.,and Mullen, E. G.,"Geosynchronous Environment for Severe Spacecraft Charging,"*Journal of Spacecraft and Rockets*,v.20, pp.26-32, 1983.

Haskell, H.B., Heinz, O., and Lorents, D.C., "Multistage Gun for Production of low energy ion beams," *The Review of Scientific Instruments*, v.37, pp.607-614, 1966.

Heinz, O.,and Reaves, R. T., "Lithium Ion Emitter for Low Energy Beam Experiments," *The Review of Scientific Instruments*, v.39, pp.1229-1230, 1968.

Hess, W., and others, "Artificial Aurora Experiment: Experiment and Principal Results," *Journal of Geophysical Research,* v.76, pp 6067-6081, 1971.

Homa, J.M., and Wilbur, P.J., "Ion Beamlet Vectoring by Grid Translation," AIAA/JSASS/DGLR 16th International Electric Propulsion Conference, New Orleans, Louisiana, 17-19 November, 1982.

Hunter,R.E., and others, "Cesium Contact Ion Microthruster Experiment Aboard Applications Technology Satellite (ATS-4)," *Journal of Spacecraft and Rockets*, v. 6, p. 968, 1969.

Jet Propulsion Laboratory Report GL-TR-89-0222, *Spacecraft Environmental Anomalies Handbook,* by P.A. Robinson, 1 August 1989.

Johnson, F. M., "Studies of the Ion Emitter Beta-Eucryptite," *RCA Review*, pp.427-446, September 1962.

Koons, H.C., and others, "Severe Spacecraft-Charging Event on SCATHA in September 1982," *Journal of Spacecraft and Rockets*, v. 25, pp.239-243, 1988.

McPherson, D.A. and Schober, W.R., "Spacecraft Charging at High Altitudes: The SCATHA Satellite Program," *Spacecraft Charging by Magnetospheric Plasmas*, v.47, AIAA, ed. A. Rosen, AIAA with MIT Press, 1976.

Moore, J.H., Davis, C.C., and Coplan, M.A., *Building Scientific Apparatus: A Practical Guide to Design and Construction*, pp. 305-321, Addison-Wesley Publishing Company,, 1983.

Norwood, C.W., Olsen, R.C., and Li, W.W., "Observations of Ions Generated on or Near Satellite Surfaces", paper presented at the AIAA 26th Aerospace Sciences Meeting, Reno, Nevada, 11-14 January, 1988.

Olsen, R.C., and Whipple, E.C., "Operations of the ATS-6 Ion Engine", paper presented at USAF/NASA Spacecraft Technology Conference, USAF Academy, Colorado, 31 October - 2 November, 1978.

Olsen, R.C., "Modifications of Spacecraft Potentials by Plasma Emission," *Journal of Spacecraft and Rockets,* v.18, pp.462-469, 1981.

Olsen, R.C., "Experiments in Charge Control at Geosynchronous Orbit, ATS-5 and ATS-6," *Journal of Spacecraft and Rockets,* v. 22, pp. 254-264, 1985.

Olsen, R.C., "Record Charging Events from Applied Technologies Satellite," *Journal of Spacecraft and Rockets,* v.24, p.362, 1987.

Olsen, R.C., Lowery, D.R., and Weddle, L.E., "Plasma Wave Observations During Electron and Ion Experiments," paper presented at the AIAA 26th Aerospace Sciences Meeting, Reno, Nevada, 11-14 January, 1988.

Olsen, R.C., *"Charging Characteristics of Dynamics Explorer I Retarding Ion Mass Spectrometer and the Consequence for Core Plasma Measurements,"* Naval Postgraduate School Technical Report NPS-61-89-014, September 1989.

Olsen, R.C., Weddle, L.E. and Roeder, J.L., "Plasma Wave Observations During Ion Gun Experiments," *Journal of Geophysical Research,* v. 95, pp. 7759-7771, 1990.

Pollock, C. J., *Rocket-borne Low Energy Ion Measurements in Space,* Phd dissertation, University of New Hampshire, 1987.

Purvis, C.K., and Bartlett, R.O., "Active Control of Spacecraft Charging," *Progress in Astronautics and Aeronautics*, v.71, pp.299-317, 1980.

Rovang, D.C., and Wilbur, P.J., "Ion Extraction Capabilities of Very Closely Spaced Grids," AIAA/JSASS/DGLR 16th International Electric Propulsion Conference, New Orleans, Louisiana, 17-19 November, 1982.

Spectra-Mat Inc.,Watsonville, California,*Technical Bulletin #118,Ion Sources*, 1980.

Tascione,Thomas F.,*Introduction to the Space Environment*, pp.97-100, Orbit Book Company, 1988.

Werner, P.W., *Ion Gun Operations at High Altitudes,* Master's Thesis, Naval Postgraduate School, Monterey, California, June, 1988.

Whipple, E.C., "Potentials of Surfaces in Space," *Report on Progress in Physics,* v. 44, pp. 1197-1240, 1981.

Winkler, J.R., "The Application of Artificial Electron Beams to Magnetospheric Research," *Reviews of Geophysics and Space Physics,* 1980.

INITIAL DISTRIBUTION LIST

1.	Defense Technical Information Center Cameron Station, Alexandria, VA 22304-6145	2
2.	Library, Code 52 Naval Postgraduate School Monterey, CA 93943-5002	2
3.	Department Chairman, Code Ph Department of Physics Naval Postgraduate School Monterey, CA 93943-5000	1
4.	Dr. R. C. Olsen, Code Ph/Os Department of Physics Naval Postgraduate School Monterey, CA 93943-5000	3
5.	Dr. S. Gnanalingam. Code Ph/Gm Department of Physics Naval Postgraduate School Monterey, CA 93943-5000	1
6.	Mr. Gracen Joiner Code 1114SP Office of Naval Research 800 N. Quincy Street Arlington, VA 22217	1
7.	Mr. Kim Gunther Spectra-Mat, Inc. 100 Westgate Drive, Watsonville, CA 95076	1
8.	LCDR M. E. Melvin Commander, Operational Test and Evaluation Force Code - 714 Norfolk, VA 23511-5225	1

9. Dr. E. C. Whipple — 1
NASA/HQ/SS-1
Washington, DC 20546

10. Major C. W. Beatty — 1
DNA/RAEV
6801 Telegraph Road
Alexandria, VA 22310-3398

11. Mr. Herb Cohen — 1
W. J. Schafer Assoc. Inc.
1901 N. Fort Meyer Drive
Suite 800
Arlington, VA 22209